COGNITIVE DYNAMIC SYSTEM FOR VEHICLES

COGNITIVE DYNAMIC SYSTEM FOR CONNECTED AND AUTONOMOUS VEHICLES

By SHUO FENG, B.Sc., M.Sc.

A Thesis Submitted to the School of Graduate Studies in Partial Fulfilment of the Requirements for the Degree Doctor of Philosophy

McMaster University DOCTOR OF PHILOSOPHY (2019) Hamilton, Ontario (Computational Science and Engineering)
TITLE: Cognitive Dynamic System for Connected and Autonomous Vehicles
AUTHOR: Shuo Feng, B.Sc., M.Sc. (McMaster University)
SUPERVISOR: Distinguished University Professor Simon Haykin
NUMBER OF PAGES: xxi, 150

Lay Abstract

As an essential part of the emerging Internet of Things, connected and autonomous vehicles have the potential to reshape future transportation systems and change the commute style in people's everyday life. Unfortunately, they are typically faced with various threats and attacks that could endanger the entire vehicle network. The recent development of cognitive dynamic systems has provided a very powerful research tool to study complex systems operating in an open and possibly adversarial environment. The key goal of this thesis is to apply cognitive dynamic systems to connected and autonomous vehicles with emphasis on improved driving safety and system security. The function of cognitive risk control is utilized in respective vehicular systems in order to achieve robust target-tracking and anti-jamming vehicle-to-vehicle communication performance. For validation, extensive simulation results have shown that the proposed methods have desirable performance in the face of motion perturbation and/or jamming attacks under various scenarios.

Abstract

As an essential part of the emerging people-centric Internet of Things, connected and autonomous vehicles (CAVs) have the potential to reshape future transportation systems and impact the physical and/or social environment. While CAVs are currently being developed all over the world, they are unfortunately faced with various potential threats that could endanger the entire CAV network. Among others, risk-related concerns such as motion perturbation and jamming attacks are extremely critical to the survival of CAV networks and urgently need effective countermeasures.

This research addresses the aforementioned challenges by employing cognitive dynamic systems (CDS). Inspired by certain features of the human brain, CDS is a very powerful research tool to study complex systems operating in an open and possibly adversarial environment. As a special function of CDS, cognitive risk control (CRC) actualizes the concept of predictive adaptation to bring risk under control when encountered with unexpected uncertainty.

The primary research objective of this thesis is to apply CDS to CAV networks with emphasis on improved driving safety and system security. The function of CRC is utilized in respective vehicular systems in order to achieve robust target-tracking and anti-jamming vehicle-to-vehicle communication performance. For validation, extensive simulation results have shown that the proposed methods have desirable performance in the face of motion perturbation and/or jamming attacks under various scenarios.

This thesis contributes to the body of knowledge by presenting the following four achievements: the first theoretical work that integrates the research tool of CDS with the engineering application of CAVs; the first experimental work of CRC being applied to a practical vehicular system; the first experimental work on V2V communication that involves anti-jamming, power control, and channel selection at the same time; and a brand-new design of coordinated vehicular radar and communication systems that builds upon all the research efforts made previously.

Preface

A. Included Manuscripts

This thesis contains four manuscripts, as listed below:

1. S. Feng, and S. Haykin, "Cognitive Dynamic System for Future RACE Vehicles in Smart Cities: A Risk Control Perspective," *IEEE Internet of Things Magazine*, accepted, June 2019.

2. S. Feng, and S. Haykin, "Cognitive Risk Control for Transmit-Waveform Selection in Vehicular Radar Systems," *IEEE Transactions on Vehicular Technology*, vol. 67, no. 10, pp. 9542-9556, Oct. 2018.

3. S. Feng, and S. Haykin, "Cognitive Risk Control for Anti-Jamming V2V Communication in Autonomous Vehicle Networks," *IEEE Transactions on Vehicular Technology*, accepted, Aug. 2019.

4. S. Feng, and S. Haykin, "Coordinated Cognitive Risk Control for Bridging Vehicular Radar and Communication Systems," *IEEE Transactions on Intelligent Transportation Systems*, under review, 2019.

B. Details on Included Manuscripts

(1) Manuscript 1 Presented in Chapter 2

The work was completed between March 2017 and February 2019. The manuscript was submitted in February 2019 and accepted in June 2019. My contributions are:

- Discussion on various risk-related issues in connected and autonomous vehicle networks.
- Development of a generic CDS architecture for performing cognitive risk control on RACE vehicles.
- Manuscript authorship and journal submission corresponding author.

(2) Manuscript 2 Presented in Chapter 3

The work was completed between March 2017 and February 2018. The manuscript was submitted in February 2018, revised in May 2018, and accepted in July 2018. My contributions are:

- Development of cognitive risk control for transmit-waveform selection in vehicular radar systems.
- Algorithm design, simulation implementation, and performance analysis.
- Manuscript authorship and journal submission corresponding author.

(3) Manuscript 3 Presented in Chapter 4

The work was completed between March 2018 and September 2018. The manuscript was submitted in September 2018, revised in January and May 2019, and accepted in August 2019. My contributions are:

- Development of cognitive risk control for anti-jamming V2V communication in autonomous vehicle networks.
- Algorithm design, simulation implementation, and performance analysis.
- Manuscript authorship and journal submission corresponding author.

(4) Manuscript 4 Presented in Chapter 5

The work was completed between September 2018 and May 2019. The manuscript was submitted in June 2019. My contributions are:

- Development of coordinated cognitive risk control for bridging vehicular radar and communication systems.
- Algorithm design, simulation implementation, and performance analysis.
- Manuscript authorship and journal submission corresponding author.

List of Publications

1. S. Feng, and S. Haykin, "Cognitive Dynamic System for Future RACE Vehicles in Smart Cities: A Risk Control Perspective," *IEEE Internet of Things Magazine*, accepted, June 2019.

2. S. Feng, and S. Haykin, "Cognitive Risk Control for Transmit-Waveform Selection in Vehicular Radar Systems," *IEEE Transactions on Vehicular Technology*, vol. 67, no. 10, pp. 9542-9556, Oct. 2018.

3. S. Feng, and S. Haykin, "Cognitive Risk Control for Anti-Jamming V2V Communication in Autonomous Vehicle Networks," *IEEE Transactions on Vehicular Technology*, accepted, Aug. 2019.

4. S. Feng, and S. Haykin, "Coordinated Cognitive Risk Control for Bridging Vehicular Radar and Communication Systems," *IEEE Transactions on Intelligent Transportation Systems*, under review, 2019.

5. S. Feng, P. Setoodeh, and S. Haykin, "Smart Home: Cognitive Interactive People-Centric Internet of Things," *IEEE Communications Magazine*, vol. 55, no. 2, pp. 34-39, Feb. 2017.

6. S. Haykin, P. Setoodeh, S. Feng, and D. Findlay, "Cognitive Dynamic System as the Brain of Complex Networks," *IEEE Journal on Selected Areas in Communications*, vol. 34, no. 10, pp. 2791-2800, Oct. 2016.

7. S. Haykin, J. M. Fuster, D. Findlay, and S. Feng, "Cognitive Risk Control for Physical Systems," *IEEE Access*, vol. 5, pp. 14664-14679, July 2017.

8. S. Feng, and S. Haykin, "Anti-Jamming V2V Communication in an Integrated UAV-CAV Network with Hybrid Attackers," *IEEE International Conference on Communications (IEEE ICC)*, pp. 1-6, May 2019.

9. S. Feng, and S. Haykin, "V2V Communication-Assisted Transmit-Waveform Selection for Cognitive Vehicular Radars," *IEEE Canadian Conference on Electrical and Computer Engineering (IEEE CCECE)*, pp. 1-6, May 2019.

Copyright Permission

I have secured permission to include copyright material in this Ph.D. thesis from the copyright holders. The permission includes a grant of an irrevocable, non-exclusive license to McMaster University and to Library and Archives Canada to reproduce the material as part of the thesis.

Acknowledgements

First and foremost, I would like to sincerely thank my supervisor, Professor Simon Haykin, for his invaluable guidance and unparalleled support during my entire Ph. D. study. I am extremely grateful to him for always believing in me, encouraging me to tackle many challenging projects, and providing me with tremendous help whenever I needed it. His enthusiasm and dedication have motivated me to do my best in all things that matter. Working closely with him all these years has given me the opportunity to observe a unique personality, which will always inspire me to be a hard worker and a good person. I am truly honored and feel very fortunate to have him as my supervisor.

I would like to express my deepest gratitude to the members of my supervisory committee, Professor Sue Becker and Professor Matheus Grasselli, for their insightful comments, valuable instructions, and encouragement. Their understanding, patience, and kindness have provided the most friendly research environment a Ph. D. student could ever ask for. Those pages with handwritten comments from Professor Sue Becker during each meeting will always be kept, and the constructive suggestion of keeping engineering-related research work realistic for practical use from Professor Matheus Grasselli will never be forgotten.

I'm indebted to Dr. Bartosz Protas for his invaluable suggestions in the first academic year on choosing courses, which have laid the foundation for this research. Just as importantly, I would also like to extend my gratitude to Dr. Peyman Setoodeh for many helpful suggestions that led to some interesting ideas in the early stages of this research. During the final stage pertaining to the thesis defence, I am truly blessed to have Professor Lajos Hanzo from the University of Southampton, United Kingdom, serving as my external examiner, and to have Professor Peter Macdonald serving as my examining committee chair. They both are very gracious and thoughtful.

Special thanks to Dr. Wade Genders and his wife Virginia Viscardi, the time we spent together over lunches or on games was always delightful and enjoyable. Sincere thanks to Xiang Song and Jiawen Wang, the few trips we took together have shown us the raw and majestic beauty of nature. Many thanks to Moyang Wang, your cooking skills made everyday life tasty and helped me focus on my research work. I also wish to thank Guoxin Li, who had helped me with a lot of things including preparing conference presentations and making well-thought travel plans. My sincere gratitude to David and Katrina Stairs, Suzanne and Colin Boot, your hospitality and loving homes have made a number of my holidays much warmer.

I also had great pleasure of working with my friends in the Cognitive Systems Laboratory, Dr. Eduardo Santos and Irshaad Oozeer, thank you for all the inspiring discussions and practical

suggestions. I am grateful to Dr. Jingshan Shi, Dr. Yangliu Dou, Dr. Ri Chen, Dr. Shasha Han, Jinfeng Huang, Xueli Zhao, Fanwang Meng, Xiaohong Liu, Tao Xie, Chenhe Zhang, Xiaotian Ju, Dr. Kiret Dhindsa, Markimba Williams, and many other friends who have made my life in Canada much more colorful.

I cannot leave McMaster University without mentioning Ms. Diana Holmes and Ms. Julie Fogarty from the Department of Mathematics and Statistics and the School of Computational Science and Engineering, Ms. Tracey Coop, Ms. Cheryl Gies, Ms. Delcia Aguiar, Ms. Kerri Hastings, and Mr. Joe Peric from the Department of Electrical and Computer Engineering, Ms. Ana Pereira from the International Student Services, and Mr. Frank Coruzzi from the School of Graduate Studies. During my entire time at McMaster, they are always welcoming, supportive, and considerate.

I would like to express my appreciation to my former advisors, Professor Jinlong Wang and Professor Qihui Wu, who had led me into the fascinating academic world during my Master's study. I gratefully acknowledge the support from Professor Xiang-Gen Xia, University of Delaware, Newark, United States, Professor Yulong Zou, Nanjing University of Posts and Telecommunications, Nanjing, China, and Professor Yujian Cheng, University of Electronic Science and Technology of China, Chengdu, China, for their profound belief in my abilities and providing me with strong recommendation letters years ago. I also owe many thanks to my former colleagues, Dr. Yuhua Xu, Dr. Guoru Ding, Dr. Luliang Jia, Dr. Changju Kan, Dr. Linyuan Zhang, Dr. Yuli Zhang, and Dianxiong Liu, for staying close and giving me enormous help during all these years. I also wish to thank Dr. Long Wang, Yutao Jiao, and Junfei Qiu, the similar studying experiences we had have given us a lot of bitter-sweet memories.

Also, I want to thank everyone who ever helped me, cared for me, or was there for me, especially during those hard times. It all meant a lot to me and is much appreciated.

Finally, I would like to thank my family from the bottom of my heart. Without their patience and sacrifice, completion of the Ph.D. study would not have been possible. Their endless support, understanding, and unconditional love is something I will never be able to repay in my entire life. To my wife Meng and my son Qiuheng, you make me happier than I ever thought I could be, and I will spend the rest of my life trying to make you two feel the same way.

Only a life lived for others is a life worthwhile.

—Albert Einstein

Dumbledore watched her fly away, and as her silvery glow faded he turned back to Snape, and his eyes were full of tears. "After all this time?" "Always," said Snape.

—J. K. Rowling, *Harry Potter and the Deathly Hallows*

Contents

List of Figures

List of Tables

List of Abbreviations

3GPP 3rd Generation Partnership Project

ABS Anti-lock Braking System

ACC Adaptive Cruise Control

ACE Autonomous, Connected, and Electric

ACES Autonomous, Connected, Electric, and Shared

ADAS Advanced Driver-Assistance System

AEB Autonomous Emergency Braking

AI Artificial Intelligence

BSD Blind Spot Detection

C-CRC Coordinated Cognitive Risk Control

CACC Cooperative Adaptive Cruise Control

CAV Connected and Autonomous Vehicle

CCH Control Channel

CDS Cognitive Dynamic System

CKF Cubature Kalman Filter

CNN Convolutional Neural Network

CRC Cognitive Risk Control

CSS Cooperative Spectrum Sensing

CVR Cognitive Vehicular Radar

DARPA Defense Advanced Research Projects Agency

DDPG Deep Deterministic Policy Gradient

DMV Department of Motor Vehicles

DoS Denial of Service

DRL Deep Reinforcement Learning

DSRC Dedicated Short-Range Communication

EBA Electronic Brake Assist

EU European Union

EV Electric Vehicle

FCW Forward Collision Warning

FDI False Data Injection

GM General Motors

GPS Global Positioning System

ICT Information and Communication Technology

IEEE Institute of Electrical and Electronics Engineers

IMM Interacting Multiple Model

IoT Internet of Things

IoV Internet of Vehicles

ITS Intelligent Transportation System

LDW Lane Departure Warning

LFM Linear Frequency Modulation

LiDAR Light Detection And Ranging

LOS Line-of-Sight

LRR Long-Range Radar

LSTM Long Short-Term Memory

LTE Long-Term Evolution

M2M Machine-to-Machine

MAB Multi-Armed Bandit

MAP Maximum A Posteriori

MIMO Multi-Input Multi-Output

NHTSA National Highway Traffic Safety Administration

OBU On-Board Unit

OEM Original Equipment Manufacturer

OSA Opportunistic Spectrum Access

PAC Perception-Action Cycle

PACE Personalized, Autonomous, Connected, and Electric

PCS Physical Carrier-Sensing

PSD Power Spectral Density

QoS Quality of Service

RACE Risk-sensitive, Autonomous, Connected, and Electric

RKRL Radio Knowledge Representation Language

RMSE Root Mean-Square Error

RNN Recurrent Neural Network

RSU Roadside Unit

SAE Society of Automotive Engineers

SCH Service Channel

SINR Signal-to-Interference-plus-Noise Ratio

SLAM Simultaneous Localization And Mapping

SNR Signal-to-Noise Ratio

TJC Traffic Jam Chauffeur

TSC-A Task-Switch Control-A

TSC-B Task-Switch Control-B

UAV Unmanned Aerial Vehicle

UCB Upper Confidence Bound

V2C Vehicle-to-Cloud

V2D Vehicle-to-Device

V2G Vehicle-to-Grid

V2I Vehicle-to-Infrastructure

V2P Vehicle-to-Pedestrian

V2V Vehicle-to-Vehicle

V2X Vehicle-to-Everything

VANET Vehicular ad hoc Network

WAVE Wireless Access in Vehicular Environments

WHO World Health Organization

Declaration of Academic Achievement

Shuo Feng is the main contributor and first author for all manuscripts in this thesis. Any co-author contributions are detailed at the beginning of each chapter that includes a published or submitted manuscript.

Chapter 1

Introduction

1.1 Background on Connected and Autonomous Vehicles (CAVs)

1.1.1 Basic Concept

The topic of connected and autonomous vehicles (CAVs) is among the most heavily researched areas in vehicular technologies and transportation systems [1, 2]. Its development is driven by innovations in many fields, including artificial intelligence (AI), information and communication technology (ICT), embedded systems, and mechanical engineering, just to name a few [3, 4]. As a representative example for the pervasive connection between cyber world and physical world, CAVs occupy a distinctive place in the emerging Internet of Things (IoT) and the ongoing fourth industrial revolution (i.e., Industry 4.0) [5, 6].

Although often studied together, connected vehicles and autonomous vehicles refer to two distinct technologies that could potentially be complementary and work cooperatively [7]. Vehicles with some levels of automation do not necessarily need to be connected, and vice versa. Technology convergence, however, will definitely result in intelligent vehicles that are both connected and autonomous, hence the concept of CAVs [8].

1.1.2 Connected Feature

In general, the term "connected" refers to vehicular features that allow vehicles to communicate with each other and with other road users in their surrounding environment using built-in or add-on devices that continuously share important safety and mobility information [9]. As a broad concept, connected vehicle technology enables communications among vehicles, infrastructure, and personal communication devices operated by passengers, pedestrians, bicyclists, or other road users [10]. Some of the connected functionality of a vehicle include Internet access, satellite navigation, congestion notification, remote diagnostics, infotainment, and emergency call services [11]. This technology can

be used not only to improve vehicle safety, but also to improve transportation efficiency, accessibility, etc.

Historically speaking, the first vehicle equipped with connected feature was produced by General Motors (GM) in 1996 [12]. In the event of traffic accidents when an airbag was deployed, a voice call would be made by the in-vehicle telematics system to a call center that contacted emergency responders. It has gradually led to the development of a modern emergency call system named "eCall", which was made mandatory in all new vehicles sold within the European Union (EU) from April 2018 onwards [13]. This is one of many practical and beneficial applications that rely on the connectivity of vehicles.

The connected feature is typically supported by a number of different communication technologies, which include [9, 14–16]:

(i) Vehicle-to-Vehicle (V2V): It refers to the wireless communications between vehicles via various technologies, such as dedicated short-range communications (DSRC), cellular networks, Wi-Fi, or satellite. Through exchanging real-time driving information regarding the position, velocity, and/or acceleration, V2V enables many safety and non-safety applications with high reliability and low latency. For example, V2V communication extends and enhances currently available crash-avoidance systems to detect collision threats more effectively, and then warns the driver about potentially dangerous situations if required. Additionally, V2V technology can also be combined with existing radar and camera systems to provide even greater benefits than either approach alone.

(ii) Vehicle-to-Infrastructure (V2I): V2I technologies capture vehicle-generated traffic data (which can then be used to make informed decisions such as temporary traffic management or long-term transportation planning by transportation agencies in a centralized manner), and wirelessly provide information such as advisories from the infrastructure to the vehicle that inform the driver of safety, mobility, or environment-related conditions.

(iii) Vehicle-to-Pedestrian (V2P): The V2P approach encompasses a broad set of road users including people walking or using wheelchairs, passengers embarking and disembarking buses and trains, and bicyclists. It will not only facilitate pedestrian detection and provide notifications to the driver, but also enable vehicle detection and send collision alerts to the pedestrians' personal mobile devices.

(iv) Vehicle-to-Grid (V2G): The V2G is developed particularly for electric vehicles (EVs), which use electric motor and battery energy for propulsion, and need to recharge frequently when the battery is running low. V2G communication allows energy exchange between the vehicles and a (smart) power grid, which will potentially bring revenues for the vehicle owners and increase the service capacity a power grid can provide.

(v) Vehicle-to-Cloud (V2C): The V2C concept allows on-board computing resources of vehicles to be integrated with the cloud computing environment, which is a virtual network that aims to transparently and ubiquitously share a large number of computing resources. By making the

cloud available to vehicular systems, V2C also helps vehicles to access information from other cloud-connected entities, such as the power grid, a regulation center, or emergency services.

(vi) Vehicle-to-Everything (V2X): The V2X is an integrated technology that interconnects all types of vehicles and infrastructure systems. This connectivity will help provide more precise knowledge of the traffic situation across the entire road network, which may also be extended to trains, airplanes, ships, etc.

Each of these connectivity mechanisms could be enhanced by one another. For example, the V2P could be enhanced by V2V or V2I with more accurate interpretation and prediction of pedestrian movement derived from various sources. Furthermore, connectivity contributes to subsequent automation, which gradually transforms the human driver's role by reassigning driving tasks previously performed by humans to autonomous systems [17].

1.1.3 Autonomous Feature

Although the primitive idea of the autonomous vehicle or driverless car originated almost a century ago [18], it really started to blossom and bear fruit in the past few decades [19, 20]. According to the U.S. Department of Transportation's description, "autonomous" or self-driving vehicles are "those in which operation of the vehicle occurs without direct driver input to control the steering, acceleration, and braking and are designed so that the driver is not expected to constantly monitor the roadway while operating in self-driving mode" [21]. When fully developed, autonomous vehicles will be able to reduce the accidents caused by human errors to a great extent, provide a comfortable travel experience, improve accessibility for disadvantaged groups, and so on. Additionally, vehicle connectivity is very important to realizing the full potential benefits of autonomous vehicles.

For research and development purposes, there are multiple definitions for various levels of driving automation proposed over the years. The most commonly adopted one is the Society of Automotive Engineers (SAE) International's definition, as prescribed by the SAE International Standard J3016 on Levels of Driving Automation (first issued in 2014, revised in 2016 and 2018) with the following six levels [22]:

(i) Level 0—No Driving Automation: Human driver controls all aspects of driving during the entire time, even when enhanced by some active safety systems. Example features include automatic emergency braking, blind spot warning, and lane departure warning.

(ii) Level 1—Driver Assistance: Human driver is assisted with either steering or brake/acceleration by driving automation system with the expectation that the human driver will perform all remaining functions. Example features include lane centering or adaptive cruise control.

(iii) Level 2—Partial Driving Automation: Driving automation system provides steering and brake/acceleration support to human driver with the expectation that the driver will perform all other driving tasks. Example features include lane centering and ACC at the same time.

(iv) Level 3—Conditional Driving Automation: Driving automation system undertakes all aspects of the dynamic driving task with the expectation that the human driver will respond appropriately to a request to intervene. One example feature is the traffic jam chauffeur.

(v) Level 4—High Driving Automation: Driving automation system undertakes all aspects of the dynamic driving task and will not require a human driver to take over driving. Example features include local driverless taxi, in which pedals/steering wheel may or may not be installed.

(vi) Level 5—Full Driving Automation: Driving automation system can drive the vehicle everywhere under all conditions.

Generally speaking, for Levels 0-2, the human driver is considered to be driving even when the driving support features are engaged. The driver must constantly supervise these support features, and must steer, brake or accelerate as needed to maintain safety. On the other hand, for Levels 3-5, the human driver is not considered to be driving when the automated driving features are engaged even if he/she is seated in the driver's seat.

It is not surprising that the world of CAVs is rapidly growing and evolving. The main contributors to this rapid evolution include technology companies, automotive manufacturers, research institutions/universities, and regulatory agencies, etc. Putting legal and ethical issues related to the development of CAVs aside, the next two subsections will briefly discuss recent industrial activities and academic research trends within this area, respectively.

1.1.4 Recent Industrial Activities

Since the earliest work on car-following controllers undertaken by GM and Radio Corporation of America in the late 1950s [23], tremendous research and development efforts were made worldwide in the past few decades. A recent milestone is a series of Grand Challenge competitions that were funded by the Defense Advanced Research Projects Agency (DARPA) between 2004 and 2007, which have spurred the most recent wave of interest and innovations for this field [24].

Currently, there are about 50 large companies (and the number is still increasing) that are working on the development of highly/fully autonomous vehicles [25, 26]. This fierce competition involves a diverse group of players, ranging from automotive makers to leading technology brands and telecommunications companies.

Since Google's first public announcement in October 2010 [27], its "Self-Driving Car Project" has been one of the leading banner-carrier autonomous vehicle programs. In May 2016, Google began working with its first automotive partner Fiat Chrysler, which remains its main original equipment manufacturer (OEM). In December 2016, this project formally became Waymo, which publicly revealed its custom-designed, self-driving hardware in February 2017. In August 2018, Waymo launched a program to provide residents of the Phoenix area with rides to bus stops and train stations using the autonomous fleet. Until October 2018, Waymo's autonomous vehicles have driven 10 million miles on public roads in various areas, including Mountain View, California, Austin, Texas, Kirkland, Washington, and Phoenix, Arizona. Most recently, Waymo partnered with ride-sharing company Lyft to make autonomous vehicles available to Lyft riders in June 2019.

Another high-profile company in this battleground is Tesla, which pushed its "Autopilot" software update to properly equipped Model S vehicles in October 2015, enabling auto steering, lane changing, and parking features. Since October 2016, all Tesla vehicles have been built with Autopilot Hardware 2, which allows Tesla vehicles on the road to receive self-driving capabilities through software updates. The release of Autopilot Hardware 3 was schedule for 2019.

A number of the world's largest automakers are following behind Waymo very closely in the race of developing CAVs. Besides a partnership with Lyft formed in January 2016, GM Cruise has been developing its own semi-autonomous technology in-house and launched Super Cruise in the 2018 Cadillac CT6. GM also filed a petition in January 2018 to run a commercial ride-sharing business through autonomous Chevrolet Bolts. In early 2015, Ford announced its "Smart Mobility Plan" to push the company forward in innovative areas including vehicle connectivity and autonomous cars. In February 2017, Ford acquired AI startup Argo, whose technology has been tested out with Ford's third-generation Fusion model sedan since 2018. Bosch and Mercedes joined forces to develop Levels 4-5 vehicles in April 2017, and they also partnered with GPS maker TomTom for its high-resolution mapping data. Honda introduced semi-autonomous advanced-driver assistance systems (ADAS) options on its entry-level Civic in 2016, offering lane-keeping, automatic braking, and ACC functionality, which have become ubiquitous on luxury models offered by brands like Tesla and Mercedes. In July 2017, Audi unveiled its A8 model, which had an autonomous driving feature that let drivers fully take their hands off the wheel. It was the first vehicle in production that could actually allow its users to "drive" hands-free at the time, and therefore can be counted as the world's first production car to offer Level 3 driving automation [28]. Volvo announced a self-driving joint venture with Swedish supplier Autoliv in January 2017. Later in June 2018, Volvo announced another partnership with LiDAR (Light Detection and Ranging) startup Luminar to work on vehicle-mounted sensors and software design. BMW teamed up with Intel and Mobileye in July 2016 to create an open standards-based platform for bringing Levels 3-5 autonomous vehicles to market. German auto supplier Continental AG has been focusing on driver-assistance technologies instead of building a physical vehicle. In April 2017, Continental opened a new lab to work on connected vehicles that can communicate with one another and with roadway infrastructure. Then in February 2018, a partnership with Nvidia was formed to integrate its software with Nvidia's platform and to develop top-to-bottom self-driving solutions.

Some world-leading technology companies with less auto manufacturing experiences are also participating in this competition. With a shift in strategy for "Project Titan", Apple registered 66 vehicles with the California Department of Motor Vehicles (DMV) in July 2018, making Apple the owner of the third-largest autonomous test-vehicle fleet in the state, behind GM and Waymo. In April 2014, Chinese tech company Baidu partnered with German automaker BMW to develop a semi-autonomous prototype. In late 2017, Baidu began testing its open-source Apollo software system, and then received permission to test Apollo on the open road in Beijing in March 2018. Amazon is experimenting on autonomous package delivery, which is viewed to be the solution to the last-mile delivery problem. Through a partnership with Toyota, Amazon started working on multi-function autonomous and electric vehicles in January 2018. Focusing on providing automakers with technological assistance, Microsoft collaborated with Volvo in November 2015 and with Toyota

in April 2016. In July 2017, Microsoft announced to offer its Azure cloud services to companies using Baidu's Apollo self-driving platform for autonomous projects. In January 2016, GPU and semiconductor company Nvidia unveiled its new processing platform Nvidia Drive PX2, which supported deep learning, sensor fusion, and computer vision applications for autonomous vehicles. Since then, Nvidia has partnered with Baidu, Tesla, Bosch, and Toyota. In May 2016, Uber revealed its in-house autonomous prototypes for the first time. In March 2018, a developmental self-driving Uber vehicle was involved in a fatal crash in Arizona, leading to a suspension of all of its road trials. In February 2018, Chinese ride-hailing company Didi reported that it had built the software and constructed the hardware for functioning self-driving cars in partnership with various automakers and suppliers. Three months later, Didi received permission from California DMV to undertake further public testings of its technology.

Among the technology companies, some specialized in telecommunications have paid extra interest in improving the connectivity of autonomous vehicles. In October 2017, Cisco began working on a project called "Cisco Connect Roadways" that aimed at connecting individual vehicles on the road with the infrastructure around them. Through a partnership with Hyundai, Cisco announced its intention to focus on bringing gigabit-speed connectivity to CAVs. Chinese telecommunication company Huawei has also shifted resources toward the development of CAVs. In December 2016, Huawei Wireless X Labs released a white paper detailing how mobile network operators could actively participate in the connected vehicle and smart transportation area. Partnered with Vodafone, Huawei demonstrated innovative cellular technology used to connect cars called cellular V2X in February 2017.

In addition, many other companies are also making huge research and development efforts, such as Hyundai, Iveco, Jaguar Land Rover, Nissan, Toyota, Volkswagen, Yutong, and so on [25].

There are different views regarding how far these companies have gone and for how long they need to continue before arriving at the end of this journey. In early 2019, Navigant Research released a new leaderboard report that assessed the strategy and execution for 20 leading companies that were developing CAVs [29]. Based on 10 criteria, vendors are profiled, rated, and ranked with the goal of providing industry participants with an objective assessment of these companies' relative strengths and weaknesses in the global automated driving market. In their report, the top three players are Waymo, GM, and Ford. Another ranking by Bloomberg stated that Waymo, GM, and Mercedes-Benz are in the lead [30].

Navigant Research's leaderboard also pointed out that, as of the end of 2018, there is one thing in common: no company is providing commercial services without a human safety operator onboard the vehicle when carrying passengers. It indicates that with all the progresses being made, there is still a long way to go.

1.1.5 Advanced Driver-Assistance Systems (ADAS)

Regarding the academic research trends, there are two major research directions that have received a great deal of attention in recent years. One of the directions takes a relatively more radical approach, which mainly relies on machine learning or computer vision techniques and tries to solve the

autonomous driving problem by inventing brand new methods and algorithms. The other direction takes an incremental innovation path, which builds upon the currently available or under development ADAS systems and moves towards the full realization of CAVs gradually. This subsection will briefly describe the first approach and then discuss ADAS systems of the second approach in more detail, for which the research work presented in this thesis can be of use.

For the first approach, a representative example using a supervised learning method is to train a convolutional neural network (CNN) to map raw pixels from a single front-facing camera directly to steering commands [31], which might be combined with a recurrent neural network (RNN) for the sequence-to-sequence mapping [32–34]. Additionally, researchers have used reinforcement learning methods, which can be viewed as the brute-force propagation of outcomes to knowledge about states and actions. To deal with continuous action spaces as in the driving problem, one possible way is to use the deep deterministic policy gradient (DDPG) method for the training process [35]. Additional representative work in this direction can be found in the literature [36–42].

For the second approach, the philosophy is to enrich, improve, and integrate current ADAS systems so that one day they will be elevated to meet the requirements for the realization of CAVs. Emerging ADAS systems will also take advantage of externally supplied data through V2V (or V2X in general) connections, which indicates that development of connected vehicles, autonomous vehicles, and ADAS systems is starting to overlap.

Compared with passive safety systems, a common feature of ADAS systems is that they directly intervene with the driving operations and aim at helping drivers to improve traffic safety. Over the years, many off-the-shell systems of such kind have been developed and deployed in the market, including [43–45]:

(i) Adaptive cruise control (ACC): The ACC is a sensor based technology that automatically adjusts the vehicle's velocity to maintain a safe distance from the vehicle ahead in the same lane. It is expected to keep a short distance to improve the transportation efficiency while ensuring that there is enough space if the vehicle ahead suddenly brakes. Visual feedback will also be provided to the driver when ACC system is engaged. The new generation of ACC systems uses multiple sensory inputs, which help to make more accurate judgments regarding which vehicles are in-lane and relevant to be tracked.

(ii) Lane departure warning (LDW): The LDW system uses a front camera to recognize lane markings and notifies the driver when he/she is about to leave the current lane without using their blinker signal. In such cases, the driver will experience a combination of steering wheel vibrations and a slight automatic correction to help the vehicle to stay in its lane.

(iii) Blind spot detection (BSD): Due to physical limitations, there are typically some areas that are out of the sight for a human driver. These blind spots exist both on the side and behind the vehicle. The BSD system provides the driver with information on whether there are any vehicles, cyclists or pedestrians in the blind spots, which can be detected by using active radar or passive infrared sensors.

(iv) Traffic jam chauffeur (TJC): As a complement function to the ACC, a TJC or traffic jam assist

is particularly designed for traffic congestion, which is very common in urban areas during rush hours. When TJC is engaged, the system finds a reference vehicle ahead and keeps their distance by making the vehicle stop and go automatically without the driver's intervention.

(v) Electronic brake assist (EBA): The EBA system takes a quick step on the brake pedal as the sign for an emergency braking action and complements the applied braking power if the driver has not stepped with enough pressure. The system is included in various anti-lock braking systems (ABS) and optimizes the vehicle's braking capacity in emergency braking situations and thereby also possibly shortens the stopping distance.

This list is not exhaustive and has only included some of the most common ADAS systems. Forward collision warning (FCW), parking assist, and automatic lighting are among well-developed ADAS systems as well. New ADAS systems may provide automated traffic warnings via GPS signals, detect drivers' drowsiness level based on facial expression recognition, or allow hands-free voice activated smartphone connections, etc. As mentioned in the list, these ADAS systems highly rely on a number of vehicle-mounted sensors for primary tasks such as data gathering and scene understanding. To be specific, the hardware components for supporting ADAS systems include [46–48]:

(i) Radar: Radar is an active detection system that uses radio waves to determine the range, angle, or velocity of target objects. Radar sensors monitor the position of other vehicles or road users nearby to improve environmental awareness. They are already widely used in many ADAS systems such as the ACC and the BSD.

(ii) LiDAR: LiDAR sensors bounce pulses of light off the surrounding objects. The reflected pulses are analyzed to form three dimensional point clouds for identifying lane markings and the edges of roadways.

(iii) Video camera: Video camera detects traffic lights and signals, reads road signs, keeps track of the position of other vehicles, and looks out for pedestrians, cyclists, and obstacles on the road.

(iv) GPS: A GPS system provides satellite-based geolocation information, which could be more accurate when GPS signals are combined with the readings from gyroscopes, accelerometers, tachometers, and altimeters, etc.

(v) Ultrasonic sensor: Compared with radar sensors, ultrasonic sensors can provide more accurate positioning of the surroundings at a short range, for example the curbs or passing-by pedestrians when the driver is parking.

(vi) Radio transceiver: A radio transceiver enables the vehicle to receive signals from other vehicles as well as roadside infrastructures, so that additional information from external sources can be utilized.

(vii) Central computer: The information gathered from all of the sensors is processed by a central computer that manipulates the steering, accelerator and brakes. It must understand the driving scene and then make proper decisions.

Later in this thesis, radar and radio transceivers will be the main focus, and the design of vehicular radar and communication systems will be studied thoroughly.

1.1.6 Benefits and Concerns

Safety is indisputably the single most important factor for modern transportation. According to the World Health Organization (WHO), approximately 1.35 million people die each year worldwide as a result of road traffic crashes [49]. Between 20 and 50 million more people suffer non-fatal injuries, with many incurring a disability as a result of their injury.

In the United States, according to the National Highway Traffic Safety Administration (NHTSA) of the U.S. Department of Transportation, there were 37,133 people killed in motor vehicle traffic crashes on U.S. roadways during 2017 [50]. The injury rates were nearly 100-fold higher; the estimated number of people injured in traffic accidents in the United States was 2.44 million in 2015 [51]. Astonishingly, the NHTSA revealed that about 94% of the traffic crashes were caused by human errors, be it recognition errors, decision errors or performance errors [52]. In particular, the act of impaired driving could lead to all kinds of human errors; it was reported by the NHTSA that alcohol-involved impaired driving fatalities accounted for 29% of all motor vehicle traffic fatalities in 2017 [53, 54], and 18% of all fatally injured drivers were tested positive for drug involvement in 2009 in the United States [55].

In the EU, according to the European Commission's reports, more than 25,000 people lose their lives on EU roads every year (25,300 fatalities in 2017) [56]. In addition, about 135,000 people sustain serious road traffic injuries on EU roads per year. Serious injuries are not only more common but also often more costly to society because of long-time rehabilitation and healthcare needs. The socio-economic consequences of this alone are estimated at 120 billion euros annually for the EU. Reducing the number of fatalities and injuries has been identified as an important objective of transport policy worldwide.

Over the past few decades, a number of safety programs/regulations leading to increased seat-belt use and reduced impaired driving have significantly lowered the number of traffic fatalities. Moreover, vehicle improvements such as air bags, anti-lock brakes, and electronic stability control have also contributed greatly to the reduction of traffic deaths [50].

There is much more to be gained with CAVs. The development and adoption of CAVs could impart significantly greater reductions in traffic injuries and fatalities. Based on an analysis report released by the NHTSA, the full adoption of DSRC and V2V technology could prevent 439,000 to 615,000 crashes, and save 987 to 1,366 lives each year in the United States [57]. Another study predicted that the widespread embrace of CAVs could ultimately cause vehicle crashes in the United States to fall from second to ninth place in terms of their lethality ranking among accident types [58]. Needless to say, this would be an enormous benefit to individuals, families and society as a whole.

However, despite the great benefits that CAVs would deliver, the future deployment of CAVs has also raised a number of risk-related concerns. With the connected and autonomous features being made popular, the same hardware, software, and electronics that have enabled them also introduce new risks to the driving safety. As vehicle cybersecurity threats have emerged, CAVs will face serious

cyber attacks, unauthorized access, privacy invasions, damage, or disruptions that interfere with system performance.

For example, dangerous situations would appear when other vehicles suddenly stop on the road ahead, speed recklessly through intersections, or maneuver unexpectedly to get through a congestion. Intentionally or not, these motion perturbations will raise the risk for driving safety and need to be tracked as accurately as possible in a timely manner. Besides, some on-road vehicles may be adversarial and equipped with radio jamming capabilities. They would specifically target V2V links and disrupt regular information exchange. This kind of attack will disable the communication between CAVs and all the critical applications that are supported by connectivity. Countermeasures should be taken to mitigate jamming attacks and keep V2V communication as reliable as possible in an efficient manner. This topic will be further discussed and elaborated in the next chapter.

1.2 Research Tool of Cognitive Dynamic Systems (CDS)

1.2.1 Basic Concept

As an emerging and fascinating research field, the study of cognitive dynamic systems (CDS) integrates many fields that are rooted in neuroscience, cognitive science, computer science, mathematics, physics, and engineering, just to name a few [59]. For justifying that a so-called CDS is indeed "cognitive", several key aspects of human cognition are adopted as the frame of reference, the principles of which will be explained in the next subsection. Regarding the second key word of "dynamic", it emphasizes that the factor of time plays a key role in the system's input-output behavior. The idea of CDS is firstly presented in [60] and has evolved significantly over the course of time [61–64].

1.2.2 Five Principles

From the perspective of neuroscience and cognitive science, there are five distinctive principles of human cognition as stated in Fuster's paradigm: perception-action cycle (PAC), memory, attention, intelligence, and language [65]. These distinctive properties of human cognition constitute the ideal framework, against which a dynamic system should be assessed for it to be cognitive.

To implement the fundamental principles within Fuster's paradigm, the formulation of CDS lives up to the well-known engineering paradigm: "divide and conquer". Step by step, CDS is built upon these fundamental principles.

1.2.2.1 Perception-Action Cycle (PAC)

The name of PAC implies that a CDS has two primary functional parts: perceptor and actuator (i.e., executive), as shown in Fig. 1.1. Deeply rooted in biology, PAC is the cybernetic information-processing loop that adapts the system to its environment during goal-directed behavior [66]. As the structural backbone of CDS, PAC begins with the perceptor perceiving the external environment by processing the incoming stimuli, called observables or measurements. In response to the feedback information from the perceptor about the environment, the executive makes decisions and acts

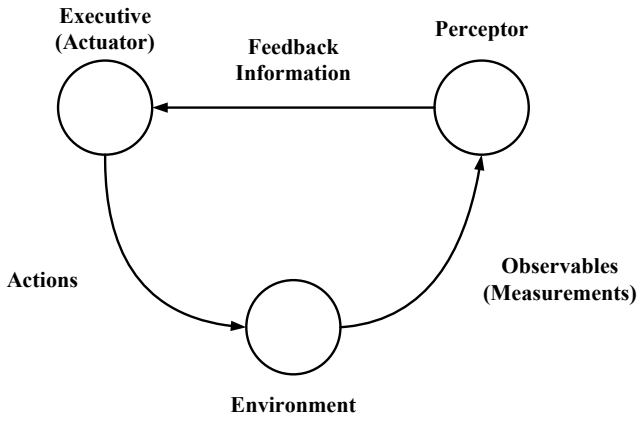

Figure 1.1: CDS in its most simplified form.

accordingly. That particular action produces change in the environment that is again processed by the perceptor for further action, and so the cyclic behavior goes on until the goal of interest is reached. The outcome of each PAC is informative for subsequent cycles, and the benefit resulting from PAC is that of improved information gained from the environment [59].

1.2.2.2 Memory

Typically, the environment that a CDS operates in is nonstationary and continually changes with time. Given such an environment, it is a must for a CDS to have memory, desirably of a multiscale variety. The PAC incorporates the acquisition and retrieval of memory. The component of memory is necessary for learning from the environment and storing the knowledge so acquired, continually updating the stored knowledge in light of environmental changes, and predicting the consequences of actions taken and/or selections made by the system as a whole. Specifically, perceptual memory (episodic, semantic, conceptual, etc.) is the memory acquired through the perception and includes a large amount of individual experiences, from the simplest forms of sensory memory to the most abstract knowledge. Executive memory is the representation of motor acts and behaviors; it plays an important role in supporting the execution of both elementary motor acts and complex goal-directed actions [67].

1.2.2.3 Attention

In general, attention can be added to both the perceptor part and the executive part of a PAC as perceptual attention and executive attention, respectively. Attention prioritizes the allocation of available resources in such a way that the information gathering and processing power is focused on what is of critical strategic importance to the system. While perceptual attention deals with the information overflow problem, executive attention tries to maintain the system operation with minimum disturbance.

1.2.2.4 Intelligence

Intelligence is an emergent property of a system that makes decisions based on the PAC, incorporating memory and attention. While attention serves all other principles, intelligence is served by all. It is safe to say that intelligence is the single most important function in a CDS. It should be noted that the abundant presence of feedback at multiple levels, including both global and local feedback loops, facilitates intelligence, which, in turn, makes it possible for the system to make intelligent decisions in the face of inevitable uncertainties in the environment.

1.2.2.5 Language

Just as language plays a distinctive role in the human brain, so it does in a CDS where language provides the means for connectivity among different parts/components of the system, for instance, via effective and efficient machine-to-machine (M2M) communications. Challenging research issues involved in enabling M2M communications include architecture, standardization, identification, addressing, security, and so on [68]. However, detailed consideration of how one would incorporate the language is outside the scope of this study.

1.2.3 Generic Structure

Four basic components that constitute a generic CDS are described in the following order: a perceptor, an executive, a feedback channel linking the perceptor to the executive, and an embedded module called task-switch control that regulates the inner pathways of a CDS, the entire structure of which is embraced within an environment [63].

1.2.3.1 Perceptor

The perceptor is usually composed of Bayesian generative model, Bayesian filter, and entropic information-processor.

(1) Bayesian Generative Model

As the underlying objective of a perceptor is perception of the environment, we typically find the perceptor starts with modeling of the incoming observables. With Bayesian dynamics being the framework of choice [69], we look to the generative model as the first processing stage.

(2) Bayesian Filter

The second part in the perceptor, namely filtering, requires a procedure for estimating the state of the system model conditional on the generative posterior. In a generic sense, the Bayesian filter is the optimal solution for the filter needed for the perceptor [70]. However, when the system can be characterized by a linear model and a Gaussian distribution, the well-known Kalman filter can be employed [71].

Additionally, in order to account for perceptual attention, the Bayesian generative model and the Bayesian filter are reciprocally coupled, and therefore, a local feedback loop is formed. From a neuroscience point-of-view, the Bayesian filter picking up relevant information from the generative model represents the selective-focusing of the excitation component of attention, and the generative

model putting aside irrelevant observables (due to the suppression of Bayesian filter) represents the inhibition component [72].

(3) Entropic Information-Processor

Due to the presence of PAC, CDS is characterized by a directed flow of information from the perceptor to the executive in a continuous cyclic manner [73, 74]. Part of that information is the entropic state of the perceptor that progresses from one PAC to the next. With the outcome of the Bayesian filter at our disposal, Shannon's information theory is invoked to calculate the entropy we need [75, 76].

1.2.3.2 Feedback Channel

As mentioned previously, the feedback channel occupies a distinctive place within the CDS in that it links the executive to the perceptor, thereby closing the global feedback loop around the environment and completing the PAC.

In addition, the feedback channel is fully occupied with internal rewards, which is based on the entropic state of the perceptor and can be calculated in various ways depending on the application of interest. Furthermore, the internal rewards play a critical role for both reinforcement learning in the executive and the task-switch control at the same time, discussed next.

1.2.3.3 Executive

As a dominant part of the CDS, the executive consists of reinforcement learning, cognitive control (that embodies a planner, action library, a policy, and working memory), and a subsystem composed of executive memory and a classifier.

(1) Reinforcement Learning

The objective of reinforcement learning is to transform the incoming internal rewards computed in the feedback channel into an output called the value-to-go function [77]. Recognizing that the internal rewards are probabilistic, the function of reinforcement learning is therefore also defined in probabilistic terms, which would be influenced by variations in the environment from one PAC to the next.

(2) Planner and Action Library

Taking the value-to-go function as input, the planner extracts a set of prospective actions from the action library and performs several planning updates in a predictive way.

In order to account for executive attention, the reinforcement learning module and the planner are also reciprocally coupled, resulting in a local feedback loop again. From a neuroscience point-of-view, the planner picking up relevant information from the reinforcement learning represents the selective-focusing of the excitation component of attention, and reinforcement learning putting aside irrelevant information (due to the suppression of planner) represents the inhibition component. It is similar to the reciprocal coupling we have observed in the perceptor.

To be more precise, the shunt cycle accounts for top-down attention in the perceptor, followed by bottom-up attention in the executive. There will be many shunt cycles performed in each PAC as the shunt cycle is only performed within the interior of the CDS. As a result, relevant information in

both the perceptor and the executive is enhanced, while at the same time irrelevant information is diminished.

(3) Policy and Working Memory

Policy leads to decision-making, and therefore, a cognitive action. As for the working memory, it is a temporary active retention of information to be used in the short term. It consists of a limited set of past actions that is immediately relevant to the task at hand and is updated from one PAC to the next. With the immediate past action from working memory on the one hand and a set of prospective actions put forward by the planner on the other hand, the cognitive action is derived from the set of prospective actions in a probabilistic manner.

The fundamental function performed by the planner (along with the action library) and the policy (along with working memory) can be called "cognitive control", the expression of which was first used to describe cortical functions and mechanisms in cognitive neuroscience [78]. More importantly, cognitive control is the over-arching function of the executive by acting on the environment on a cycle-by-cycle basis.

However, the environment in a realistic world is prone to the unexpected occurrence of unpredicted events. Whenever a system of interest experiences such uncertainty, it is a must that cognitive control expands its functionality in order to deal with unexpected adverse events, which are collectively called risk. As the solution for tackling uncertainties, we bring into play "cognitive risk control (CRC)", which is built upon the regular cognitive control with the addition of an executive memory and a classifier [79].

(4) Executive Memory

In the human brain, the prefrontal cortex is at the highest level of the cortical executive hierarchy, representing the rules and schemas of goal-directed action [67, 80]. According to Fuster's notion of an executive memory system, the physiological activity of the executive memory supports the prefrontal cortex in establishing temporal organization of behavior, speech, and logical reasoning [81]. From an engineering perspective, the executive memory provides valuable historical references for appropriate goal-directed actions to be made in the current situation.

In a distinctive way, the executive memory for CRC is the dual of the working memory for regular cognitive control. To expand on this duality, we highlight the contextual differences between executive memory and working memory as follows: the action library of the executive memory has a large time-frame and more options, whereas the action library of the working memory is limited to the "here and now". It is also noteworthy that the executive memory and the working memory are both dynamic in their respective ways; it is therefore expected that both of them learn from their respective past experiences. Here, the past experiences refer to a record of actions that were taken and stored in the past.

As for inputs, the executive memory picks up past experiences to be used in the future irrespective of what the environmental conditions are in reality. Nonetheless, all the past experiences stored in the action library of executive memory are free from uncertainties: in the presence of uncertainty, the regular cognitive action that is perturbed will be replaced with a risk-sensitive cognitive action, which is generated by the classifier.

(5) Classifier

In the presence of uncertainty, the regular cognitive control operates under a perturbed condition and we would have a perturbed cognitive action as one of the inputs for the classifier. In a corresponding way, the executive memory selects a set of prospective past experiences that serves as the second input for the classifier. Therefore, the stage is set for the classifier to perform decision-making and produce the risk-sensitive cognitive action, which is finally applied to the environment.

1.2.3.4 Task-Switch Control

In order to alternate between regular cognitive control and the CRC in a CDS, a network of switches is formulated to prevent the perturbed cognitive action from affecting the environment as well as to facilitate the generation of risk-sensitive cognitive action. These switches are the results of addressing two completely different environmental conditions, one involving the absence of uncertainties and the other one involving their presence.

To identify the presence of uncertainties and help bring risk under control given the observables, a module called task-switch control is introduced. It manages the status of the network of switches, and therefore, regulates the inner pathways of a CDS.

At this point, we should reemphasize that this generic structure of CDS merely serves as a guideline for its use in practice. The exact composition of a specialized CDS varies from one system to another, depending on the specific application of interest.

1.2.4 Regular PAC vs. Complex PAC

Looking back to the first fundamental principle of cognition, namely the PAC, we can now elaborate on the simplistic CDS shown in Fig. 1.1 to some extent. Moreover, two types of PAC, a regular one and a complex one, are depicted in Figs. 1.2 and 1.3, respectively.

Fig. 1.2 presents a regular PAC that follows and enriches the global cycle depicted in Fig. 1.1, representing the operation of regular cognitive control in the absence of unexpected uncertainties. It is noteworthy that past experiences regarding the cognitive actions are preserved in the executive memory, and the classifier is currently non-functional.

In contrast, Fig. 1.3 illustrates a complex PAC that is much more informative in the presence of uncertainties on two accounts. First, the executive memory is now activated to provide prospective past experiences that were accumulated before. Second, the classifier will now take the role to compute a risk-sensitive cognitive action with both perturbed cognitive action and prospective past experiences at hand. In addition, the end result of risk-sensitive cognitive action will also be stored in the executive memory for future use.

Simply put, for every gain made, there is a price to pay. Compared with the regular PAC, the complex PAC is relatively more complicated, and by the same token, much more powerful in the context of information processing.

As is increasingly recognized in the modern neuroscience literature, the prefrontal cortex makes the brain a pre-adaptive system [82]. From the same viewpoint, it is not surprising to see that an engineering framework of CDS manifests the predictive-adaptation feature of the human brain. Specifically, the planner accounts for the outcome of CRC to be consistently ahead of the observables

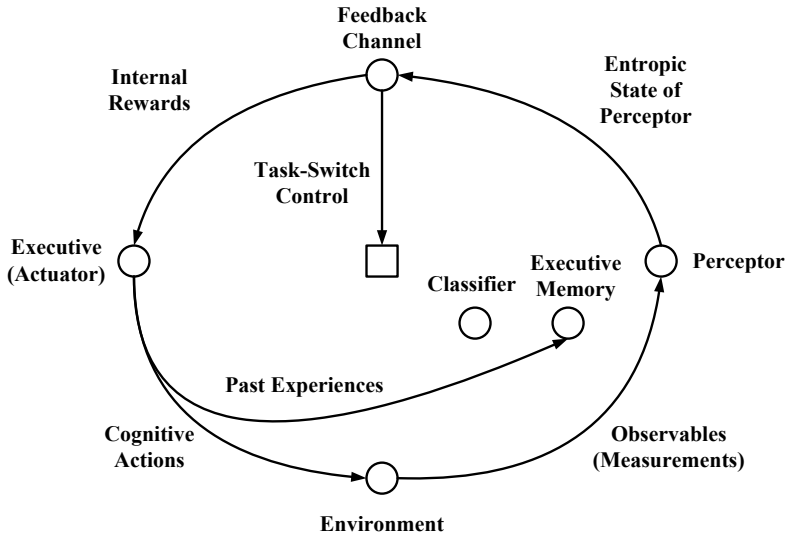

Figure 1.2: The regular PAC of a CDS.

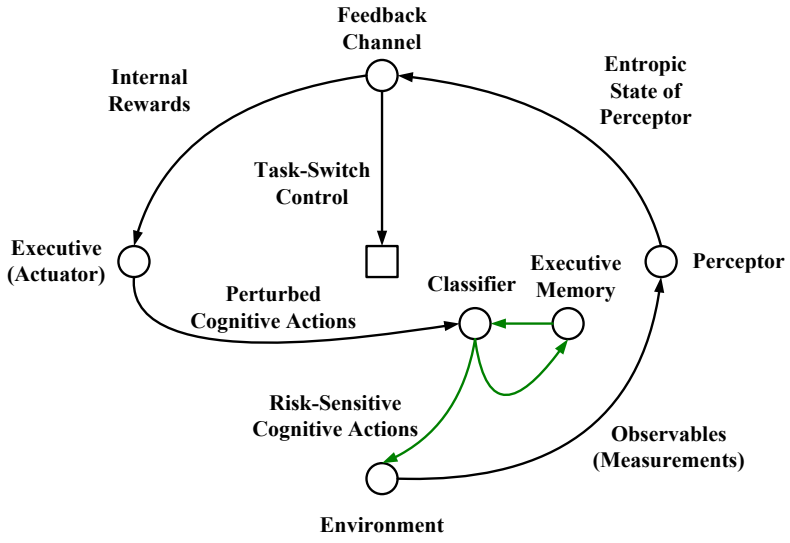

Figure 1.3: The complex PAC of a CDS.

by one PAC due to its predictive property. Besides, the working memory provides the immediate historical references, according to which cognitive action is derived, and the executive memory bypasses the influence of uncertainty and brings risk under control in an adaptive way.

1.2.5 Engineering Applications

Among other engineering systems enabled with cognition, two distinctive applications of CDS stand out over the years: cognitive radio [83] and cognitive radar [84]. In short, cognitive radio aims at facilitating

dynamic spectrum management and solving the problem of an underutilized electromagnetic spectrum, while cognitive radar aims at improved performance in both accuracy and reliability for remote-sensing applications.

1.2.5.1 Cognitive Radio

The term "cognitive radio" was coined by Joseph Mitola and Gerald Q. Maguire in 1999 [85]. From a computer science perspective, cognitive radio was envisioned to enhance the flexibility of personal wireless services through a new language called the radio knowledge representation language (RKRL), the idea of which was further studied and expanded in 2000 [86]. In 2005, a seminal paper on cognitive radio was published by Simon Haykin [83]. Viewing cognitive radio as a novel approach for improving the utilization of the radio electromagnetic spectrum from an engineering perspective, detailed expositions of signal processing and adaptive procedures that lay at the heart of cognitive radio were presented for the first time. Since then, the topic of cognitive radio has been extensively studied [87–92].

In realistic wireless communication networks, we typically find that only a small fraction of the radio spectrum assigned to legacy operators by government agencies is actually employed by primary (i.e., licensed) users [93, 94]. Indeed, if we were to scan portions of the radio spectrum including the revenue-rich urban areas, we would find that: 1) some frequency bands in the spectrum are largely unoccupied most of the time; 2) some other frequency bands are only partially occupied; and 3) the remaining frequency bands are heavily used. The underutilized subbands of the spectrum are commonly referred to as spectrum holes [95, 96].

The function of a cognitive radio may then be summarized as follows [59]:

(i) The radio receiver is equipped with a radio scene analyzer, the purpose of which is to identify where the spectrum holes are located at a particular point in time and space.

(ii) Through an external feedback link from the receiver to the transmitter, the information on spectrum holes is then passed to the radio transmitter, which is equipped with a dynamic spectrum manager and transmit-power controller. The function of the transmitter is to allocate the spectrum holes among multiple secondary (i.e., cognitive radio) users in accordance with prioritized needs.

Therefore, cognitive radio offers a new way of thinking on how to promote efficient use of the radio spectrum by exploiting the existence of spectrum holes. From a different angle, it can be seen that CDS is well suited for the engine of complex wireless communication networks. The perceptor of CDS can be responsible for modeling spectrum environment and building the dynamic-interference map, based on which the executive will perform decision-making and generate cognitive actions to address the resource-allocation issues [97].

1.2.5.2 Cognitive Radar

The term "cognitive radar" was described for the first time by Simon Haykin in 2006 [84]. Generally, radar is a remote-sensing system with numerous well-established applications in surveillance, tracking,

and imaging of targets, just to name a few [98]. Cognitive radars are systems based on the PAC for cognition that senses the environment, learns relevant information from it about the target and the background, and then adapts the radar sensor to optimally satisfy the needs of the mission according to a desired goal [99, 100]. The feature of cognition provides the basis for enabling a new generation of radar systems with reliable and accurate tracking capability that is beyond the reach of traditional radar systems [101, 102].

Specifically, the function of the receiver in a radar system is to produce an estimate of the state of an unknown target located somewhere in the environment by processing a sequence of observables dependent on the target state. In effect, perception of the environment takes the form of state estimation. As for the transmitter in the system, its function is to adaptively select a transmitted waveform that illuminates the environment in the best manner possible. In target detection, the issue of interest is to decide as reliably as possible whether a target is present or not in the observables. In target tracking, on the other hand, the issue of interest is to estimate the target parameters (e.g. range and velocity) as accurately as possible [59, 103].

Three ingredients are basic to the constitution of cognitive radar [84]:

(i) Intelligent signal processing, which builds on learning through interactions (i.e., experiences) of the radar with the surrounding environment.

(ii) Feedback from the receiver to the transmitter, which is a facilitator of intelligence.

(iii) Preservation of the information content of radar returns and adjustment of the transmitted signals in an intelligent manner.

All three of these ingredients feature in the echo-location system of a bat [104, 105], which may be viewed as a physical realization (albeit in neurobiological terms) of cognitive radar. The bat is endowed with the ability to build up its own rules of behavior over the course of time, through what we usually call "experience". To be more precise, experience, gained through the bat's interactions with the environment, is built up over time with the development continuing well beyond birth. Simply put, the "developing" nervous system of a bat, or for that matter a human, is synonymous with a plastic brain: plasticity permits the developing nervous system to adapt to its surrounding environment [71]. The importance and usefulness of experience will be further discussed in this thesis later on.

For a more detailed discussion on the engineering applications of cognitive radio and cognitive radar, the interested reader is referred to [59] and the references therein.

1.3 Research Motivation and Objectives

The introduction on CAVs has revealed that there are a number of risk-related concerns to be addressed before CAVs' large-scale manufacturing and full commercialization are possible. Among others, the potential threats of motion perturbation and jamming attacks are extremely critical to the survival of CAV networks and urgently need effective countermeasures, which is the main motivation for conducting this research.

Fortunately, the recent development of CDS has provided a very powerful research tool to study complex systems operating in an open and possibly adversarial environment. To address the aforementioned problems, the primary research objective of this thesis is to apply CDS to CAV networks with emphasis on improved driving safety and system security. A number of secondary objectives which will aid in achieving the primary objective include answering the following questions:

(i) What kind of potential threats would prevail in a CAV network and what difference will CDS make?

(ii) How can CDS and CRC be of help for vehicular radar systems in the face of motion perturbation?

(iii) How can CDS and CRC be of help for vehicular communication systems in the face of jamming attacks?

(iv) Can we make further improvements when radar and communication systems are jointly considered?

1.4 Research Outline

Fig. 1.4 shows the research outline of the thesis. The main body of this thesis can be briefly described as a theoretical overview followed by three technical works (on different applications).

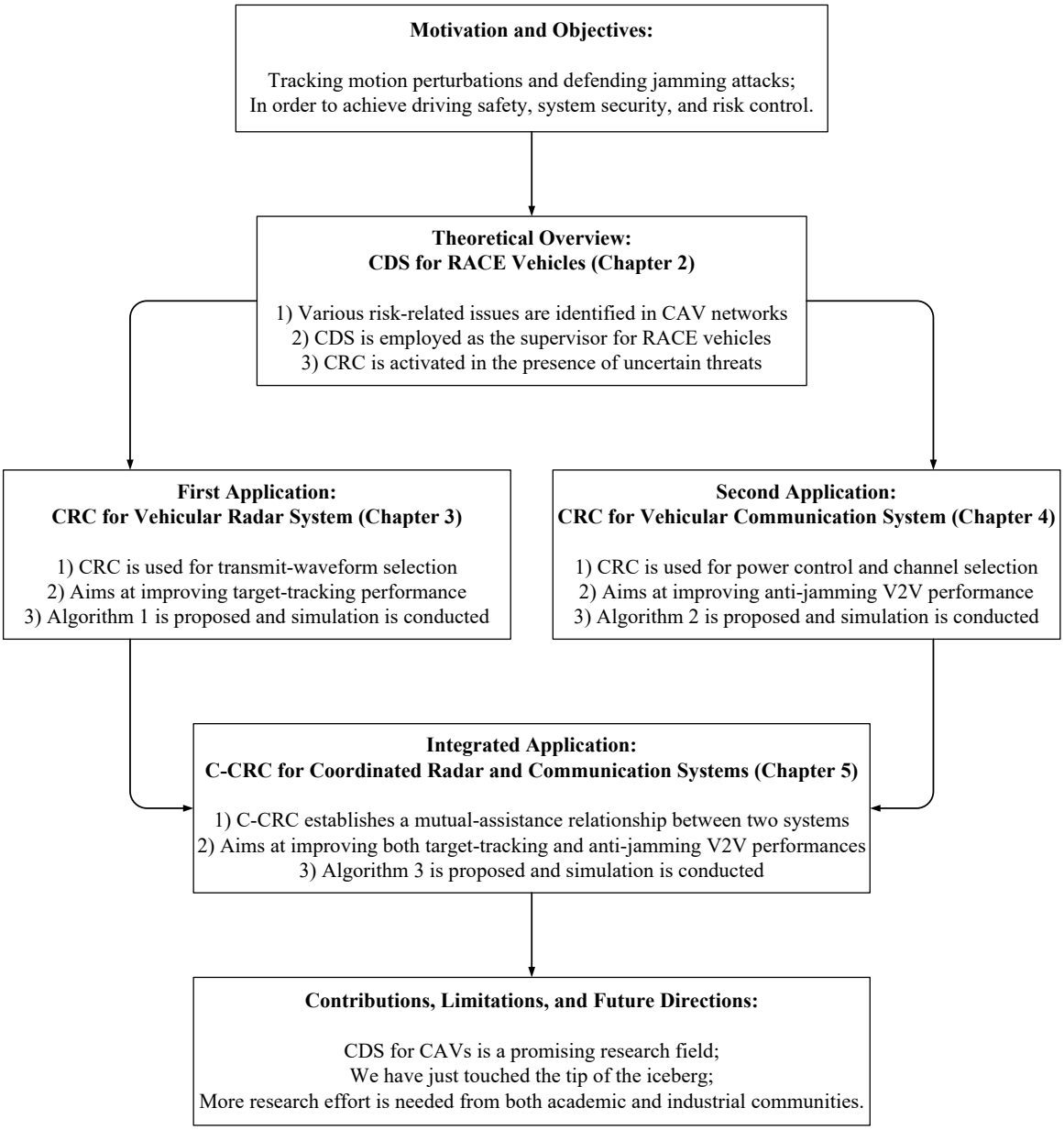

Figure 1.4: Research outline of the thesis.

1.5 Thesis Organization

This thesis is composed of the following chapters:

Chapter 1 provides an introduction about the important concepts of CAV and CDS, discusses the research motivation and associated objectives, presents the research outline, and describes the overall organization of this thesis.

Chapter 2 provides a theoretical overview mainly about how the CDS can be of use for CAVs.

This chapter is more of a high-level tutorial style, which presents a general picture of this research area and lays down the foundation for subsequent studies. To the best of the author's knowledge, this is the first theoretical work that integrates the research tool of CDS with the engineering application of CAVs.

Chapter 3 proposes to employ the CRC for transmit-waveform selection in vehicular radar systems. Focusing on the improvement of robust target-tracking performance, this chapter studies a vehicular radar system, which is the first application for CRC investigated in this thesis. To the best of the author's knowledge, the scholarly work presented herein is the first experimental work of CRC being applied to a practical vehicular system.

Chapter 4 proposes to employ the CRC for power control and channel selection in CAV networks. Focusing on the improvement of anti-jamming V2V performance, this chapter studies a vehicular communication system, which is the second application for CRC investigated in this thesis. To the best of the author's knowledge, the scholarly work presented herein is the first experimental work on V2V communication that involves anti-jamming, power control, and channel selection at the same time.

Chapter 5 introduces a new notion called coordinated cognitive risk control (C-CRC), which serves as a cognitive mediator and establishes a mutual-assistance relationship between vehicular radar and communication systems. This chapter builds upon all the research efforts made in previous chapters and takes them one step further.

Chapter 6 concludes the thesis by summarizing the work presented, its main contributions, limitations and prospective areas for future work.

Chapter 2

Cognitive Dynamic System for Future RACE Vehicles in Smart Cities: A Risk Control Perspective

2.1 Preceding Introduction

As part of the emerging people-centric Internet of Things, CAVs have the potential to reshape future transportation systems and impact the physical and/or social environment. Along with the rapid developments of CAVs also arise numerous potential threats, which would severely endanger the safety and security of CAV networks. Being a powerful research tool inspired by certain features of the human brain, in this chapter, CDS will take the role of a supervisor or system orchestrator in order to deal with risk-related issues and to provide possible countermeasures.

To the best of the author's knowledge, this is the first theoretical work that integrates the research tool of CDS with the engineering application of CAVs.

The publication included in this chapter is:

S. Feng, and S. Haykin, "Cognitive Dynamic System for Future RACE Vehicles in Smart Cities: A Risk Control Perspective," *IEEE Internet of Things Magazine*, accepted, June 2019.

The co-author's contributions to the above work include:

- Technical supervision and financial support of the study presented in this work.
- Manuscript revising and editing.

Abstract

As one of the largest applications for Internet of Things (IoT) in smart cities, Internet of Vehicles (IoV) has attracted increasing attention over the years due to its great potential for reshaping both transportation systems and human society. While connected and autonomous vehicles (CAVs) are currently being developed all over the world, they are unfortunately under various potential threats that could endanger the entire CAV network. In this article, we envision a new class of future vehicles, namely the risk-sensitive, autonomous, connected and electric (RACE) vehicles, to cope with uncertain attacks and potential threats. The safety, security and privacy issues in CAV networks are identified first. Next, the cognitive dynamic system (CDS) is introduced as the supervisor of RACE vehicles for improving and coordinating multiple vehicle-mounted systems. A special function of CDS, namely cognitive risk control (CRC), is described then in the presence of uncertain threats. Last but not least, we present the future directions and research challenges ahead.

2.2 Introduction

Internet of Things (IoT), being one of the most critical pillars of the fourth industrial revolution, has dramatically reshaped the physical-cyber-social environment that surrounds each and every one of us [106]. Under the umbrella of pervasive IoT, a lot of attention has been paid to a specific category pertaining to the Internet of Vehicles (IoV) in recent years [107]. The upgrading and modernization of transportation system in smart cities will offer a great potential to prevent traffic collisions, increase transport capacity, reduce commute costs, etc.

To fulfill the goals of IoV in smart cities, connected and autonomous vehicles (CAVs) are viewed as a promising way of the future [108, 109]. Ranging from middle-level to high-level automation, CAVs are capable of taking a course of actions in terms of adjusting steering angles and accelerating/decelerating based on the perceived environmental information with minimal (if any) human interventions. Aimed at bringing this life-changing innovation into reality, the research and development of CAVs is now one of the fiercest battlegrounds in both academic and industrial communities. Some early-stage products are already being tested and deployed worldwide in small-scale applications, while more matured and reliable technologies are urgently needed before the full commercialization is considered possible.

Another field that overlaps with CAVs is the electric vehicles (EVs), which differ from the fuel-powered vehicles in that the electricity they consume can be generated from a wide variety of renewable energy sources, and therefore, are more environment-friendly [110]. In addition, the personalized and shared features are also regarded as key factors for future intelligent vehicles. The integration of these characteristics has led to many insightful concepts: autonomous, connected and electric (ACE) vehicles, personalized ACE (PACE) vehicles, shared ACE (ACES) vehicles, to just name a few [111]. With safety-related issues being the undisputable priority of modern transportation systems, we are emboldened to envision a new class of future vehicles, namely the risk-sensitive ACE (RACE) vehicles. Here, the term risk-sensitive refers to the intrinsic attribute of being sensitive to uncertain threats in the vehicular environment and having the built-in capability to bring risk under control.

To realize this vision, it is instructive to learn lessons from the recent advances in cognitive dynamic systems (CDS) and utilize cognitive risk control (CRC) for addressing the uncertain attacks and potential threats [63], which have already begun to endanger the safety of CAV networks and will only get severer for there are more RACE vehicles yet to come. Inspired by certain features of the human brain, from the perspectives of both neuroscience and engineering, CDS is a theoretical construct designed to explain and explore the mechanisms of adaptation of a complex system to its environment. As a special function of CDS, CRC takes over and actualizes the notion of predictive adaptation learned from the prefrontal cortex when encountered with uncertain threats [82]. Acting as the supervisor or system orchestrator, CDS provides a desirable unified framework for bringing multiple vehicle-mounted systems together, which would remarkably improve the intelligence and security level of future RACE vehicles.

This article is organized as follows. After this introductory section, an analysis is presented on the safety, security and privacy issues in the CAV networks, where potential threats and possible countermeasures are discussed. Next, the CDS acting as the supervisor of RACE vehicles is described

along with several example applications, after which the functionality of CRC in the presence of uncertain threats is discussed. Then, future directions and research challenges are identified, followed by a brief summary that concludes the article.

2.3 Safety, Security, and Privacy in CAV Networks

While the connected feature of CAVs and the large-scale open nature of public roads are generally beneficial for the transportation system, they leave the system itself quite vulnerable to malicious activities, unfortunately [17]. CAV networks can easily be chosen as the attacking target by different adversaries, who may have their respective purposes, such as causing traffic accidents, stealing critical information, hijacking, etc. Moreover, with CAV networks essentially being one kind of newly rising cyber-physical systems, the threats posed on CAV networks include not only traditional types of attack in vehicular networks such as eavesdropping, but also new forms of attack like jamming signal or compromised instructions from unmanned aerial vehicles (UAVs) [112]. Fig. 2.1 has illustrated a number of potential threats that deserve our attention. It is accompanied by Tab. 2.1, which also presents the affected aspects of interest and possible countermeasures correspondingly. It should be pointed out that the list therein is not intended to be exhaustive, but rather to give an idea of the scope of possible malicious activities that could appear in CAV networks.

As a major threat in many other engineering applications, jamming is still viewed as a serious attack in CAV networks. Generally speaking, any type of vehicle-to-everything (V2X) communications can be the victim of jamming attacks, which emits high-power electromagnetic interference to make the legitimate signal unrecognizable [113]. Here, V2X refers to vehicle-to-vehicle (V2V), vehicle-to-infrastructure (V2I), vehicle-to-pedestrian (V2P), vehicle-to-device (V2D), and vehicle-to-grid (V2G), as illustrated in Fig. 2.1 (for detailed descriptions, the readers are referred to [114] and the references therein). Targeting at a CAV or regular vehicle, jamming attacks can be launched from various sources such as other vehicles, malicious devices, unauthorized UAVs or adversary personnel on the roadside. In such circumstances, the CAVs will no longer be connected and the automation level would inevitably be degraded due to insufficient information. Moreover, the missing of critical messages (for example, road-closure announcement, overtaking signal) may even lead to fatal traffic accidents. Therefore, effective anti-jamming communication mechanisms (such as spread spectrum or cognitive radio techniques) should be designed and employed to deal with this kind of attack.

A similar yet different type of attack is blinding, which mainly targets at new equipments such as LiDAR (light detection and ranging) or video cameras by shedding obtrusive light or feeding them with strong noise. Since many computer vision based technologies highly rely on these data-gathering equipments, their disruption would result in a serious failure of environmental awareness. To tackle blinding attacks, some mitigation methods can be adopted, such as signal filtering, noise reduction, or adaptive adjustment of sensing directions. As both jamming and blinding are basically one-way denial-of-service (DoS) attack, there is no information leakage from the target vehicle to the attackers. Therefore, the privacy of involved individuals (i.e., drivers, passengers, pedestrians) will not be violated directly, while the safety of individuals and the security of assets (i.e., vehicles, infrastructures, devices) would be in grave danger. From a defense point of view, these kinds of attack have emphasized the

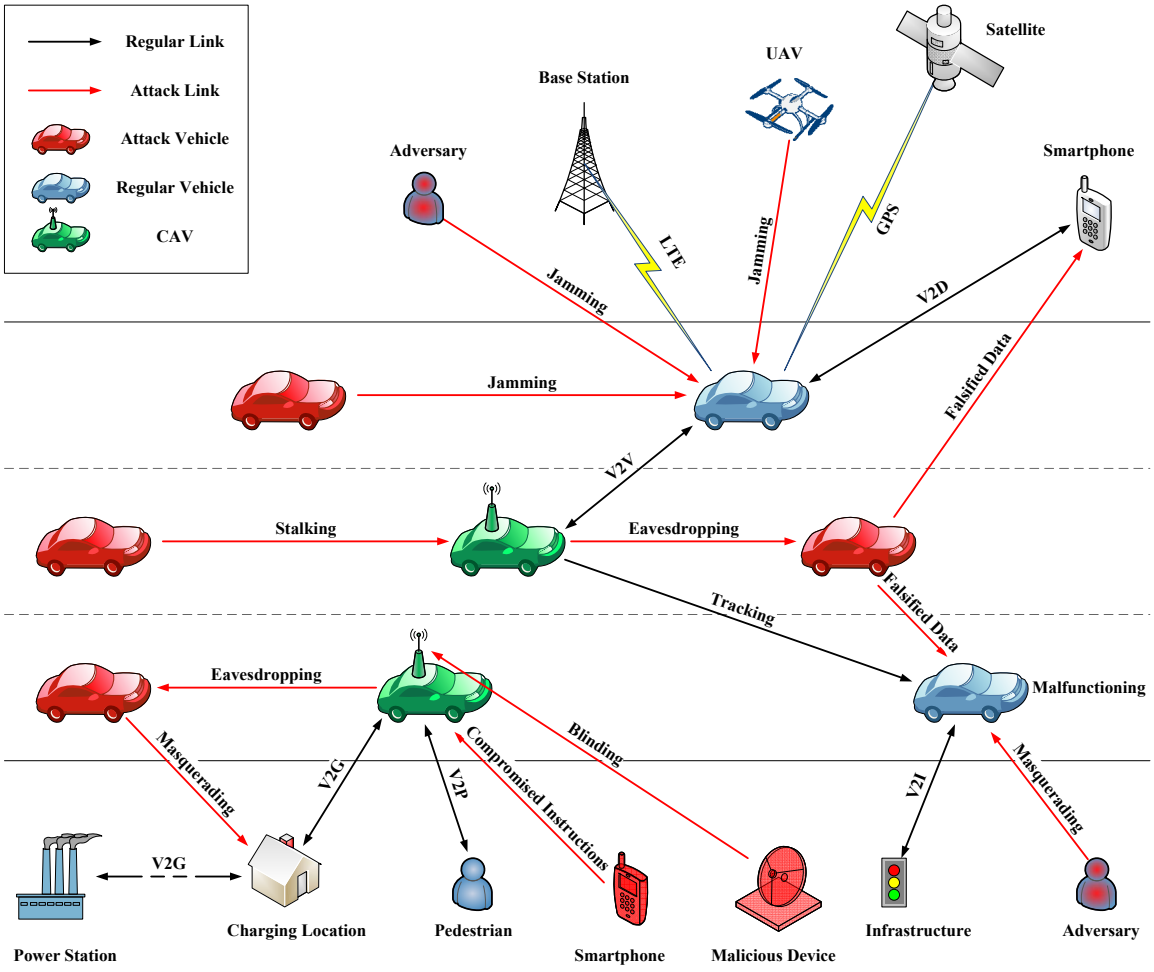

Figure 2.1: An illustration of the CAV network under various potential threats.

necessity of ensuring data availability in CAV networks.

With a huge potential of profits to be gained from the offense point of view, more sophisticated attacks will soon become common, such as compromised instructions, falsified data, masquerading/impersonation [115]. Specifically, compromised instructions are controlling signals tampered by adversaries for the purpose of gaining partial or complete control of the vehicle. Falsified data attacks are initiated at a lower level in that they do not instruct the CAV directly; rather, they exploit the internal vulnerabilities of vehicle-mounted systems and inject falsified/altered data in order to mislead the CAV into making wrong decisions by itself. Masquerading or impersonation attack takes place when an attacker pretends to be a legitimate entity to gain privileges or cause damages, for example, requesting the travel profile or exploiting vehicle repair-record. Due to the destructive capability of these sophisticated attacks, the aspects of safety, security, and privacy will all be endangered. Effective countermeasures for these attacks include digital authentication, data cleansing, digital watermarking, identification, etc., the overall objective of which is ensuring data integrity in CAV networks.

Table 2.1: Potential threats and corresponding countermeasures for safety, security, and privacy in CAV networks

Potential Threats		**Aspects of Interest**			**Possible Countermeasures**	
		Safety of individuals (Drivers/ passengers/ pedestrians)	Security of assets (Vehicles/ infrastructures/ devices)	Privacy of individuals (Activities/ preferences/ trajectories)		
Active	Jamming	✓	✓		Anti-jamming communication	Ensuring availability
	Blinding	✓	✓		Signal filtering, noise reduction	
	Compromised instructions	✓	✓	✓	Digital authentication	Ensuring integrity
	Falsified data	✓	✓	✓	Data cleansing, digital watermarking	
	Masquerading/ Impersonation	✓	✓	✓	Identification	
Passive	Eavesdropping		✓	✓	Data encryption	Ensuring confidentiality
	Stalking			✓	Anonymization	
	Misbehaving/ Malfunctioning	✓	✓		Emergency response	Ensuring reaction capability

Unlike the active attacks as discussed above, passive attacks without explicit aggressive behavior are stealthier since they are usually more difficult to be detected. One representative example is eavesdropping, which tries to intercept and record the messages being exchanged by others without the consent of involved parties. For instance, an attack vehicle may eavesdrop a private conversation, or an electricity-consumption report in V2G communication; the information illegally gathered by the attacker can then be utilized to request energy transmission from power grid using the victim vehicle's ID, which is again one form of the masquerading attack. Although eavesdropping does no physical harm to the affected individuals, it greatly violates the security of assets (such as an ACE vehicle with low battery) and privacy of the individuals, putting emphasis on the necessity of applying data encryption techniques to establish secure communications. Another example of passive attacks

is stalking, which targets valuable CAVs and gathers their detailed travel information by following them intentionally. It should be noted that the data obtained by adversaries can be used to analyze and derive behavior pattern, social activities and personal habits of involved individuals. Therefore, the potential threat of stalking makes anonymization methods useful for protecting privacy through ensuring confidentiality. Furthermore, the misbehaving or malfunctioning of a vehicle could be a result of successful attack, or just an unexpected failure in software and/or hardware. Either way, it will pose a threat on the road to other CAVs, which should be able to detect the threat immediately and make emergency responses accordingly. Ensuring reaction capability is also of great importance to enhance the safety and security for CAVs.

2.4 The Cognitive Dynamic System as the Supervisor of RACE Vehicles

In face of various potential threats in CAV networks, it is imperative to put safety and security as the first priority and accelerate the development of future RACE vehicles. To achieve that, many of the current vehicle-mounted systems should be upgraded to cope with the complex, dynamic, and adversarial vehicular environment. The CDS, being a structured engineering model and research tool inspired by certain features of the human brain, is a competent candidate for dealing with such an environment [59]. In its most simplified form, CDS consists of two major components, the perceptor on one side and the executive on the other side, with a feedback channel linking them together to form a perception-action cycle (PAC). It is the presence of feedback channel that facilitates intelligence and makes it possible for multiple vehicular systems to make intelligent decisions in the face of inevitable uncertainties in the environment. Acting as the supervisor or system orchestrator, CDS provides a desirable unified framework for bringing these vehicular systems together in an interoperable manner and having them interact with the environment jointly on a cyclic basis, as illustrated in Fig. 2.2.

Specifically, the perceptor side of a RACE vehicle takes observables and measurements from the adversarial vehicular environment through diverse input devices, such as radio receiver, radar receiver, LiDAR receiver, video cameras, photoelectric sensors, etc. Based on the incoming signals and gathered data, the environmental context (such as the communication-link quality, distance to obstacles, weather condition) is extracted and analyzed by the RACE vehicle. The results of this information processing are not only utilized by the algorithms specifically designed for controlling steering angle and vehicle velocity (which is omitted in Fig. 2.2 for simplicity), but also passed on to the executive side of a RACE vehicle through feedback channel. The executive side consists of multiple actuators, such as radio transmit-power and channel controller, radar transmit-waveform controller, LiDAR transmit-wavelength controller, camera-orientation controller, lighting controller, etc., which are reciprocally coupled with their counterparts on the perceptor side of RACE vehicles. As a result, cognitive actions (be it risk-sensitive or not) are applied to the environment and the next PAC begins.

For example, cognitive radio technology can be used in V2X communications for better utilization of spectrum resources in either DSRC (dedicated short-range communication) bands or LTE (long-term

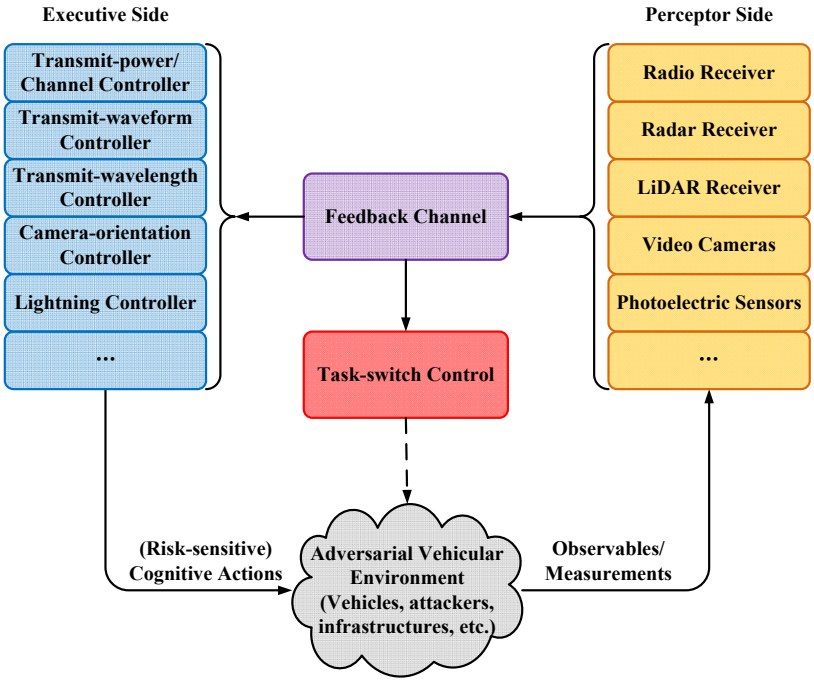

Figure 2.2: The cognitive dynamic system as the supervisor of RACE vehicles.

evolution) bands. If the received signal strength in the radio receiver is lower than the requirement for correct demodulation, it would raise the transmit power or switch to another channel on executive side accordingly without causing too much interference for other communication links. For a cognitive vehicular radar system, it is able to adjust the transmit waveform (and transmit power as well) in accordance with the distance to a target as perceived by the radar receiver, in such an adaptive way that is very much like what an echo-locating bat would do. Similarly, the LiDAR system is anticipated to have better performance in constructing three-dimensional point clouds by tuning its transmit parameters such as wavelength based on the feedback from its receiver. Due to the mobility of RACE vehicles, the environment that surrounds them is always changing. It would be beneficial if extra attention can be paid to those environmental changes that are of importance to the safety and security concerns. Therefore, the video cameras on RACE vehicles should be capable of adjusting their orientations to focus on the entities or incidents of interest, based on the feedback information extracted from the images or video clips captured by the cameras. The lighting system can also be upgraded to turn the lights on and off automatically as well as switch between main and dipped beam, which can already be found in some of the advanced driver-assistance systems (ADAS). It is noteworthy that the lighting control will depend not only on the feedback from photoelectric sensors, but also on the information regarding the quality of images or clips from video cameras. Furthermore, it should be pointed out that many other vehicular systems can also be improved and coordinated under the supervision of CDS (such as side window control, multi-speed wiper, air conditioner) for more advanced RACE vehicles.

With cognition capability being introduced to RACE vehicles by the unified framework of CDS, the uncertainties in the environment can be handled and mitigated to some extent. However, since CAV network is frequently under various potential threats with different attacking patterns, it is not sufficient for the regular cognitive control as described herein to operate on its own. Therefore, CRC is undoubtedly required to be brought into play for addressing those threats. More detailed discussions on this point are given in the next section.

2.5 Cognitive Risk Control in the Presence of Uncertain Threats

When encountered with attacks and threats in CAV networks, the perceptor of a RACE vehicle will be perturbed inevitably. The feedback channel will be occupied with abnormal values for some metrics, and therefore, the executive as discussed previously will also be perturbed. Under such circumstances, the regular cognitive control must expand its functionality to deal with the risk raised by the occurrence of uncertain threats, which naturally results in the formulation of CRC. By incorporating a new subsystem composed of executive memory and classifier into the executive, CRC serves as a special yet critical function of CDS and actualizes the concept of predictive adaptation, which is learned from the prefrontal cortex of the human brain. In order to switch between two operational modes, a mechanism called task-switch control is introduced into the CDS, which enables the provision of CRC whenever it is needed for combating uncertain threats and bringing risk under control.

The compositional architecture of CDS for RACE vehicles is illustrated in Fig. 2.3 (modified from [63]). It should be pointed out that this figure serves as a generic guideline for the practice; the exact architecture varies from one system to another, depending on the specific application of interest. In accordance with Fig. 2.3, Tab. 2.2 has listed the objective of each component in CDS and the corresponding functionalities that are improved in RACE vehicles.

Specifically, the perceptor of CDS is composed of Bayesian generative model, Bayesian filter, and entropic-information processor: Bayesian generative model characterizes the measurements originated from the adversarial vehicular environment, Bayesian filter makes estimation and prediction based on the generative posterior, while entropic-information processing is responsible for calculating the entropic state of the perceptor. Assisted by the perceptor side of RACE vehicles, the functionalities that relate to driving-scene understanding and context awareness will be significantly improved.

The feedback channel, bridging the perceptor on its right-hand side and the executive on its left-hand side, is filled with internal rewards/costs for evaluations such as the quality of service (QoS) of corresponding vehicular systems. Occupied a distinctive place within the CDS, task-switch control is mainly responsible for assessing the risk level that indicates whether the uncertain threats is present or not, and therefore, switching between two operational modes. To achieve that, two pairs of switches are formulated as shown in Fig. 2.3. When the risk level is relatively low, the first pair of switches (S1, S2) is closed and the second pair (S3, S4) is opened so that the regular cognitive control is solely functional; on the contrary, if the risk level is escalated to high due to the presence of

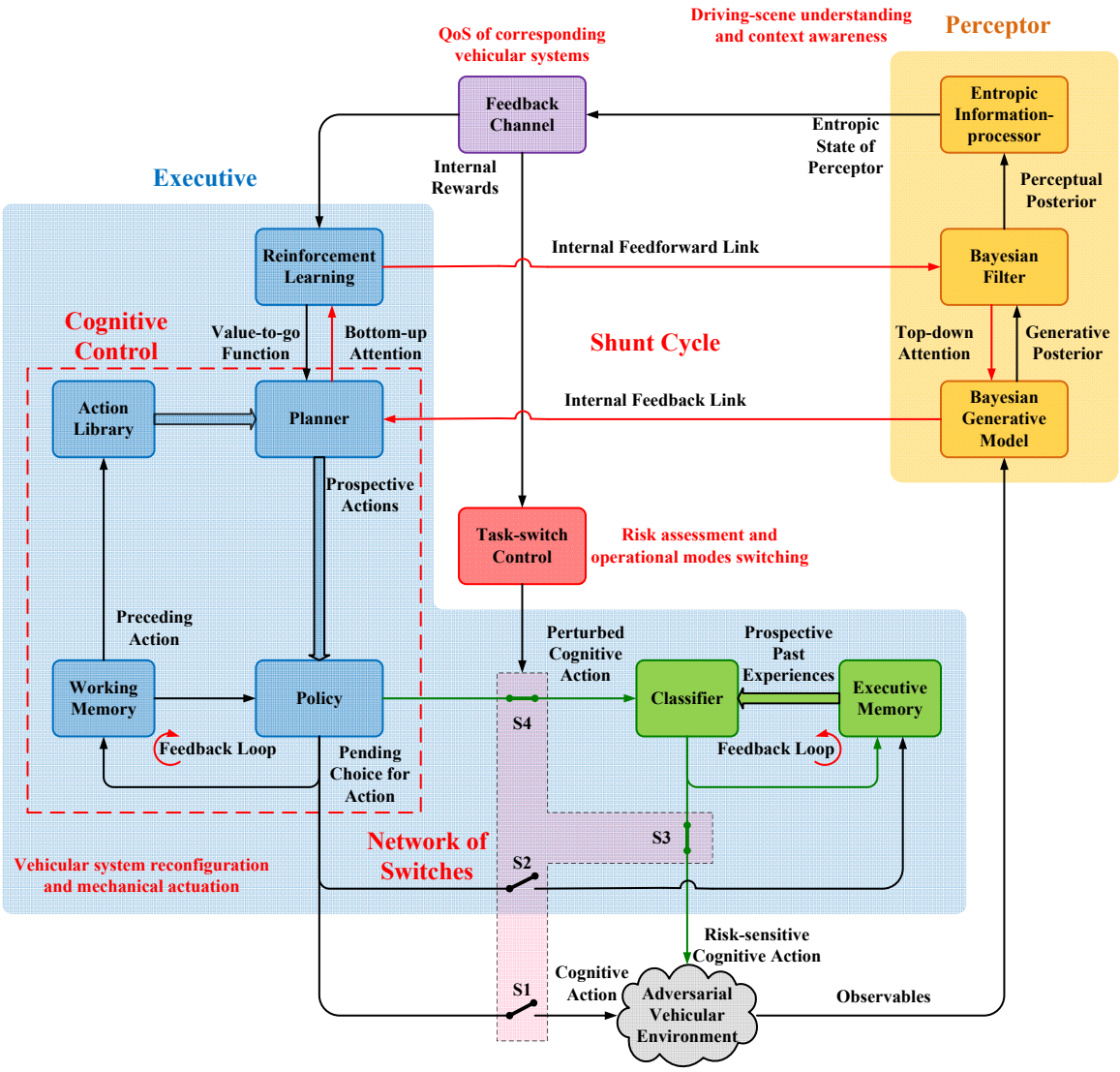

Figure 2.3: The compositional architecture of CDS for RACE vehicles.

uncertain threats, those two pairs of switches will be reversed so that CRC is now in function as the countermeasure.

As the dominant part of the CDS, the executive is composed of reinforcement learning, planner, action library, policy, working memory, executive memory, and classifier. Reinforcement learning gains knowledge of previous actions based on the feedback information, while planner extracts a set of prospective actions from the action library and initiates several shunt cycles for improved information capacity in a predictive way. When the regular cognitive control is solely functional, the policy and working memory are responsible for selecting cognitive action, which is then applied to the environment in a straightforward way. However, in the presence of uncertain threats, CRC will activate the subsystem consisting of executive memory and classifier to address the problem. As a

long-term memory stored with abundant past experiences, executive memory can provide a set of prospective past experiences for the use of current PAC. With perturbed cognitive action (provided by the policy) on one hand and the set of prospective past experiences (provided by executive memory) on the other, the classifier will then be able to pick out the risk-sensitive cognitive action, which is finally applied to the environment. It is noteworthy that the risk-sensitive cognitive action thus obtained has two distinctive features: first, it is always ahead of the perturbed observables by one PAC due to the predictive nature of planner; and second, it neutralizes the negative influence of uncertain threats due to the adaptive nature of executive memory. The theoretical originality and importance of this framework rests mainly on the application to risk control of the predictive adaptation feature of the prefrontal cortex. As a result, the functionalities that relate to vehicular system reconfiguration and mechanical actuation will be remarkably improved on the executive side. More descriptions can be found in Tab. 2.2.

For better comparison, Tab. 2.3 has listed the main differences between two operational modes for CDS acting as the supervisor of RACE vehicles. For brevity, we only need to point out that the cognitive control can be viewed as the principal function of CDS and is functional all the time, while CRC performs as a special function of CDS since it only comes into play when large part of the system is unfortunately perturbed in the presence of uncertain threats. Due to the page limit of this article, the interested readers are referred to [116] for a detailed experimental demonstration in cognitive vehicular radar systems.

Table 2.2: Objective of each component in CDS and improved functionalities in RACE vehicles

Components in CDS		**Objective of each component in CDS**	**Improved functionalities in RACE vehicles**
Adversarial vehicular environment		Multi-domain environment pertaining to vehicles, attackers, infrastructures, pedestrians, etc.	N/A
Observables/ Measurements		Measurements from various sources about the adversarial vehicular environment in multi-domains, i.e., time, space, spectrum, power, etc.	Overall observability and availability
Perceptor	Bayesian generative model	Bayesian formulation of the measurements	Cooperative spectrum sensing (CSS), dynamic interference-map generation, target tracking, 3-D data-points construction, simultaneous localization and mapping (SLAM), intruder recognition, traffic-signal detection, ambient illumination, traffic analysis, service-demand data collection, etc.
	Bayesian filtering	Bayesian estimation and prediction	
	Entropic-information processing	Information-theoretic evaluation of the perceptual posterior	
Feedback channel		Internal feedback (rewards or costs) for the entropic state of the perceptor	Channel-occupation state, interference metrics, attacking strength evaluation, quality of service (QoS) of corresponding vehicular systems
Task-switch control		Risk assessment and operational modes switching	System rescheduling and coordination for multiple vehicular systems
Executive	Reinforcement learning	Learning from trial-and-error experience	Opportunistic spectrum access (OSA), interference cancellation, target/crash avoidance, trajectory and movement planning, path updating, intruder isolation, resource reallocation, radio transmit-power and channel selection, radar transmit-waveform selection, LiDAR transmit-wavelength selection, camera-orientation control, lighting control, etc.
	Planner and action library	Predicting and learning from predictive trial-and-error experience	
	Policy and working memory	Decision-making for selecting cognitive action	
	Executive memory and classifier	Risk-sensitive decision-making for selecting risk-sensitive cognitive action	
(Risk-sensitive) Cognitive actions		System reconfiguration: transmit power/channel/waveform/ wavelength, camera orientation, lighting strength, etc.	Overall operation and reaction capability

Table 2.3: Two operational modes of CDS acting as the supervisor of RACE vehicles

Topics in CDS	**Mode I: In the Absence of Uncertain Threats**	**Mode II: In the Presence of Uncertain Threats**
Environmental observables	Regular observables	Perturbed observables
Perception-action cycle	Regular PAC	Complex PAC
Perceptor	Regular perceptor	Perturbed perceptor
Feedback channel	Regular metric values	Abnormal values for some metrics
Task-switch control	Two pairs of switches: (S1, S2) closed; (S3, S4) opened	Reversed pairs of switches: (S1, S2) opened; (S3, S4) closed
Cognitive control	Regular functionality	Perturbed and expanded functionality
Planner and action library	A number of shunt cycles for prediction	Same number of shunt cycles with timing expansion
Policy and working memory	Active	Active and perturbed
Cognitive risk control	Non-functional	Functional
Executive memory	Passive	Active
Classifier	Non-functional	Functional
Predictive adaptation	Planner for prediction and working memory for adaptation	Planner for prediction and executive memory for adaptation
Decision-maker	Policy for decision-making	Classifier for risk-sensitive decision-making
End result	Cognitive action	Risk-sensitive cognitive action

2.6 Future Directions and Research Challenges

Although the development of CAVs or ACE vehicles has made tremendous progresses recently, it is still in its nascent stage right now. Taking it one step further, the concept of RACE vehicles shows a bright prospect in the application of intelligent and secure transportation systems, which also urgently requires more research work to be done. Among many interesting topics that should draw further attention, some of the future directions and research challenges are discussed below.

(i) A universal standardization for secure V2X communications within the whole vehicular network needs to be established. While the framework of CDS is adequate for coordinating multiple vehicle-mounted systems for one RACE vehicle, the continuous interactions among RACE vehicles and many other entities require a universal standardization, which also guarantees the interoperability and extendibility for large-scale vehicular networks.

(ii) The mechanisms for harmonious coexistence of RACE vehicles and regular vehicles should be well designed. There are no stand-alones in a connected world. With different types of autonomous vehicles being deployed on the road at different stages, it will be a heterogeneous, complex, and dense network for many years to come. How to share the road with other vehicles that are enabled with different levels of automation or intelligence remains to be an open issue.

(iii) The capability of joint defense should be enhanced in order to counter with more sophisticated and possibly colluded attacks. With RACE vehicles being intelligent and collaborative in general, the potential attackers can also plot new schemes or collude with each other for causing greater damage. Therefore, building on the universal standardization and coexistence mechanisms, the CDS of a RACE vehicle will be anticipated to cooperate with other defense systems/software of another vehicle through standard interfaces, which is another research challenge yet to be solved.

(iv) More research effort could and should be made to seek new inspirations from the human brain. For example, it would be extremely instructive to exploit the lateral connections within each layer of human brain at the neuronal level, and therefore, construct a non-restricted multilayered CDS for improved information capacity. Mathematical formulations and experimental validations are also needed. There is a great opportunity to advance this promising field by learning from neuroscience, cognitive science, data science, general artificial intelligence, cybernetics, engineering practices, etc.

2.7 Conclusion

This article envisions the future RACE vehicles for intelligent transportation systems in smart cities from a risk control perspective. We first identify the safety, security and privacy issues in CAV networks. Acting as the supervisor of RACE vehicles, the CDS is then brought into play for improving and coordinating multiple vehicle-mounted systems. Next, the function of CRC is described in the presence of uncertain threats, which is followed by a brief discussion on future directions and

research challenges. The theoretical originality and importance of this framework rests mainly on the application to risk control of the predictive adaptation feature of the prefrontal cortex. We firmly believe that this article has discovered a fruitful research field, and we have just touched the tip of the iceberg. We sincerely hope that this article, with interdisciplinary perspectives, will stimulate more interests in brain-inspired CDS or RACE vehicles in both academic and industrial communities.

Chapter 3

Cognitive Risk Control for Transmit-Waveform Selection in Vehicular Radar Systems

3.1 Preceding Introduction

Among many vehicle-mounted systems, vehicular radar is an essential component for CAVs. The main responsibility of a vehicular radar system is to detect and estimate the movements of possible on-road targets, such as vehicles, pedestrians, bicyclists, etc. Aiming at the improvement of robust target-tracking performance, in this chapter, CDS and its special function of CRC are adopted to develop transmit-waveform selection method for vehicular radar systems.

To the best of the author's knowledge, the scholarly work presented herein is the first experimental work of CRC being applied to a practical vehicular system.

The publication included in this chapter is:

S. Feng, and S. Haykin, "Cognitive Risk Control for Transmit-Waveform Selection in Vehicular Radar Systems," *IEEE Transactions on Vehicular Technology*, vol. 67, no. 10, pp. 9542-9556, Oct. 2018.

The co-author's contributions to the above work include:

- Technical supervision and financial support of the study presented in this work.
- Manuscript revising and editing.

Abstract

A cognitive dynamic system (CDS) is a structured engineering model and research tool inspired by certain features of the human brain. As a special function of CDS, cognitive risk control (CRC) actualizes the concept of *predictive adaptation* to bring risk under control when encountered with unexpected uncertainty. In this paper, the first experimental demonstration of CRC is presented in the practical application of vehicular radar systems, and an algorithm for transmit-waveform selection in cognitive vehicular radar (CVR) based on CRC is proposed. During each perception-action cycle (PAC), the perceptor of CVR processes new environmental inputs and provides the processed information to the executive through feedback channel for the selection of cognitive action. With the mechanism of *task-switch control* being functional all the time, the CVR will switch to a more capable operation mode in the face of unexpected disturbances or adverse events. In such cases, a new subsystem of executive is brought into play, in which the risk-sensitive cognitive action is finally selected and applied to the environment. Simulation results have shown the robustness and effectiveness of the proposed CVR system, which can make the next-generation vehicular radars more intelligent and play an important role in future self-driving cars.

3.2 Introduction

3.2.1 Cognitive Dynamic System and Cognitive Risk Control

Cognitive risk control (CRC) is firstly introduced and described in [63] as a special function within a general framework called the cognitive dynamic system (CDS). CDS, firstly presented in [60], is constructed as an engineering system that simulates certain features of the human brain, which is the ultimate adaptive system in biology. Ever since the early applications such as cognitive radio [83] and cognitive radar [84], CDS has evolved significantly over the course of time. In its most simplified form, CDS consists of two major components, the *perceptor* on one side and the *executive* on the other, with a *feedback channel* linking them together. From the perspective of neuroscience, there are five principles of cognition as stated in *Fuster's paradigm* [65]: perception-action cycle (PAC), attention, memory, intelligence, and language (which is often put aside), upon which CDS is built step-by-step [59].

From an engineering point-of-view, cognitive control and CRC—both of which are inspired by the prefrontal cortex of human brain—aim at dealing with different situations of the environment. To be specific, cognitive control conforms well to a statistically stationary cyber-physical system; when encountered with unexpected uncertainty, cognitive control must expand its functionality to deal with the occurrence of adverse events, which naturally results in the formulation of CRC. By incorporating a new subsystem that consists of executive memory and classifier, CRC serves as a special function of CDS and actualizes the concept of *predictive adaptation* in order to bring risk under control.

Following on the model of CRC provided in [63], this paper is our latest effort to test it in a practical application where the first experimental demonstration is conducted.

3.2.2 Self-Driving Cars and Vehicular Radar Systems

The fourth industrial revolution has witnessed remarkable breakthroughs in a number of fields, including next-generation wireless communications [89, 117, 118], Internet of Things [112, 119], robotics, unmanned aerial vehicles [120, 121], self-driving cars [108, 122, 123], etc. Being part of this ongoing revolution, enormous efforts made on the development of self-driving cars by companies like General Motors, Ford, Hyundai, Waymo, and Tesla have started to blossom and bear fruit [124]. Specifically, the rise of self-driving cars is mainly attributed to the recent development of enabling technologies such as machine learning and accelerated computing, which are gradually pushing and elevating the advanced driver-assistance system (ADAS) to meet the requirement for the realization of fully autonomous vehicles [19, 109]. They are viewed as a promising solution to reduce or even eliminate vehicle accidents caused by human error, for which millions of lives can be saved every year [125]. Moreover, the benefits of self-driving cars include giving people back countless hours of time, empowering the disabled and the elderly, and cutting down on CO_2 emissions for a green world, etc.

In most of the current designs for self-driving cars, multiple sensory equipments with different merits and limitations—LiDAR (i.e., light detection and ranging), radar, radio, camera, GPS, just to name a few—are required on the vehicle to provide multi-domain information, which is then utilized by a central computer to make informed decisions about steering angles and accelerations/decelerations

[126]. For instance, LiDAR can be used for obstacle detection and representation using rotating laser beams, while radio can be used to establish vehicle-to-vehicle (V2V) communications. As one of the most important vehicle-mounted systems, vehicular radar is involved in many ADAS systems and responsible for determining the distance, velocity, and/or angle of targets [127, 128]. Therefore, a sophisticated and well-designed vehicular radar is indispensable for the development of self-driving cars.

Currently, for each individual service provided by the in-market ADAS, a different set of sensor specifications is needed. As the new services provided by ADAS are ever growing, it would lead to an intractable number of technical specifications designated to various services eventually. To address this issue, we argue that cognitive radar is a good candidate to make the vehicular radars more intelligent [103]. By actively adapting its operational parameters—such as transmit power or waveform type—according to the dynamic changes in the surrounding environment, cognitive radar is able to have continued interactions with the environment and operate in various settings of specifications, and therefore, reduce the number and types of radar sensors required on board.

Unfortunately, the driving environment is full of uncertainty and may change suddenly [17, 114]. For example, the safety can be endangered by sudden moves made by careless pedestrians, mental condition of tired drivers, imperfection of vehicle mechanicals, failure of electronic systems, severe weather condition, or uneven pavement on the road, and so on. Any of this can raise the risk dramatically and cause serious accidents, which should be dealt with in a timely and effective manner. The first and most direct approach is to improve the radar performance in the face of such disturbances. To this end, this paper focuses on the problem of transmit-waveform selection under the influence of unexpected uncertainty and proposes a new design of cognitive vehicular radar (CVR) system based on CRC.

3.2.3 Contribution and Organization

The main contributions of this paper can be summarized as follows:

(i) The architectural structure of CRC within CDS is investigated and tailored for CVR systems. Our model is based on what we know about the mechanisms that the nervous system uses to guide the organism in behavior. The theoretical originality and importance of this model rests mainly on the application to risk control of the predictive adaptation feature of the prefrontal cortex.

(ii) An algorithm for transmit-waveform selection in CVR systems is proposed based on CRC. In these systems, the transmit waveforms employed by the executive side of the CVR are regarded as the cognitive actions, which are continuously updated and improved under the influence of PACs. In addition, a smooth transition of the transmit waveform from one PAC to the next is guaranteed by taking localized attention mechanism into account, which will prolong the lifespan of radar hardware as well.

(iii) The first experimental demonstration of CRC is presented in the application of CVR systems. It is demonstrated that this new design will be able to achieve a performance comparable to

other existing designs in the absence of uncertainty, and more importantly, to make a significant improvement in the performance even when faced with unexpected disturbances or adverse events.

The rest of this paper is organized as follows: after this introductory Section I which outlines the basics of CRC, CDS, and CVR, Section II briefly describes a simple vehicle-following scenario that is of interest in this paper. Section III presents the architectural structure of CRC tailored for the application of CVR. Section IV is devoted to the proposed algorithm for transmit-waveform selection in CVR system. Section V discusses the simulation results of different algorithms. Finally, Section VI concludes this paper.

3.3 A Simple Vehicle-Following Scenario

In this section, we briefly describe a simple scenario on the road with one host vehicle following another target vehicle, which is typically used for studying the vehicle longitudinal motions in ACC [129, 130]. As shown in Fig. 3.1, the host vehicle is moving forward with velocity v_x^0 and acceleration a_x^0, while the target vehicle is moving in the same direction with velocity v_x^1 and acceleration a_x^1. The longitudinal distance and lateral distance between these two vehicles are denoted by d_x^1 and d_y^1, respectively. In addition, the host vehicle is mounted with radar sensor for keeping track of motion dynamics. Specifically, the longitudinal dynamics can be expressed as

$$\boldsymbol{x}_{k+1} = \mathbf{F}_{k+1,k}\boldsymbol{x}_k + \boldsymbol{\Gamma}_{k+1,k}u_k + \boldsymbol{w}_k, \tag{3.1}$$

with

$$\mathbf{F}_{k+1,k} = \begin{bmatrix} 1 & \delta & 0 & 0 & 0 \\ 0 & 1 & 0 & 0 & 0 \\ -\delta & -\delta^2/2 & 1 & \delta & \delta^2/2 \\ 0 & 0 & 0 & 1 & \delta \\ 0 & 0 & 0 & 0 & 1 \end{bmatrix}, \boldsymbol{\Gamma}_{k+1,k} = \begin{bmatrix} \delta \\ 0 \\ -\delta^2/2 \\ 0 \\ 0 \end{bmatrix}.$$

Here, $\boldsymbol{w}_k = \boldsymbol{\Psi}_{k+1,k}\hat{\boldsymbol{w}}_k$, with

$$\boldsymbol{\Psi}_{k+1,k} = \begin{bmatrix} 0 & \delta^2/2 & 0 & 0 & 0 \\ 0 & \delta & 0 & 0 & 0 \\ 0 & -\delta^3/6 & 0 & 0 & \delta^3/6 \\ 0 & 0 & 0 & 0 & \delta^2/2 \\ 0 & 0 & 0 & 0 & \delta \end{bmatrix}.$$

Vector $\boldsymbol{x}_k$ represents the underlying state that can be written as

$$\boldsymbol{x}_k = \left[v_{x,k}^0, a_{x,k}^0, d_{x,k}^1, v_{x,k}^1, a_{x,k}^1\right]^T.$$

The state for the next time step is denoted by $\boldsymbol{x}_{k+1}$. Scalar u_k represents a known acceleration or deceleration that can be derived from engine maps and brake characteristics of the host vehicle. $\boldsymbol{w}_k$

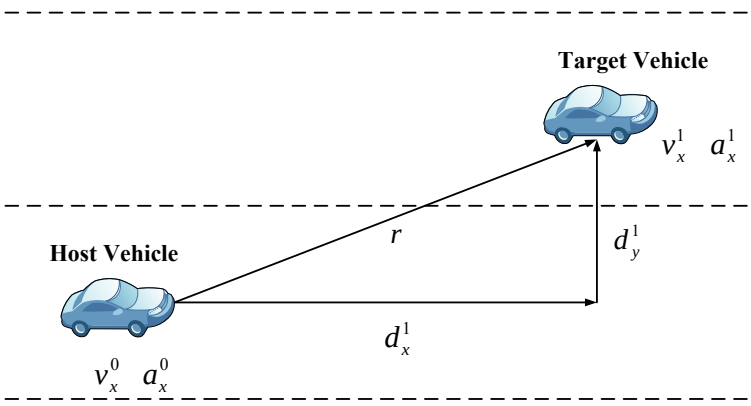

Figure 3.1: Geometry of a simple vehicle-following scenario.

denotes the additive process noise in the system with $\hat{\boldsymbol{w}}_k$ being Gaussian $\hat{\boldsymbol{w}}_k \sim \mathcal{N}\left(0, \hat{\mathbf{Q}}_{w,k}\right)$. The predictive transition matrix from one time step to the next is denoted by $\mathbf{F}_{k+1,k}$. Matrix $\boldsymbol{\Gamma}_{k+1,k}$ describes how constant u_k will affect the evolution of state vector, while matrix $\boldsymbol{\Psi}_{k+1,k}$ describes how the stochastic changes in accelerations for both vehicles will affect the system. The symbol k denotes discrete time and δ is the time step used for discretization.

Since $\hat{\boldsymbol{w}}_k$ is assumed to be zero-mean Gaussian, we can write the covariance matrix of process noise $\boldsymbol{w}_k$ as follows:

$$\begin{aligned}\mathbf{Q}_{w,k} &= \boldsymbol{\Psi}_{k+1,k}\hat{\mathbf{Q}}_{w,k}\boldsymbol{\Psi}_{k+1,k}^T \\ &= \begin{bmatrix} \delta^4/4 & \delta^3/2 & -\delta^5/12 & 0 & 0 \\ \delta^3/2 & \delta^2 & -\delta^4/6 & 0 & 0 \\ -\delta^5/12 & -\delta^4/6 & \delta^6/18 & \delta^5/12 & \delta^4/6 \\ 0 & 0 & \delta^5/12 & \delta^4/4 & \delta^3/2 \\ 0 & 0 & \delta^4/6 & \delta^3/2 & \delta^2 \end{bmatrix} \hat{\mathbf{Q}}_{w,k}.\end{aligned}$$

The diagonal of $\mathbf{Q}_{w,k}$ represents the variance of each state variable, while each of the off-diagonal entries represents the covariance between the associated two state variables. This simple model will serve as the starting point for the design of CVR, which is discussed in the next section.

3.4 Architectural Structure of Cognitive Risk Control Tailored for Cognitive Vehicular Radar

As introduced earlier, the CDS is mainly composed of two parts—the perceptor and the executive—with a feedback channel linking them together. Through interacting with the environment constantly, a PAC is formulated in the form of a global feedback loop, which functions as the backbone of the entire CDS. In this section, the perceptor is described first, followed by the feedback channel and another key element in CRC called the task-switch control. Then, the executive is discussed, for which much of the attention is given to a subsystem designated to bring risk under control.

3.4.1 Perceptor

In a generic sense, the perceptor of CDS should start with the *Bayesian generative model*, which characterizes the observables originated from the environment. However, in the case of vehicular radars, the Bayesian generative model can be omitted since the observables are usually taken in a way that is ready to be processed by Bayesian filter. Therefore, Bayesian filter is positioned at the bottom of the perceptor, as shown in Fig. 3.2.

3.4.1.1 Bayesian filter

In this paper, the well-known Kalman filter is opted for modeling the vehicle-following scenario described in the previous section, due to its features of linear state and additive Gaussian noise. With the system equation of Kalman filter presented as eq. (3.1), the measurement equation can be expressed as

$$\boldsymbol{z}_k = \mathbf{L}_k \boldsymbol{x}_k + \boldsymbol{v}_k, \tag{3.2}$$

where $\boldsymbol{z}_k$ is the observables taken at time k (i.e., in the kth cycle of PACs), $\mathbf{L}_k$ is the measurement matrix, and $\boldsymbol{v}_k$ is the measurement noise whose covariance matrix is denoted by $\mathbf{Q}_{v,k}$.

It has been shown in [131] that, for the transmit waveform obtained by combining linear frequency modulation (LFM) with Gaussian amplitude modulation, the measurement noise covariance matrix is defined by

$$\mathbf{Q}_{v,k} = \mathbf{Q}_{v,k}\left(\theta_{k-1}\right) = \begin{bmatrix} \frac{c^2\lambda^2}{2\eta} & -\frac{c^2 b\lambda^2}{2\pi f_c \eta} \\ -\frac{c^2 b\lambda^2}{2\pi f_c \eta} & \frac{c^2}{(2\pi f_c)^2 \eta}\left(\frac{1}{2\lambda^2} + 2b^2\lambda^2\right) \end{bmatrix}, \tag{3.3}$$

where θ_{k-1} denotes the parameter vector for the transmit waveform generated at cycle $k-1$, f_c and η denote the carrier frequency and the received signal-to-noise ratio (SNR), respectively. Constant c denotes the speed of light. Vector

$$\theta_{k-1} = \left[\lambda_{k-1}, b_{k-1}\right]^T,$$

where λ and b denote the duration of the Gaussian envelope for the LFM chirp transmit signal and the chirp rate of the LFM pulse, respectively. In a way, the transmitter (executive) controls accuracy of the state estimation in the receiver (perceptor) since measurement noise is dependent on the vector θ_{k-1}, which is one of the fundamental principles for designing a CVR system.

Assuming that the transmitter and the receiver of a CVR are co-located, the received signal energy depends inversely on the fourth power of the distance between two vehicles. For this reason, the received SNR η in eq. (3.3) for the target vehicle observed at distance $r = \sqrt{\left(d_x^1\right)^2 + \left(d_y^1\right)^2}$ is modeled according to

$$\eta = \left(\frac{r_0}{r}\right)^4, \tag{3.4}$$

where r_0 is the range at which 0 dB SNR is obtained.

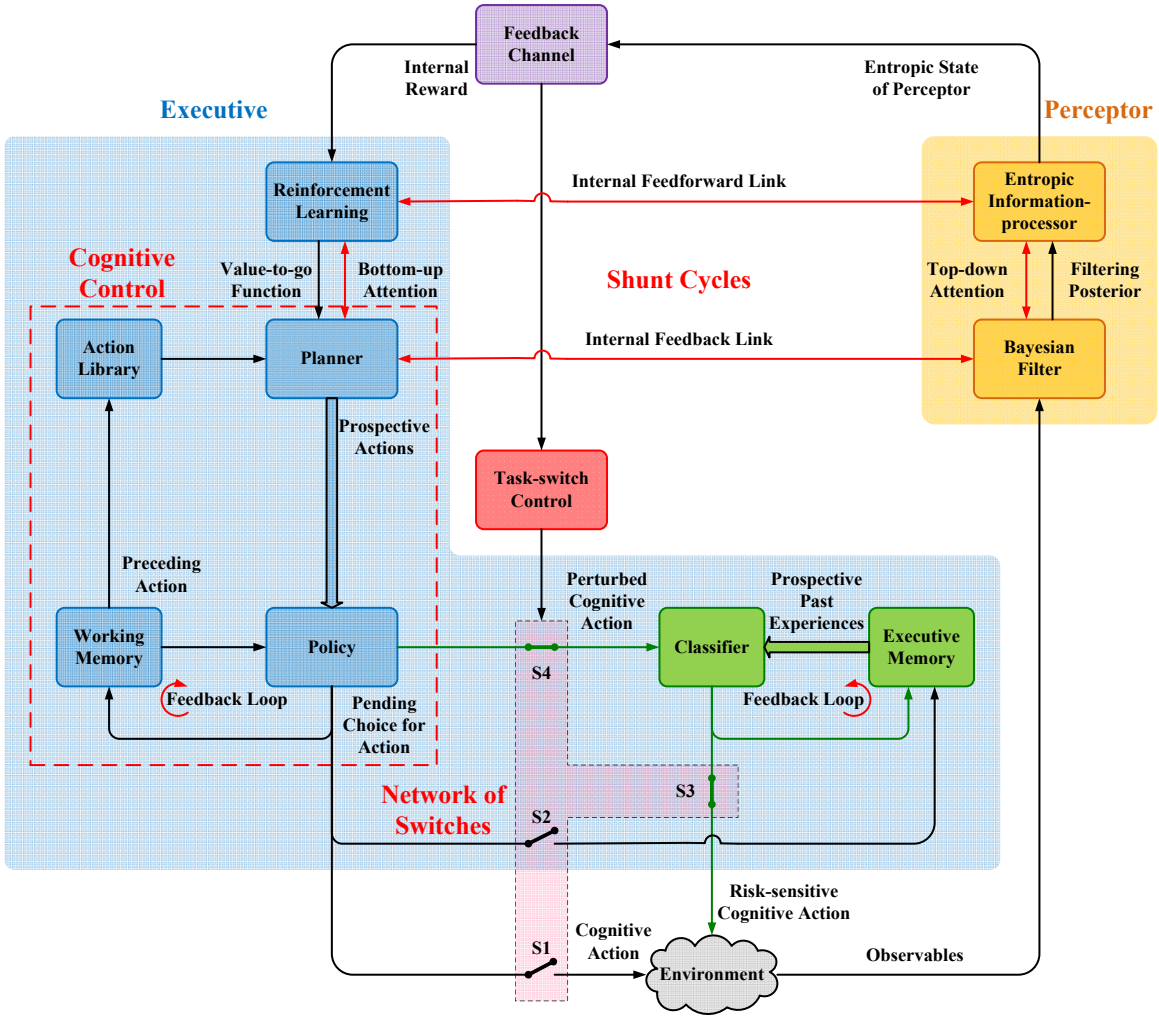

Figure 3.2: Architectural structure of cognitive risk control tailored for cognitive vehicular radar.

The process noise $\boldsymbol{w}_k$ and measurement noise $\boldsymbol{v}_k$ are both additive and assumed to be statistically independent zero-mean Gaussian processes. Assuming the velocity of the host vehicle $v^0_{x,k}$ and the longitudinal distance between two vehicles $d^1_{x,k}$ are available, measurement matrix $\mathbf{L}_k$ can then be expressed as

$$\mathbf{L}_k = \begin{bmatrix} 1 & 0 & 0 & 0 & 0 \\ 0 & 0 & 1 & 0 & 0 \end{bmatrix}.$$

With eqs. (3.1) and (3.2), a set of computational steps well formulated for the classic Kalman filter can be performed as described in [71]. In essence, the Kalman gain at time k is formulated as

$$\mathbf{G}_k = \mathbf{P}_{k|k-1}\mathbf{L}_k^T \left[\mathbf{L}_k \mathbf{P}_{k|k-1}\mathbf{L}_k^T + \mathbf{Q}_{v,k}\right]^{-1}. \tag{3.5}$$

The filtered estimate of the state at time k is written as

$$\hat{\boldsymbol{x}}_{k|k} = \hat{\boldsymbol{x}}_{k|k-1} + \mathbf{G}_k \left(\boldsymbol{z}_k - \mathbf{L}_k \hat{\boldsymbol{x}}_{k|k-1} \right), \tag{3.6}$$

given the current measurement $\boldsymbol{z}_k$, and the predicted estimate of the state at time k can be written as

$$\hat{\boldsymbol{x}}_{k+1|k} = \mathbf{F}_{k+1,k} \hat{\boldsymbol{x}}_{k|k} + \boldsymbol{\Gamma}_{k+1,k} u_k. \tag{3.7}$$

For the next iteration, we need to calculate the filtering-error covariance matrix as

$$\mathbf{P}_{k|k} = \mathbf{P}_{k|k-1} - \mathbf{G}_k \mathbf{L}_k \mathbf{P}_{k|k-1}, \tag{3.8}$$

and the predicting-error covariance matrix as

$$\mathbf{P}_{k+1|k} = \mathbf{F}_{k+1,k} \mathbf{P}_{k|k} \mathbf{F}_{k+1,k}^T + \mathbf{Q}_{w,k}. \tag{3.9}$$

The net result of Kalman filter is an output referred to as the *filtering posterior* of the system, which is optimally updated from one iteration to the next.

3.4.1.2 Entropic-information processor

The Kalman filter is to be followed by the entropic-information processor, which takes the filtering posterior as input and calculates the *entropic state of the perceptor* in a continuous cyclic manner.

Invoking Shannon's information theory [76], the entropic state at time k can be expressed as

$$h_k = \int_{\mathbb{R}} p\left(\boldsymbol{x}_k | \boldsymbol{z}_k\right) \log \frac{1}{p\left(\boldsymbol{x}_k | \boldsymbol{z}_k\right)} d\boldsymbol{x}_k, \tag{3.10}$$

where $p\left(\boldsymbol{x}_k | \boldsymbol{z}_k\right)$ is the conditional probability distribution of $\boldsymbol{x}_k$ given $\boldsymbol{z}_k$. $\mathbb{R}$ denotes the entire space where the state $\boldsymbol{x}_k$ resides.

Note that the measurement $\boldsymbol{z}_k$ is the reason for the so-called *innovation process* embedded in Kalman filter, which leads to the calculation of the filtered estimate $\hat{\boldsymbol{x}}_{k|k}$ as shown in eq. (3.6). Under such circumstances that $p\left(\boldsymbol{x}_k | \boldsymbol{z}_k\right)$ has a multivariate normal distribution, the entropic state can be written as [76, 132, 133]

$$h_k = \frac{1}{2} \log \left[(2\pi e)^n \left| \mathbf{P}_{k|k} \right| \right],$$

where $|\cdot|$ takes the determinant of a matrix. In a more general sense, the $p\left(\boldsymbol{x}_k | \boldsymbol{z}_k\right)$ essentially describes the distribution of $\boldsymbol{x}_k$ given the information on $\hat{\boldsymbol{x}}_{k|k}$, whose characteristics are also captured by the filtering-error covariance matrix $\mathbf{P}_{k|k}$. Recalling that the filtering-error covariance matrix is defined as [71]

$$\mathbf{P}_{k|k} = \mathbb{E}\left[\boldsymbol{\varepsilon}_{k|k} \boldsymbol{\varepsilon}_{k|k}^T \right],$$

with the state-filtering-error vector as

$$\boldsymbol{\varepsilon}_{k|k} = \boldsymbol{x}_k - \hat{\boldsymbol{x}}_{k|k},$$

we therefore avoid to calculate h_k in eq. (3.10) directly and opt to use a simplified expression, denoted as H_k, for the entropic state in this paper as follows:

$$H_k = \left|\mathbf{P}_{k|k}\right|. \tag{3.11}$$

As it goes on from one PAC to the next, the entropic state of the perceptor will decrease gradually due to the information gain, but never assume the value zero as there will always be imperfections within the perceptor.

3.4.2 Feedback Channel and Task-Switch Control

The feedback channel bridges the perceptor on its right-hand side and the executive on its left-hand side. It is occupied by the internal rewards, which are then used in both task-switch control and the reinforcement learning.

3.4.2.1 Feedback channel

To formulate the internal rewards, we first calculate the incremental deviation in the entropic state at time k as follows [133]:

$$\Delta_k^H = H_{k-1} - H_k, \tag{3.12}$$

where H_{k-1} and H_k are the entropic states computed at the $(k-1)$th and kth PAC, respectively. The internal reward, denoted by the symbol r_k, can now be defined as an arbitrary function of H_k and Δ_k^H as shown by

$$r_k = g_k\left(H_k, \Delta_k^H\right), \tag{3.13}$$

where $g_k(\cdot)$ is a single-valued operator. In this paper, the internal reward takes on a simple form:

$$r_k = \frac{\Delta_k^H}{H_k}. \tag{3.14}$$

Subject to the variations in the environmental condition, internal reward evaluates how good the action taken in the previous PAC is, and therefore, is always monitored by the task-switch control.

3.4.2.2 Task-switch control

Task-switch control occupies a distinctive place within the CDS and mainly deals with the raising of risk, which is imposed by the unexpected occurrence of uncertainty.

In general, uncertainty can manifest itself in many forms in mathematical models or experiments, such as parameter uncertainty, structural uncertainty, measurement uncertainty, experimental uncertainty, etc [134]. All kinds of uncertainty can result in erroneous control and undesired system

behavior. There are ways to mitigate the negative effect of uncertainty—such as incorporating more prior knowledge, or taking the average of repeated experiment results—but it will never be eliminated entirely. Taking the vehicle-following scenario described in Section II as an example, factors like the imperfection of vehicle mechanicals, the severe weather condition, or the uneven pavement on the road can all affect the evolution of the original system. Denote the influence of these disrupting factors by a new vector $\boldsymbol{m}_k$, the new system equation that is actually functioning during this disturbed period can be formulated as

$$\boldsymbol{x}_{k+1} = \mathbf{F}_{k+1,k}\boldsymbol{x}_k + \boldsymbol{\Gamma}_{k+1,k}u_k + \boldsymbol{m}_k + \boldsymbol{w}_k, \tag{3.15}$$

where $\boldsymbol{m}_k$ appears in the form of structural uncertainty. The whole CVR system is unaware of this new system equation when it comes into play, which can deteriorate the radar performance and raise the risk dramatically. Here, risk is regarded as a property of actions that affects choices among them [135]. The actions we select in the decision-making stage will have different outcomes, and therefore, determine the overall performance of the vehicular radar. By choosing those actions that are associated with lower risks, we can maintain the robustness and effectiveness of the radar system on a cyclic basis. In short, the uncertainty is inevitable and breeds risk, which fortunately can be brought under control with care.

To achieve this, the task-switch control—serving as a *watchdog*—aims at indentifying the presence of uncertainty and switching between two operation modes of CVR as needed. Two pairs of switches are formulated as shown in Fig. 3.2. When the structural uncertainty is absent, the first pair of switches (S1, S2) is closed and the second pair (S3, S4) is opened so that the CVR will operate in Mode I, which can be called with impunity the regular cognitive control. On the contrary, when the structural uncertainty is present, those two pairs of switches are reversed so that the CVR will operate in Mode II, which is the CRC instead.

For detecting the occurrence of unexpected uncertainty, the condition in the following formulation is checked:

$$\rho_k = \begin{cases} 0, & \text{if } \sum_{i=\max(1,k-L+1)}^{k} \left|\min\left[0, \operatorname{sgn}(r_i)\right]\right| < \beta \\ 1, & \text{otherwise} \end{cases}, \tag{3.16}$$

where ρ_k represents the result of detection, $\operatorname{sgn}(\cdot)$ is the sign function, r_k represents the internal reward at time k, L is the length of a window set for counting, and β denotes a predefined threshold. Eq. (3.16) shows one of many ways to count the number of negative internal rewards in the immediate past L cycles (or in all cycles if the total number is less than L). The reason for performing this check is the following: under normal circumstances, the internal rewards will not be negative continuously; when that happens, it indicates that the actions taken in the past few cycles have been severely affected by the presence of uncertainty, which imposes the necessity for switching to a more capable operation mode.

If $\rho_k = 0$—meaning the number of negative internal rewards in the immediate past L cycles is less than β—then the CVR will keep operating in Mode I. Otherwise, the CVR will switch to Mode II to invoke a subsystem for dealing with uncertainty and bringing risk under control. More discussions on this point will be given in the next subsection.

3.4.3 Executive

Computationally speaking, the executive as a whole is the dominant part of the CVR system. It consists of reinforcement learning, planner (and its action library), policy (and its working memory), executive memory, and classifier.

3.4.3.1 Reinforcement learning

With input being internal rewards from feedback channel, the desired output of reinforcement learning is the value-to-go function, which is formulated as follows [77]:

$$\begin{aligned} \boldsymbol{J}_{k-1}(c) &= \mathbb{E}^{\pi}\left[\sum_{i=0}^{\infty}\gamma^{i} r_{k+i} | c_{k-1}\right] \\ &= \mathbb{E}^{\pi}\left[r_k + \gamma r_{k+1} + \gamma^2 r_{k+2} + \cdots | c_{k-1}\right], \end{aligned} \tag{3.17}$$

where $\gamma \in [0,1)$ represents a discount factor that decreases the effect of future actions exponentially, $\mathbb{E}$ denotes the expectation operator for which the expected value is calculated using the policy distribution π. Here, the superscript π is a simplified version of the policy $\pi(c_{k-1}, c_k)$, where c_{k-1} is the immediate past action at $(k-1)$th PAC and c_k is the action to be selected at kth PAC.

From a computational viewpoint to be consistent with the CDS, it is instructive to reformulate the value-to-go function, $\boldsymbol{J}(c)$, so that it can be updated algorithmically from one PAC to the next. With this point in mind, eq. (3.17) is reformulated as follows [133]:

$$\boldsymbol{J}_{k-1}(c) \leftarrow \boldsymbol{J}_{k-1}(c) + \alpha\left[R_{k-1}(c) + \gamma \sum_{c_k} \pi_k(c_{k-1}, c_k)\boldsymbol{J}_k(c) - \boldsymbol{J}_{k-1}(c)\right], \tag{3.18}$$

where $\alpha > 0$ is the learning-rate parameter, $R_{k-1}(c) = \mathbb{E}^{\pi}[r_k | c_{k-1}]$ denotes the expected internal reward at cycle k as a result of the immediate past action c_{k-1} at cycle $k-1$, that is, $R_{k-1}(c) = r_k$. The left-pointing arrow indicates the updating of the algorithmic recursion from one PAC to the next.

3.4.3.2 Planner and policy

The function of planner is to extract a set of prospective actions from the action library on its left, and initiates several internal cycles (i.e., shunt cycles) for improved information capacity in a predictive way. While reinforcement learning is processed only once in each global PAC due to the fact that it involves one specific past action and the associated internal reward, planning is performed for a number of times to go through all the prospective actions that are selected as candidates for the current cycle.

With CVR being the practical issue of interest in this paper, we need to ensure that the action to be selected at the current cycle is a *neighbor* to the preceding selected action. In other words, the parameters used for two successive transmissions should not be much of a difference. The practical importance of a smooth transition of the transmit waveform from one PAC to the next is that it prolongs the life of the microwave devices (i.e., magnetron, klystron, or traveling-wave tube) in the

radar transmitter [103]. This localization can be viewed as one form of the *attention* mechanism, which is one of the basic principles of cognition and is widely distributed in the CVR system. The effect of localized attention mechanism will be further discussed along with the simulation results. In addition, for the sake of saving computing and energy resources, it is usually enough to formulate the set of prospective actions as a proportion of all the neighbors.

The planning can be performed in a similar way of reinforcement learning with the set of prospective actions at hand. However, one distinct difference is that there is no interaction with environment in the planning. Specifically, each prospective action c_k^j—representing a parameter vector θ_k^j for the transmit waveform—is only *virtually* applied to the environment. It means that the measurement noise covariance matrix $\mathbf{Q}_{v,k+1}^j\left(\theta_k^j\right)$ is calculated according to eq. (3.3) to reflect the hypothesized situation resulting from action c_k^j without this action actually being applied. Mathematically speaking, we then have the hypothesized Kalman gain

$$\mathbf{G}_{k+1}^j = \mathbf{P}_{k+1|k}\mathbf{L}_{k+1}^T\left[\mathbf{L}_{k+1}\mathbf{P}_{k+1|k}\mathbf{L}_{k+1}^T + \mathbf{Q}_{v,k+1}^j\right]^{-1}, \tag{3.19}$$

and the hypothesized filtering-error covariance matrix

$$\mathbf{P}_{k+1|k+1}^j = \mathbf{P}_{k+1|k} - \mathbf{G}_{k+1}^j\mathbf{L}_{k+1}\mathbf{P}_{k+1|k}, \tag{3.20}$$

which directly follow eqs. (3.5) and (3.8) for each prospective action. Here, $j = 1, 2, \cdots, N$, and N is the total number of prospective actions. The hypothesized entropic state of the perceptor can be expressed as

$$H_{k+1}^j = \left|\mathbf{P}_{k+1|k+1}^j\right|. \tag{3.21}$$

Then, the hypothesized internal reward for prospective action c_k^j is written as

$$r_{k+1}^j = \frac{\Delta_{k+1}^{H\ j}}{H_{k+1}^j}. \tag{3.22}$$

where $\Delta_{k+1}^{H\ j} = H_k - H_{k+1}^j$. Note that the entities without superscript j still represent the actual entities rather hypothesized ones. Based on the hypothesized internal rewards, the value-to-go function can be updated for the whole set of prospective actions as follows:

$$\boldsymbol{J}_k(c) \leftarrow \boldsymbol{J}_k(c) + \alpha\left[R_k^j(c) + \gamma\sum_{c_{k+1}}\pi_k(c_k, c_{k+1})\,\boldsymbol{J}_{k+1}(c) - \boldsymbol{J}_k(c)\right], \tag{3.23}$$

where $R_k^j(c) = \mathbb{E}^\pi\left[r_{k+1}^j|c_k^j\right] = r_{k+1}^j$.

The calculations through eq. (3.19) to eq. (3.23) are conducted within multiple shunt cycles, which start at the planner and involve the Bayesian filter, the entropic information-processor, and the reinforcement learning, as shown in the red bidirectional arrows in the Fig. 3.2. Just as it is in the human brain, shunt cycles get involved in both the perceptor and the executive and therefore account for all prospective actions within each PAC.

In a related matter, it is customary practice to balance the exploitation and exploration in the policy [77]. To that end, we adopt a ϵ-greedy strategy in the policy for selecting actions. For most of the time, with probability $(1-\epsilon)$, the policy exploits current knowledge to select the particular action that maximizes the value-to-go function; with a small probability ϵ, the policy selects randomly from all the actions (with equal probability), independently of the value-to-go function.

The end result of the derived policy is indeed *cognitive action*, which is readily to be applied to the environment and thus initiates the next PAC if there is no risk involved. However, in the presence of unexpected uncertainty, it is a must to bring the subsystem consisting of executive memory and classifier into play for implementing the CRC.

3.4.3.3 Executive memory and classifier

As discussed in Section III.B, eq. (3.16) can be used to evaluate whether the structural uncertainty is present or not. If $\rho_k = 0$ is what we obtained in the stage of task-switch control, it indicates that the CVR system is currently free of uncertainty and functioning normally. Therefore, the cognitive action put forward by the policy can be applied to environment directly (with switch S1 being closed) and the next PAC begins. In addition, this cognitive action will also be recorded (with switch S2 being closed) in the executive memory, which picks up all the past experiences for future use.

However, if $\rho_k = 1$, it means that the CVR system is currently under the affection of structural uncertainty and requires further measures to be taken. In such cases, the first pair of switches (S1, S2) is opened and the second pair (S3, S4) is closed, so that CVR system will operate in Mode II for the CRC. Since the perceptor, the executive (expect for this subsystem), and therefore, the cognitive action are unfortunately perturbed, we look for a new way to bypass the uncertainty and generate the so-called *risk-sensitive cognitive action*.

Essentially, executive memory is a long-term memory occupied by abundant past experiences. It can provide a limited set of prospective past experiences for the current cycle k based on some prior knowledge, such as the historical behavior of the CVR or a prior probability distribution aligned with the policy. With perturbed cognitive action on one hand and the set of prospective past experiences on the other, we introduce a new component called classifier that is responsible for *risk-sensitive decision-making* to act on the environment [136]. In this paper, the nearest neighbor classifier is adopted to pick out the particular past experience that is the closest to the perturbed cognitive action. As a result, we write

$$c_k^* = \arg\min_{c \in \hat{\mathbb{B}}} dis\left(c_k^p, c\right), \tag{3.24}$$

where c_k^p denotes the (pending and probably perturbed) cognitive action, $\hat{\mathbb{B}}$ is the set of prospective past experiences provided by the executive memory, and c_k^* represents the risk-sensitive cognitive action. Operator $dis(\cdot)$ denotes one of the distance metrics such as Euclidean distance. Finally, the risk-sensitive cognitive action c_k^*—as the best option we can find from the past experiences gained by the PAC as a result of its continued interactions with the environment—is applied to the environment itself.

Fig. 3.3 sketches out how cognitive action and risk-sensitive cognitive action are selected in conceptual terms. Each circle in the grid represents one possible action stored in the static action

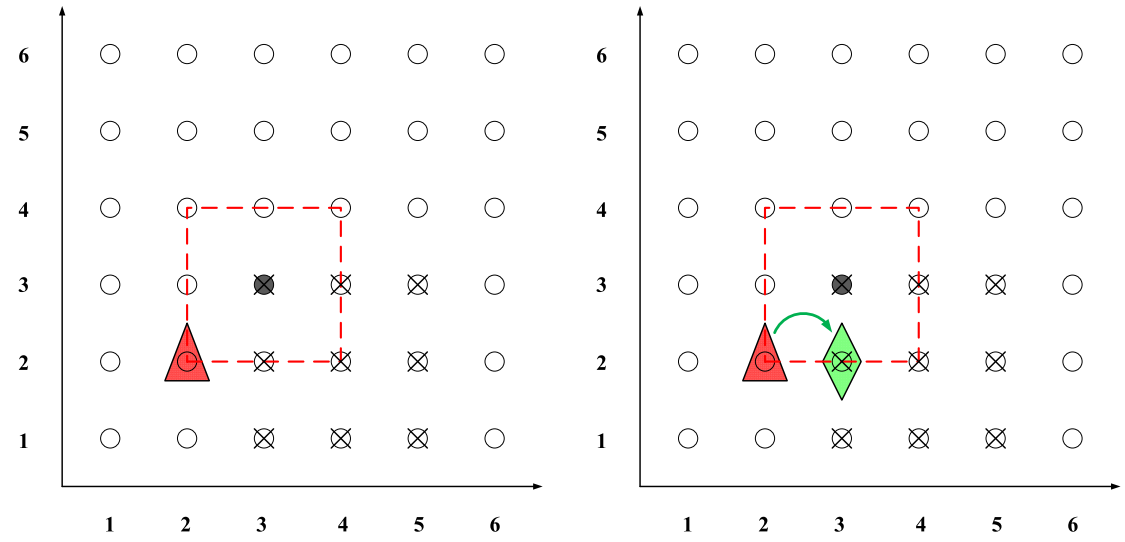

(a) Cognitive action (b) Risk-sensitive cognitive action

Figure 3.3: An illustration of the selection processes of cognitive action and risk-sensitive cognitive action.

library. The black disk represents the action applied to the environment at the preceding cycle, while the eight circles along the red dotted square represent the set of prospective actions at the current cycle. Those circles with crosses represent the set of prospective past experiences put forward by the executive memory. The red triangle represents the cognitive action selected by the policy from the ones lying on the red square. In the case of uncertainty being absent, it is already the final action for the current cycle. However, in the presence of uncertainty, one further step is needed to pick out the risk-sensitive cognitive action—represented by the green diamond that only appears in Fig. 3.3b—from the prospective past experiences that are uncertainty-free. The green arrow denotes the selecting process performed by the classifier. In this second case, the green diamond would be the final action applied to environment and the following PAC goes on.

It is noteworthy the action c_k^* will have two distinctive features after all this effort: i) consistently ahead of the observables under uncertainty by one cycle due to the predictive nature of planner, and ii) bypassing the influence of uncertainty and bringing risk under control due to the adaptive nature of executive memory. Hence, we speak of the important notion of *predictive adaptation*, which is inspired by the prefrontal cortex of human brain [82].

One last comment is in order: once the next PAC starts, there is another auxiliary approach can be taken to help counter with the uncertainty if it exists. Although both the observables and the predicted estimate of the state are perturbed, the observables taken at cycle $k+1$ are still one PAC ahead. Considering this, we may put more faith in the measurement of the state for cycle $k+1$ and introduce a confidence factor h for the following adjustment:

$$\hat{\boldsymbol{x}}_{k+1|k} \leftarrow \hat{\boldsymbol{x}}_{k+1|k} + \mathbf{L}_k^T \left[(1-h)\, \mathbf{L}_k \hat{\boldsymbol{x}}_{k+1|k} + h \boldsymbol{z}_{k+1} \right], \tag{3.25}$$

where z_{k+1} denotes the measurement at cycle $k+1$. The value of confidence factor h is naturally application dependent. Then, the Bayesian filtering comes into play and the rest procedure of processing follows. Although this adjustment has no impact on the current cycle k, it will help reduce the time for recovering from unexpected disturbances in future PACs.

3.5 Proposed Algorithm for Transmit-Waveform Selection in Cognitive Vehicular Radar

With the detailed discussions presented in previous sections, the stage is now set for an overall description of the proposed algorithm for CVR system. Algorithm 1 has outlined the complete procedure for implementing the transmit-waveform selection in one PAC, which follows the architectural structure of CRC for CVR system, as illustrated in Fig. 3.2. During the processing of each PAC, no action is required to be taken until when the final decision regarding the selected transmit-waveform—denoted as c_k—is reached at the end of that PAC. For convenience, Table 3.1 lists all the used notations in this algorithm.

Algorithm 1 Proposed Algorithm for Transmit-waveform Selection in CVR System

Input: the observables z_k, $k = 1, 2, \cdots, M$

Output: the final actions c_k

Initialization:

$\boldsymbol{x}_0$, $\hat{\boldsymbol{x}}_{1|0}$, $\mathbf{P}_{1|0}$, $w_0 = 0$, $\mathbf{A}_0 = \varnothing$, $\hat{\mathbf{A}}_0 = \varnothing$, $\mathbf{B}_0 = \varnothing$, $\hat{\mathbf{B}}_0 = \varnothing$

$c_0 \leftarrow$ an action randomly selected from $\mathbf{C}$

Apply c_0 to the environment

---

for $k = 1$ to M **do**

  Take observable z_k

  Updating:

  Calculate $\hat{\boldsymbol{x}}_{k|k}$ and $\mathbf{P}_{k|k}$

  Predicting:

  Calculate $\hat{\boldsymbol{x}}_{k+1|k}$ and $\mathbf{P}_{k+1|k}$

  Entropic-information processing:

  Calculate H_k

  Internal rewards calculating:

  Calculate r_k

  Task-switch control:

  Calculate ρ_k

  if $\rho_k = 0$ **then**

    Close (S1, S2) and open (S3, S4), i.e., Mode I

else
  Close (S3, S4) and open (S1, S2), i.e., Mode II
end if

Learning:
Update $\boldsymbol{J}_{k-1}(c)$
Planning:
Localize $\mathbf{A}_k$ according to c_{k-1}
Generate $\hat{\mathbf{A}}_k$ randomly from $\mathbf{A}_k$, $\left|\hat{\mathbf{A}}_k\right| = N$
for $j = 1$ to N **do**
  Apply c_k^j virtually ($c_k^j \in \hat{\mathbf{A}}_k$)
  Calculate $\mathbf{P}_{k+1|k+1}^j$
  Calculate H_{k+1}^j
  Calculate r_{k+1}^j
  Update $\boldsymbol{J}_k(c)$
end for
Policy:
Update π by $\boldsymbol{J}(c)$
Select the cognitive action c_k^p based on π
Risk control:
if $\rho_k = 0$ **then**
  $\mathbf{B}_k \leftarrow \mathbf{B}_k \cup \{c_k^p\}$
else
  Generate $\hat{\mathbf{B}}_k$ from $\mathbf{B}_k$
  Select the risk-sensitive cognitive action c_k^*
  Adjust $\hat{\boldsymbol{x}}_{k+1|k}$
end if
Final action:
$c_k = (1 - \rho_k) \cdot c_k^p + \rho_k \cdot c_k^*$
Apply c_k to the environment
end for

Table 3.1: Summation of Used Notations

Notation	Explanation
M	the total number of PACs
k	the time step for PACs
N	the total number of shunt cycles within one PAC
j	the time step for shunt cycles within one PAC
$\mathbf{C}$	the set of all possible actions stored in the static action library
$\mathbf{A}_k$	the set of all neighbors of the preceding action
$\hat{\mathbf{A}}_k$	the set of prospective actions for planning at the current PAC_k
$\mathbf{B}_k$	the set of all past experiences stored in the executive memory
$\hat{\mathbf{B}}_k$	the set of prospective past experiences at the current PAC_k
$\boldsymbol{x}_k$	the true state at time k
$\boldsymbol{z}_k$	the observables taken at time k
$\hat{\boldsymbol{x}}_{k\|k}$	the filtered estimate of the state at time k
$\mathbf{P}_{k\|k}$	the filtering-error covariance matrix
$\hat{\boldsymbol{x}}_{k+1\|k}$	the predicted estimate of the state at time k
$\mathbf{P}_{k+1\|k}$	the predicting-error covariance matrix
H_k	the entropic state of the perceptor at time k
r_k	the internal reward at time k
L	the length of window for counting
β	the predefined threshold
ρ_k	the result of detection
$\boldsymbol{J}(c)$	the value-to-go function
π	the policy distribution
$\mathbf{P}^j_{k+1\|k+1}$	the hypothesized filtering-error covariance matrix
H^j_{k+1}	the hypothesized entropic state
r^j_{k+1}	the hypothesized internal reward
c^j_k	the jth prospective action
c^p_k	the (pending and probably perturbed) cognitive action
c^*_k	the risk-sensitive cognitive action
c_k	the final action

It should be pointed out that in computational terms insofar as the transmit-waveform selection is concerned, the implementation of CRC would bring additional overhead. The increased complexity can be easily seen in a simplified format of what the structure could be, as depicted in Fig. 3.4 [63].

(i) In the absence of unexpected uncertainty, Fig. 3.4a shows a regular PAC that follows the

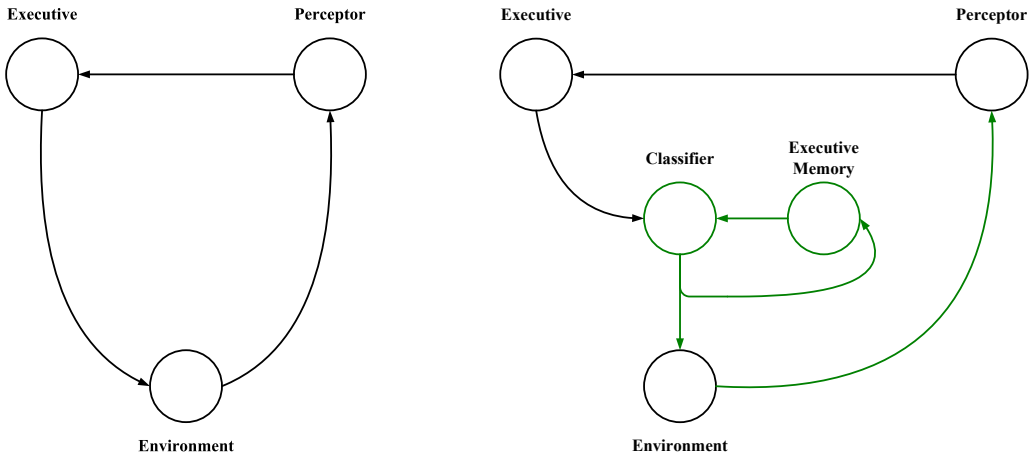

(a) Regular PAC (b) Complex PAC

Figure 3.4: Regular PAC in the absence of unexpected uncertainty, compared with complex PAC in the presence of unexpected uncertainty.

ordinary global cycle. In such cases, cognitive control is functional on its own.

(ii) In direct contrast with respect to Fig. 3.4a, Fig. 3.4b illustrates a complex PAC that is much more informative in the presence of unexpected uncertainty on two accounts. First, the executive memory is now active in order to provide prospective past experiences that are accumulated before. Second, the classifier will now take the role to compute the risk-sensitive cognitive action with both perturbed cognitive action and prospective past experiences at hand.

Simply put, for every gain made, there is a price to pay. Compared with the methods that are not involved with CRC, the proposed algorithm is relatively more complicated, and for the same token, much more powerful in the context of information processing.

3.6 Simulation Results

In this section, simulation results are presented to compare the performance of proposed algorithm for CVR system with other algorithms, as shown from Fig. 3.5 to Fig. 3.12.

Specifically, the curve of "Q" shows the vehicular radar based on traditional Q-learning algorithm described in [77], "CC" shows the vehicular radar based on regular cognitive control algorithm presented in [133], and "CRC" shows the CVR based on the proposed CRC algorithm. Accordingly, the curves of "Q-ATT", "CC-ATT", and "CRC-ATT" represent each of these three designs with the attention mechanism (as discussed in Section III.C) being taken into account, respectively. The curve of "FTW" shows the vehicular radar with fixed transmit-waveform as a reference. MATLAB is used for the simulations.

3.6.1 Radar Configurations and Parameter Settings

For the vehicle-following scenario described in Section II, the simulations are performed with two vehicles moving in adjacent lanes. The width of lane is set to be $d_y^1 = 3$ m and vehicles are assumed to be positioned in the middle of each lane. A millimeter-wave radar is mounted on the host vehicle. The carrier frequency of the transmitted radar signal is $f_c = 77$ GHz. Linear frequency modulation is adopted with both up-sweep and down-sweep chirps, which compose the (waveform) action library with

$$\Theta = \{\lambda \in [10e\text{-}6, 300e\text{-}6], b \in [-300e8, 300e8]\},$$

and grid step-size $\Delta\lambda = 10e$-6 and $\Delta b = 20e8$. For generality, the parameter vector θ_f for the radar with fixed transmit-waveform is randomly selected at the beginning of each running time and kept fixed thereafter. The bandwidth of transmitted signal is set to be 5 MHz. The range is set to be $r_0 = 2$ km, at which 0 dB SNR is received. The number of prospective actions considered in the planning stage is set to be $N = 10$ for all learning algorithms. The speed of light is $c = 2.998 \times 10^8$ m/s. The known acceleration derived from vehicle mechanics is set to be $u_k = 0$ for simplicity. The learning rate is $\alpha = 0.1$, and the discount factor is $\gamma = 0.5$. The greedy factor is set to be $\epsilon = 0.05$. The confidence factor is $h = 0.5$. For those algorithms that are equipped with attention mechanism, the neighborhood range for planning is set to be $n_r = 3$. The length of window for counting is $L = 5$ and the associated threshold is $\beta = 3$.

Without loss of generality, the true initial state of the vehicle-following problem is set to be

$$\boldsymbol{x}_0 = \left[80 \text{ km/h}, 3 \text{ m/s}^2, 400 \text{ m}, 70 \text{ km/h}, 2.5 \text{ m/s}^2\right],$$

the estimation of initial state and its covariance matrix are assumed to be

$$\hat{\boldsymbol{x}}_{1|0} = \left[75 \text{ km/h}, 0 \text{ m/s}^2, 500 \text{ m}, 65 \text{ km/h}, 0 \text{ m/s}^2\right],$$

$$\mathbf{P}_{1|0} = \text{diag}\left(\left[10^3, 1, 10^3, 10^3, 1\right]\right).$$

In this paper, the source of risk is considered to be the unexpected occurrence of structural uncertainty. The unknown vector $\boldsymbol{m}_k$ denoting the imposed disturbance is $\boldsymbol{m}_k \sim \mathcal{N}\left(0, \mathbf{Q}_{m,k}\right)$ in the perturbed system equation with $\mathbf{Q}_{m,k} = \text{diag}\left(\left[1, 1, 10^2, 1, 1\right]\right)$. It starts at 2.1s and ends at 3s, with the entire period for the experiment being set to 10s. The sampling rate is set to be $\mathrm{T}_s = 100$ ms and the simulations are conducted for $S = 50$ Monte Carlo runs.

3.6.2 Evaluation Metric and Performance Comparison

For the performance comparison, the metric of root mean-square error (RMSE) is used to evaluate the performance of different algorithms [71]. In spite of its simplicity, RMSE is effective to capture the deviations in the achieved results. Also, it is rather efficient in that its complexity follows a linear law with respect to the number of parameters of interest. Specifically, the RMSE for velocity v_x^0 is defined as

$$\mathrm{RMSE}\left(v_x^0\right) = \sqrt{\frac{1}{S}\sum_{n=1}^{S}\left(v_{x,k}^0 - \hat{v}_{x,k}^0\right)^2}, \tag{3.26}$$

where $v_{x,k}^0$ and $\hat{v}_{x,k}^0$ represent the true and filtered velocity for the host vehicle at cycle k, respectively. In a similar manner, the RMSE for other variables can also be defined and evaluated.

3.6.2.1 In the absence of unexpected uncertainty

As described earlier in Section III. B, there will be no risk involved when the CVR system operates normally, following the ordinary vehicle-dynamics model. Figs. 3.5-3.8 have shown the performance of different tracking algorithms in the absence of unexpected structural uncertainty.

In the five subfigures of Fig. 3.5, the RMSE for each element in the state vector is given, respectively. It is obvious that all algorithms can achieve a relatively low level of error for each element, except for the "FTW" design with the fixed transmit-waveform. This demonstrates that the learning algorithms—be it Q learning, cognitive control, or CRC—embedded in the executive will result in better choices of actions. With the parameter vector θ of transmit waveform being selected and adjusted according to the varying situation of surrounding environment, the measurement noise is reduced effectively, and therefore, the overall RMSE decreases.

It is noteworthy that in Fig. 3.5, the curves of "Q", "CC", and "CRC" almost coincide with one another and reach a steady state within 2s. Meanwhile, the curves of "Q-ATT", "CC-ATT", and "CRC-ATT" have similar performance, which will also reach the same steady state but in a slower fashion. The reason is that the algorithms of "Q-ATT", "CC-ATT", and "CRC-ATT" have been equipped with the attention mechanism. That is, they focus on a localized neighborhood instead of a global grid for selecting the cognitive actions, which will require more time (about 5s) to converge. By purposely confining the prospective actions for the current PAC to be the neighbors of the action selected in the preceding PAC, the physical life of the vehicle-mounted radar would last longer at the cost of slower convergence rate.

For better demonstration, Fig. 3.6 shows the sets of neighbors considered in the planning stage for "Q-ATT", "CC-ATT", and "CRC-ATT" algorithms. In the grid, each of the blue squares represents an action, i.e., a specific value for the parameter vector of transmit-waveform. Take "CRC-ATT" algorithm as an example, the red star marker represents the action selected at the preceding PAC. The red rectangular covers all the neighbors of the preceding action within a range of $n_r = 3$. For that particular single run showed in Fig. 3.6, the length of envelop $\lambda^* \in [160e\text{-}6, 220e\text{-}6]$ and the chirp rate $b^* \in [120e8, 240e8]$. However, not all the neighbors are viewed as prospective actions. Only a subset of $N = 10$ neighbors, as depicted in green circles within the red rectangular area, are randomly selected to go through the planning stage. It is foreseeable that the cognitive action for the current PAC will be one of those green circles, which will then serve as the new red star marker and it continues on.

Fig. 3.7 shows how the entropic state for each algorithm changes with PACs going on. A common phenomenon for all the radar designs is that the entropic state drops rapidly at the beginning and then slows down gradually. Besides, we can see that the entropic states of "Q-ATT", "CC-ATT", and "CRC-ATT" algorithms are higher than that of their counterparts without attention, while the

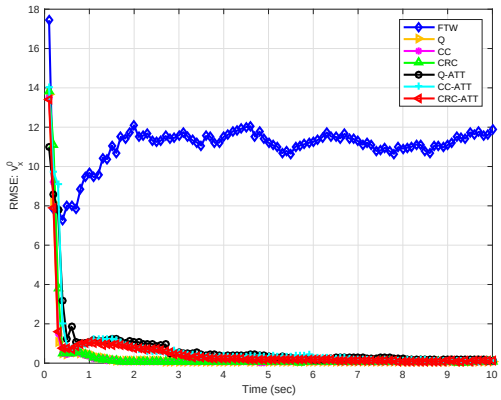

(a) RMSE for the velocity of the host vehicle v_x^0

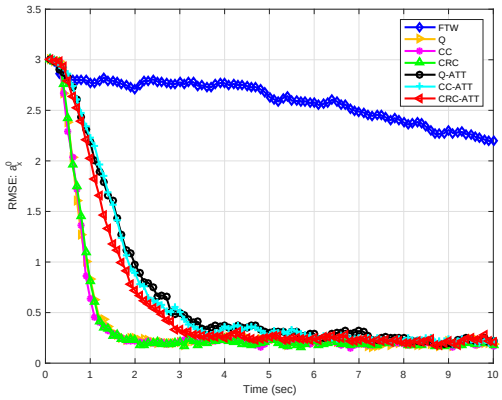

(b) RMSE for the acceleration of the host vehicle a_x^0

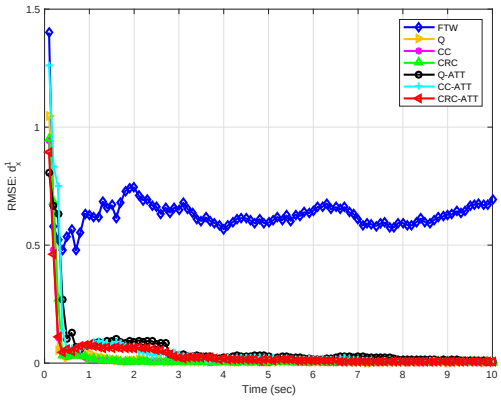

(c) RMSE for the longitudinal distance between two vehicles d_x^1

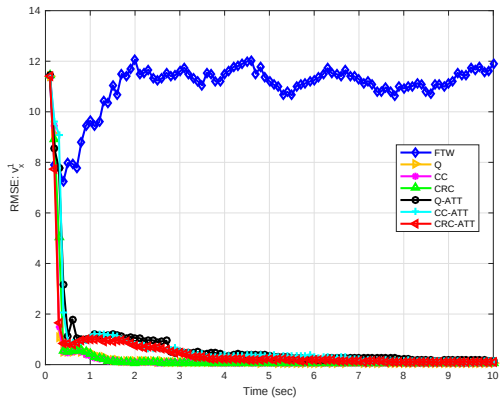

(d) RMSE for the velocity of the target vehicle v_x^1

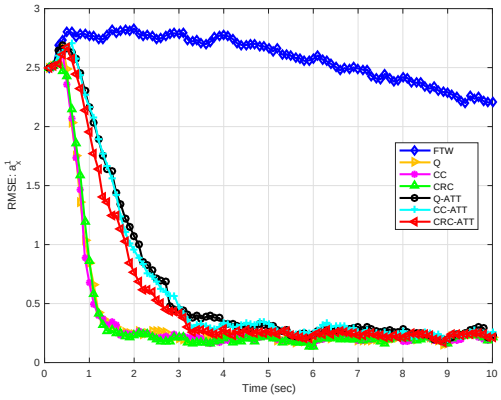

(e) RMSE for the acceleration of the target vehicle a_x^1

Figure 3.5: The RMSE for each element in the state vector (in the absence of unexpected uncertainty).

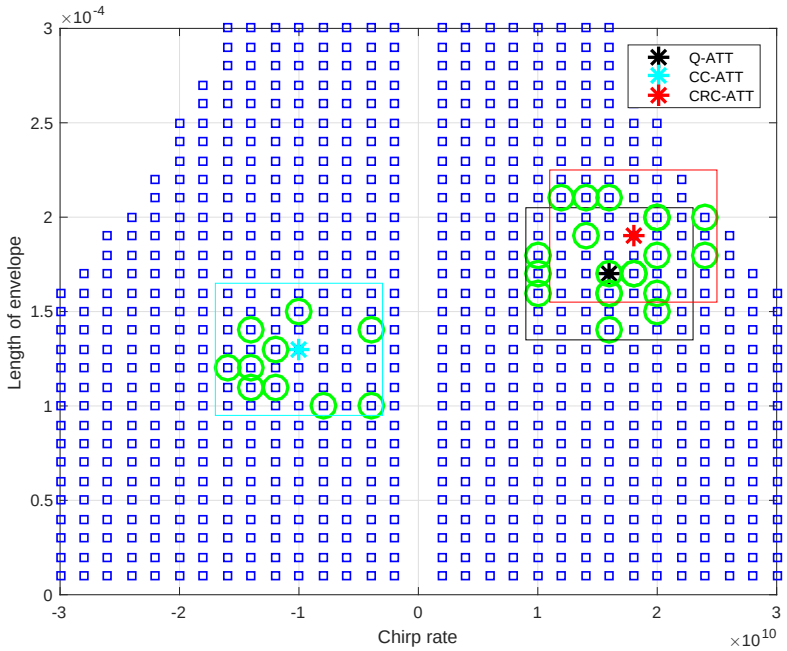

Figure 3.6: The sets of neighbors and prospective actions (in the absence of unexpected uncertainty).

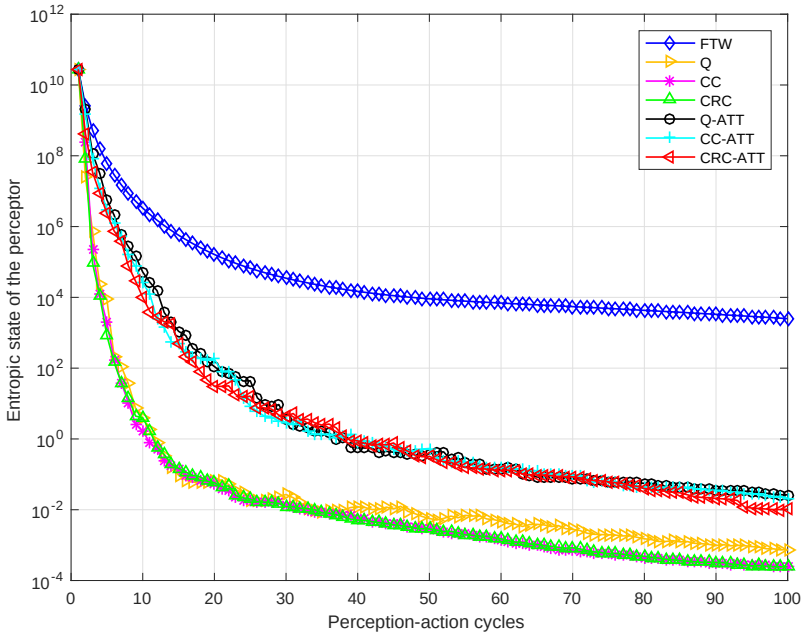

Figure 3.7: The entropic state of the perceptor (in the absence of unexpected uncertainty).

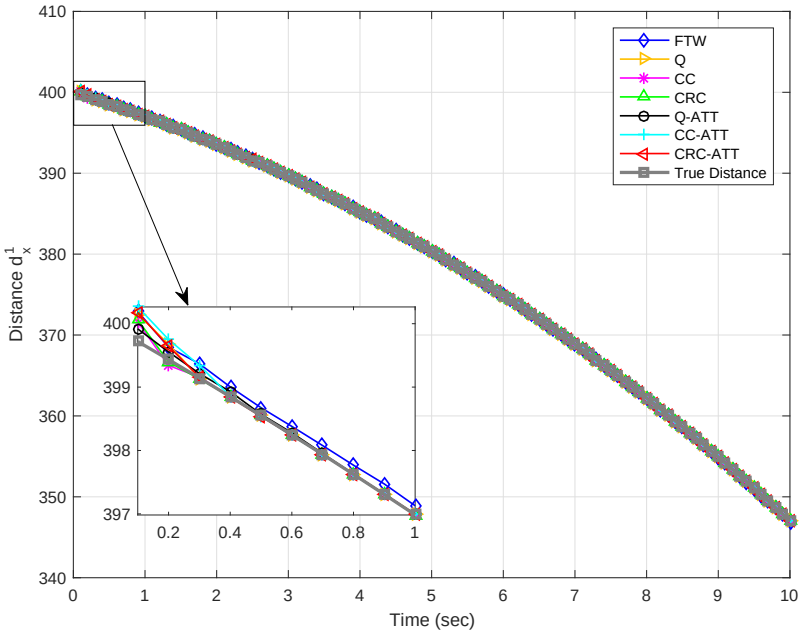

Figure 3.8: The true and estimated longitudinal distances between two vehicles (in the absence of unexpected uncertainty).

entropic state of "FTW" algorithm is the highest. The reason is as follows: with a suboptimal set of prospective actions (in terms of the performance in RMSE) for PAC_k, the final selected action c_k will lead to less accurate observations at PAC_{k+1}, the posterior $\hat{\boldsymbol{x}}_{k+1|k+1}$ will be more dispersed and the covariance matrix, $\mathbf{P}_{k+1|k+1}$, will have larger determinants. As a result, the entropic state H_{k+1} would be relatively higher.

Out of five elements in the state vector, Fig. 3.8 takes the longitudinal distance d_x^1 between two vehicles as an example. It shows how the true distance as well as the estimated distance obtained by each algorithm evolves during the simulation. Obviously, all the algorithms are capable of capturing the distance information right after the initialization and keeping track of that information thereafter, which would have been completely different if there is risk involved, as discussed in the next subsection.

3.6.2.2 In the presence of unexpected uncertainty

If the system model for vehicle-following problem experiences structural uncertainty (due to the unexpected occurrence of disturbance) during some period, the performance for all kinds of radar systems will be affected inevitably. When the unknown vector $\boldsymbol{m}_k$ is first imposed, the host vehicle will not have any information about this change in the beginning; however, it can become aware of the existence of this change soon, thanks to the information gain obtained through each PAC. The level of risk for the vehicle-following scenario depends on how well that uncertainty can be detected and handled. Figs. 3.9-3.12 have shown the performance of different algorithms in the presence of unexpected structural uncertainty.

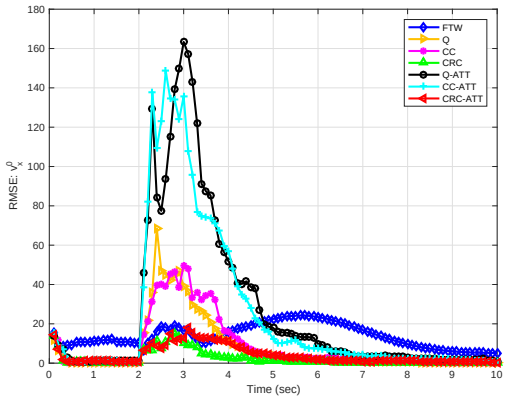

(a) RMSE for the velocity of the host vehicle v_x^0

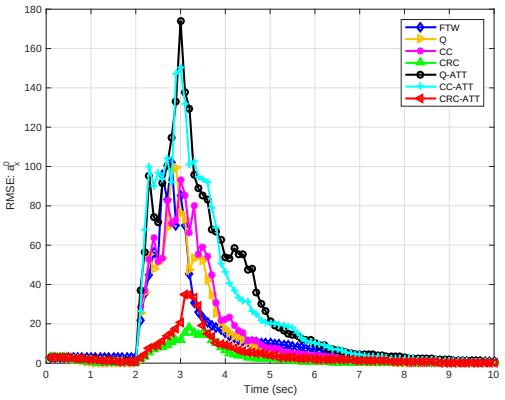

(b) RMSE for the acceleration of the host vehicle a_x^0

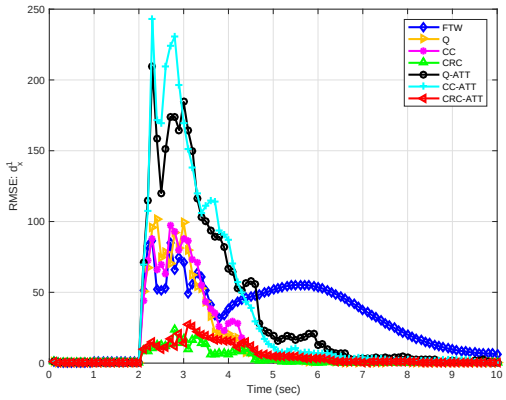

(c) RMSE for the longitudinal distance between two vehicles d_x^1

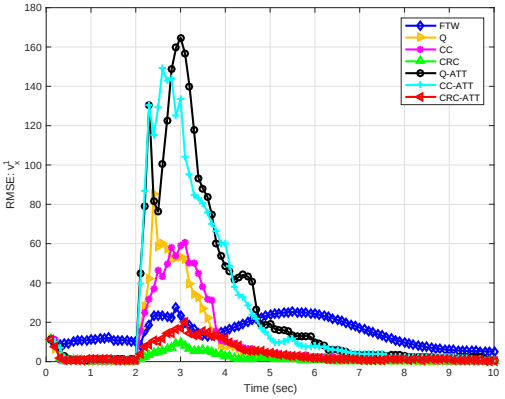

(d) RMSE for the velocity of the target vehicle v_x^1

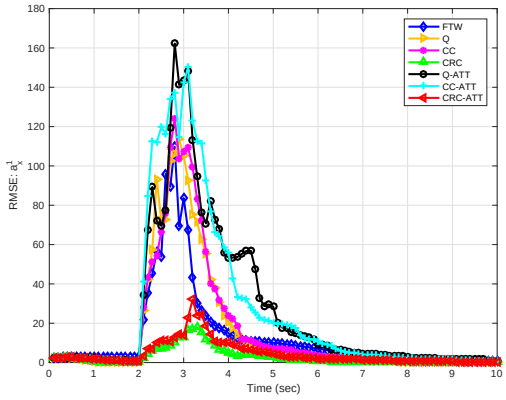

(e) RMSE for the acceleration of the target vehicle a_x^1

Figure 3.9: The RMSE for each element in the state vector (in the presence of unexpected uncertainty).

Like Fig. 3.5, Fig. 3.9 also shows the RMSE for each element in the state vector. It can be seen that the occurrence of unexpected uncertainty will have a negative effect on all algorithms to some extent. Specifically, the systems relying on "Q-ATT" or "CC-ATT" would experience the most severe deterioration in performance. When the unknown vector is suddenly imposed on the state evolution, these two algorithms still follow the original system model, which would result in inaccurate predicted values in both filtering and planning processes. Moreover, the practical constraint that the current cognitive action can only be selected from the neighbors of the preceding action makes the final decision to be a local optimum at best.

Different from "Q-ATT" and "CC-ATT", the algorithms of "Q" and "CC" do not take into consideration the hardware limitation on shifting operational parameters, and therefore, they will not suffer from that constraint and are able to search the entire action library to find the best cognitive action available. Consequently, "Q" and "CC" have better performance compared with "Q-ATT" and "CC-ATT" due to the freedom in making decisions. However, they are still confronted with inaccurate observations and predictions, and the final decisions they made are still perturbed by the uncertainty.

It is encouraging to see that "CRC" and "CRC-ATT" have the best overall performance compared with the rest. The reason is twofold. First, by putting more confidence in next cycle's observations, the filtered estimations and predictions will be more accurate in a statistical sense. Second, the subsystem composed of executive memory and classifier will come into play immediately to bring the risk under control when the unexpected uncertainty is detected. To elaborate on the latter point, we point out that the occurrence of structural uncertainty will cause the increasing of entropic state. While other learning algorithms ignore it, "CRC" and "CRC-ATT" empowered with task-switch control treat this increasing as a warning signal and will switch to a different operational mode. The cognitive action obtained by the policy will no longer be applied to the environment directly; rather, it is compared with the prospective past experiences put forward by the executive memory, from which a risk-sensitive cognitive action is finally selected and used to adjust the transmit waveform, as described in Section III. Although the RMSE performance of "CRC" is slightly better than that of "CRC-ATT", the latter one would still be a favorable choice in practice, considering the merits of attention mechanism (factors like the physical life time, maintenance cost, etc).

In addition, the curve of "FTW" displays an ordinary performance due to the fact that it can neither change for the better nor for the worse in terms of the transmit-waveform parameter.

Similar to Fig. 3.6, Fig. 3.10 also shows different sets of neighbors considered in the planning stage for "Q-ATT", "CC-ATT", and "CRC-ATT" algorithms. Note that for every PAC_k, the set of neighbors for each algorithm will be different, but it will always surround the preceding action c_{k-1} and fall within the range of n_r for the neighborhood.

Fig. 3.11 shows how the entropic state for each algorithm changes with PACs going on in the presence of structural uncertainty. At first, the entropic state drops for all algorithms with "Q", "CC", and "CRC" having the rapidest rate. After the unexpected disturbance occurs at 2.1s, it takes a short while before the entropic state starts to go up. Moreover, after the disturbance finishes and the evolution of system state returns to normal, the entropic states of "Q-ATT", "CC-ATT", and "CRC-ATT" will gradually decrease until they reach the same level with those of "Q", "CC", and "CRC". It is noteworthy that "CRC-ATT" has lower entropic state compared with the other two

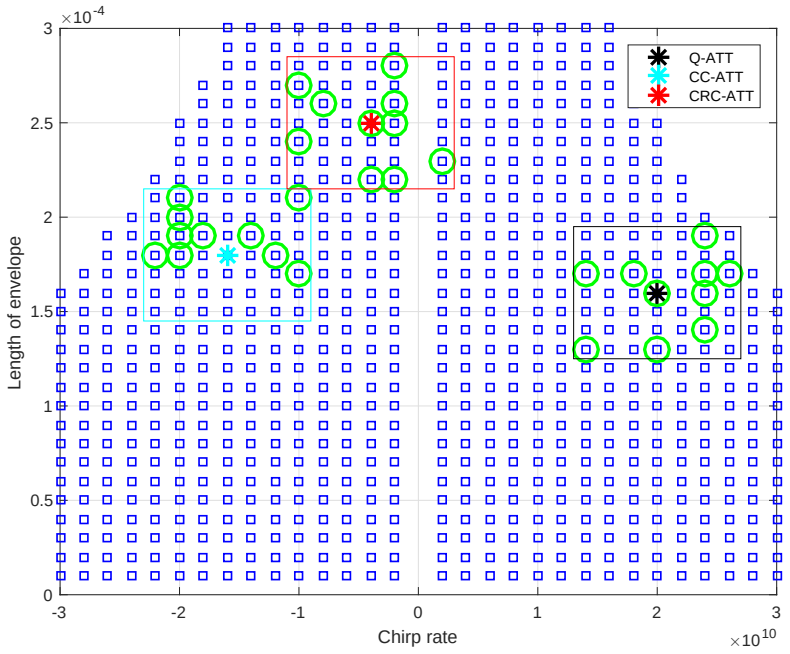

Figure 3.10: The sets of neighbors and prospective actions (in the presence of unexpected uncertainty).

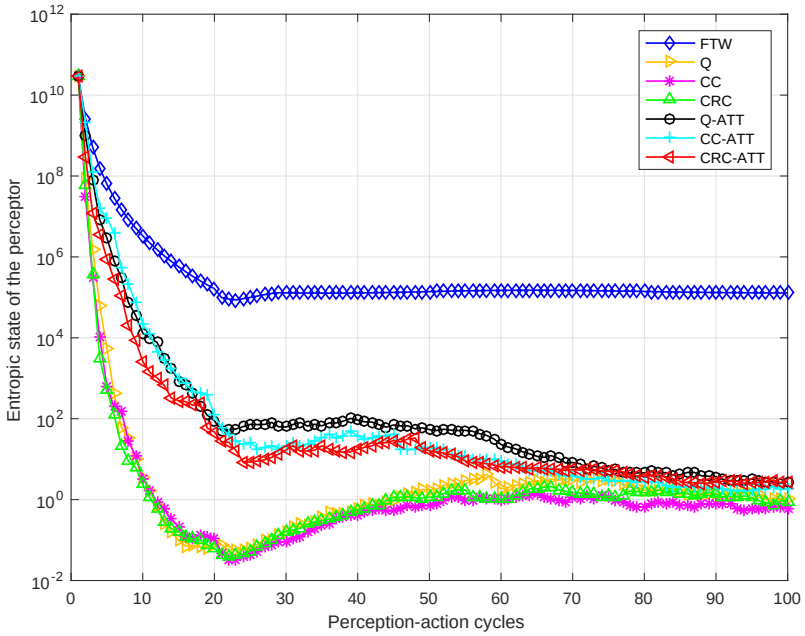

Figure 3.11: The entropic state of the perceptor (in the presence of unexpected uncertainty).

algorithms with attention features.

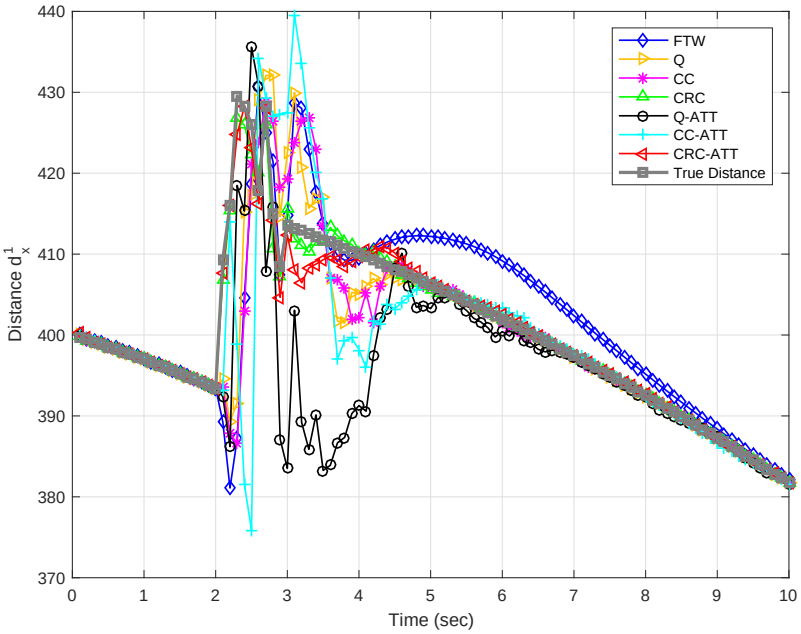

Figure 3.12: The true and estimated longitudinal distances between two vehicles (in the presence of unexpected uncertainty).

In direct contrast to Fig. 3.8, Fig. 3.12 reveals how each of the algorithms keeps track of the longitudinal distance between two vehicles during the simulation. It can be seen that "Q-ATT" and "CC-ATT" are almost incapable of tracking the distance during the presence of uncertainty, while "CRC-ATT" and "CRC" manage to stay relatively close to the true distance. This observation is in consistence with Fig. 3.9c. By improving the accuracy of predictions, and more importantly, by utilizing the subsystem composed of executive memory and classifier to benefit from the gained knowledge, the concept of predictive adaptation is brought into reality and the risk is finally brought under control in the CVR system.

3.7 Conclusion

In this paper, we have investigated and tailored the architectural structure of cognitive risk control (CRC), proposed an algorithm for transmit-waveform selection in cognitive vehicular radar (CVR) systems, and provided the first experimental demonstration of CRC in such an application. Simulation results have shown that this new design will be able to achieve a performance comparable to other classic designs in the absence of uncertainty, and more importantly, to make a significant improvement in the performance even when faced with unexpected disturbances or adverse events. The robustness and effectiveness of the proposed CVR system is in fact much needed for the self-driving cars, with safety-related issues being the undisputable priority. In addition to radar systems, assuming the role of a supervisor, the cognitive dynamic system (CDS) would substantially improve the performance of

many other vehicle-mounted systems. It envisions a remarkable contribution to the radical self-driving car revolution and one solid step toward the smart city in future. The theoretical originality and importance of this model rests mainly on the application to risk control of the predictive adaptation feature of the prefrontal cortex. Simply put, it is unique in the world of engineering as we know it today. In future work, we will improve the current approach with powerful tools like cubature Kalman filter, further investigate the possible marriage of brain-inspired CDS and self-driving cars in other aspects such as anti-jamming V2V communications, and bring out the full capacity of CRC in this promising research field.

Chapter 4

Cognitive Risk Control for Anti-Jamming V2V Communications in Autonomous Vehicle Networks

4.1 Preceding Introduction

In addition to vehicular radar, vehicular communication system is also an essential component for CAVs. The main responsibility of a vehicular communication system is to help stay connected and share information with other vehicles within a network. Aiming at the improvement of anti-jamming V2V performance, in this chapter, CDS and its special function of CRC are adopted to develop robust power control and channel selection method for vehicular communication system.

To the best of the author's knowledge, the scholarly work presented herein is the first experimental work on V2V communication that involves anti-jamming, power control, and channel selection at the same time.

The publication included in this chapter is:

S. Feng, and S. Haykin, "Cognitive Risk Control for Anti-Jamming V2V Communication in Autonomous Vehicle Networks," *IEEE Transactions on Vehicular Technology*, accepted, Aug. 2019.

The co-author's contributions to the above work include:

- Technical supervision and financial support of the study presented in this work.
- Manuscript revising and editing.

Abstract

The future of intelligent transportation system (ITS) is expected to be composed of connected and autonomous vehicles (CAVs), the development of which will have great impact on people's everyday life. Unfortunately, this progress will be accompanied by all kinds of potential threats and attacks rising in CAV network. As a legacy from traditional wireless networks, jamming attack is still one of the major and serious threats to vehicle-to-vehicle (V2V) communications. In this paper, we investigate the anti-jamming V2V communication in CAV networks through power control in conjunction with channel selection. Bringing into play a brain-inspired research tool called the cognitive dynamic system (CDS), the general structure of cognitive risk control (CRC) is well-tailored to analyze and address the jamming problem. Specifically, power control is carried out first using reinforcement learning, the result of which is then examined by a module called task-switch control. Based on the risk assessment, a multi-armed bandit (MAB) problem is formulated to perform the channel-selection process when necessary. Through continuous perception-action cycles (PACs), the feature of predictive adaptation is realized for the legitimate vehicle in its behavioral interactions with the jammer. Simulation results have shown that the proposed method has desirable performance in terms of several evaluation metrics.

4.2 Introduction

4.2.1 Connected and Autonomous Vehicles

As one of the most vigorous and active fields in the fourth industrial revolution, autonomous vehicles will play an important role in future intelligent transportation systems (ITS) and have great potential to change the landscape of our society [19, 137]. The benefits of autonomous vehicles include reducing the traffic accidents, cutting down the average commute time, reducing carbon dioxide emissions, improving travel experience, etc. [138]. According to Society of Automotive Engineers (SAE) International's standard J3016, there are six levels of driving automation [139]. Currently, enormous research efforts are being made to reach the "Level 4: High Automation", which will liberate human drivers from resuming fallback performance of the dynamic driving tasks, making it very close to the expectation of fully autonomous vehicles.

Despite the promising automation features, how do we coordinate independent autonomous vehicles in a vehicular ad hoc network (VANET) remains a challenging issue [140]. One possible answer rests on the bright prospect pertaining to connected and autonomous vehicles (CAVs). On the one hand, the autonomous driving performance can be improved by exploiting the information shared through vehicle-to-vehicle (V2V) communications; on the other hand, V2V communications will also benefit from driving automation, such as the provision of line-of-sight (LOS) path or estimated location from simultaneous localization and mapping (SLAM) [122]. Therefore, the two key features of CAVs will complement and enhance each other effectively.

To support V2V communication, different spectrum bands have been allocated for ITS applications worldwide. In the Unite States and Canada, the spectrum of 5.850-5.925 GHz is allocated for dedicated short-range communications (DSRC), which relies on IEEE 802.11p standard for wireless access in vehicular environments (WAVE) [141]. The total 75 MHz bandwidth is divided into one control channel (CCH) and six service channels (SCHs), each with 10 MHz bandwidth and 5 MHz guard band. Among these seven channels, safety applications are given priority over non-safety applications [142]. In order to extend vehicle-to-everything (V2X) communications to cellular spectrum bands, 3GPP has studied V2X specifications based on long-term evolution (LTE) technology [143]. More work is currently in progress to further pave the way for 5G-based V2X communications [144].

4.2.2 Jamming Attack and Its Countermeasures

Unfortunately, while the enabling technologies for CAVs gradually mature, all kinds of potential threats or attacks will also rise and endanger the CAV network [112, 145]. These adversarial behaviors can be driven by various motivations, such as causing traffic accidents, stealing critical cargo/information, hijacking, etc. [17]. One serious threat to CAV networks is the jamming attack, for which a jammer emits high-power electromagnetic signals to make the legitimate signals unrecognizable for on-board units (OBUs) and/or roadside units (RSUs) [146]. By reconfiguring the frequency band and signal strength, a smart jammer is able to modify the attack pattern according to the transmission specifics of targeted V2V communication links. Due to its easy implementation and disruptive impact, jamming

attack has received a lot of attention and the countermeasures have been extensively studied in the literature.

In [147], the presence of a smart jammer was considered in a traditional wireless network, and the power-control problem for the legitimate user was studied from a Stackelberg game perspective. In [148], a joint power-control and user-scheduling problem was formulated, and dynamic programming techniques were exploited to decompose and solve the problem. By utilizing the representation of spectrum waterfall, an anti-jamming scheme based on deep reinforcement learning (DRL) method was proposed in [149] to facilitate the channel-selection process. A multi-armed bandit (MAB) framework was formulated in [150] to obtain efficient channel-selection strategies, which were demonstrated to be able to defend various kinds of jamming attacks. In [151], a multi-domain anti-jamming scheme that tackles both power control and channel selection was proposed in heterogeneous wireless networks. In [152], a reputation-based anti-jamming method was proposed for large-scale wireless networks. This method is robust against collusion attacks and can significantly reduce the attacker population for a wide range of attacks. In [153], two reputation-based algorithms were proposed to deal with both naïve attackers and smart attackers, who could learn from historic information and adapt their attacking strategies accordingly to avoid being detected/punished. Due to different network characteristics, these methods are not directly applicable to the CAV networks.

Focusing on the safety-messages exchange in ITS applications, [154] investigated the real-time detection method for securing beacons against jamming attack in vehicular networks. The issue of attack detection was also studied in [155], in which unmanned aerial vehicles (UAVs) are deployed to help protect a safety-oriented vehicular network. A hideaway strategy was proposed in [156] as a countermeasure, for which an OBU or RSU will stop sending signals and keep silent upon the detection of jamming attack. In [157], a cooperative anti-jamming relaying method was proposed. When a vehicle is under attack, the neighboring vehicles will serve as relay nodes to forward received signals to the victim vehicle through other channels. The scenario of UAV-aided VANET was studied in [158], in which the UAV chooses whether to relay data while the jammer chooses its jamming power. Following on this work, [159] further investigated the stochastic game for relaying with random channel gains. In [160], the power control for anti-jamming problem in a pure UAV communication network was investigated from a game theoretic perspective. However, the jamming attack specifically targeting at V2V links remains a critical issue, and more effective anti-jamming methods are still urgently needed.

4.2.3 Cognitive Dynamic System and Cognitive Risk Control

In this paper, we study the anti-jamming V2V communication by introducing a different set of tools. We look to the recent progresses on cognitive dynamic systems (CDS) and make use of the newly developed cognitive risk control (CRC) [63, 116]. Generally speaking, CDS is a unique engineering system that is inspired by certain features of the human brain [59]. Built upon the five principles of human cognition as identified in Fuster's paradigm [65], which embodies perception-action cycle (PAC), memory, attention, intelligence, and language, CDS models the functionality of prefrontal cortex and thus exhibits the feature of predictive adaptation [62].

As established in the cognitive neuroscience and neurophysiology literature, the anatomical substrate of human brain confirms that there are two tiers of nervous structures hierarchically organized along the nerve axis: a posterior tier for sensation and perception, and an anterior tier for executive action [66]. The summit of the human PAC is occupied by the posterior association cortex and the frontal association cortex, the highest level of which is the prefrontal cortex of the PAC. That prefrontal cortex is essentially the structural and functional support of the functions we postulate and computationally formulate in the CDS.

Being a particular function of CDS, CRC aims at regulating the goal-directed behavior and averting the risk caused by internal or external disturbances. It is especially important when the surrounding environment is full of complexities or uncertainties. Accordingly, CRC can serve as a good candidate for addressing the jamming problem in CAV networks. Through the behavioral interactions with a smart jammer, the legitimate vehicle empowered by CRC adjusts its transmission power and channel, which are viewed as (risk-sensitive) cognitive actions and are continuously updated to adapt to the dynamic environment. To the best of our knowledge, this is the first paper that investigates the anti-jamming V2V communication in CAV networks through power control in conjunction with channel selection.

4.2.4 Contribution and Organization

The main contributions of this paper are summarized as follows:

(i) The brain-inspired CDS is applied to study V2V communications, and CRC is tailored for addressing the jamming problem in CAV networks. The novelty of this design rests mainly on the application to risk control of the predictive-adaptation property of human brain, which modern neuroscience attributes to the prefrontal cortex.

(ii) A new method based on CRC is designed for anti-jamming V2V communication in CAV networks. The power control is carried out first using reinforcement learning methods, the result of which is then examined by a module called task-switch control. Based on the risk assessment, an MAB problem is called upon to perform the channel-selection process when it is needed.

(iii) Performance of the proposed method is validated using a number of evaluation metrics. It is demonstrated that a network of switches will be able to coordinate the operations of power control and channel selection, in such a way that unnecessary operations are avoided while maintaining a desirable throughput.

The rest of this paper is organized as follows: after this introductory Section I that outlines the basics of CAV, V2V, and CRC, Section II briefly describes the system model that is of special interest in this paper. Sections III and IV present the detailed design of CRC for anti-jamming V2V communications from the perceptor side and the executive side, respectively. Section V gives an overall description of the proposed algorithm and its implementation process. Section VI discusses the simulation results. Finally, Section VII concludes this paper.

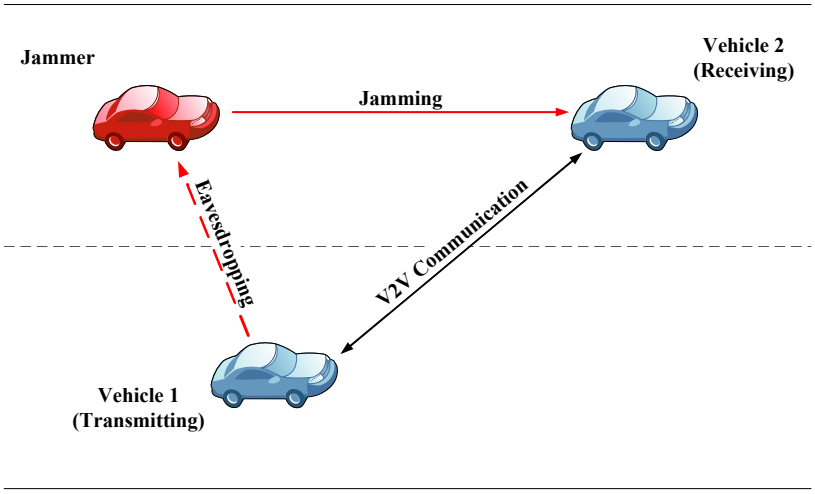

Figure 4.1: The jamming attack on V2V communication in autonomous vehicle networks.

4.3 Underlying System Model

4.3.1 Network Scenario

As illustrated in Fig. 4.1, the two CAVs, namely V_1 and V_2, are engaged in the V2V communication on a public road. An adversarial vehicle, referred to as the jammer, is trying to sabotage that communication link; it disturbs the vehicle on the receiving end by sending jamming signals, the act of which may also be assisted by potential eavesdropping from the transmitting vehicle. The vehicles V_1, V_2, and the jammer are driving in the same direction.

The set of communication channels between V_1 and V_2 can be denoted as $\mathbf{\Theta} = \{\theta_1, \cdots, \theta_c, \cdots, \theta_C\}, 1 \leq c \leq C$, where $|\mathbf{\Theta}| = C$ is the total number of available channels. The transmission-power set of vehicle V_1 can be denoted as $\mathbf{P} = \{P_1, \cdots, P_m, \cdots, P_M\}, 1 \leq m \leq M$, where $|\mathbf{P}| = M$ is the total number of discrete transmission power. Similarly, the transmission-power set of the jammer can be denoted as $\mathbf{Q} = \{Q_1, \cdots, Q_n, \cdots, Q_N\}, 1 \leq n \leq N$, where $|\mathbf{Q}| = N$.

4.3.2 Perception-Action Cycle

In its most simplified form, the CDS is mainly composed of two parts—the perceptor and the executive—with a feedback channel linking them together. Through interacting with the external environment constantly, a PAC is formulated in the form of a global feedback loop, which functions as the backbone of the entire CDS. Facing the potential threat of jamming attack, the PAC enables CAVs to monitor the dynamic changes in the environment, analyze the current quality of service and risk level, and therefore, make corresponding adjustments in transmission power and/or channel to maintain reliable V2V communications.

In hostile CAV networks, a smart jammer will also have the ability to adapt its transmission parameters over the course of time. The actions taken by CAVs will affect its counterpart, and vice

versa, which makes it more complicated. Moreover, due to the non-cooperative relationship between legitimate vehicles and the jammer, they will always take their actions in an asynchronous manner. Effective and timely PACs are therefore essential to detect and cope with the jamming attacks.

4.4 Cognitive Risk Control for Anti-Jamming V2V Communications: The Perceptor

The structure of CRC tailored for anti-jamming V2V communications is illustrated in Fig. 4.2. To some extent, it follows the basic framework of the CDS, which consists of the perceptor, the feedback channel, and the executive [59]. Specifically, the perceptor is composed of environmental sensing/modeling and interference formulation, which will result in utility metrics for feedback channel. The utilities are then viewed as internal rewards and sent to the executive. As a dominant part in CDS, the executive is composed of reinforcement learning, planner, policy, task-switch control, multi-armed bandit (MAB), executive memory, and classifier. The first half of executive focuses on power control, while the second half mainly deals with channel selection. Besides, a network of switches is introduced to facilitate the mechanism of task-switch control.

Each cyclic behavior starts with observables acquired from the external environment and ends with (risk-sensitive) cognitive actions being applied to it, accompanied by frequent behavioral interactions with the smart jammer. Generally speaking, the purpose of perceptor in CDS is to perceive the dynamic and uncertain environment, so that informed decisions can be made later on in the executive on a cyclic basis. Inspired by the human brain, the feature of predictive adaptation is incorporated in the design and exploited for engineering practice. This section mainly focuses on the perceptor of CDS, while the next section will be devoted to the executive.

4.4.1 Environmental Sensing and Modeling

In order to deal with a jamming attack effectively, vehicle V_1 needs to be aware of the status of both vehicle V_2 and the jammer, such as their relative distances or transmission-power levels. There are several possible ways that the distance between legitimate vehicles can be obtained. For example, vehicle-mounted GPS devices typically have the accuracy from a few meters to tens of meters [161, 162], which is deemed to be usable for on-road longitudinal positioning. Another way of obtaining the distance is to rely on V2V messages sent from the other legitimate vehicle in a cooperative fashion. Besides, radar-ranging methods are also desirable for the real-time distance estimation. Ideally, all these possible inputs from different sources should be analyzed to form a well-informed distance estimation.

However, the accuracy of GPS depends on factors like satellite geometry, atmospheric conditions, signal blockage, etc. It usually worsens near buildings or trees, which are very common in an urban scenario [163]. Consequently, the usefulness of GPS signals is limited. Moreover, under severe jamming situations, no meaningful information can be extracted from the received V2V messages. In such cases, neither GPS nor V2V will fulfill the requirement, which makes radar-ranging method necessary for distance estimation due to its robustness.

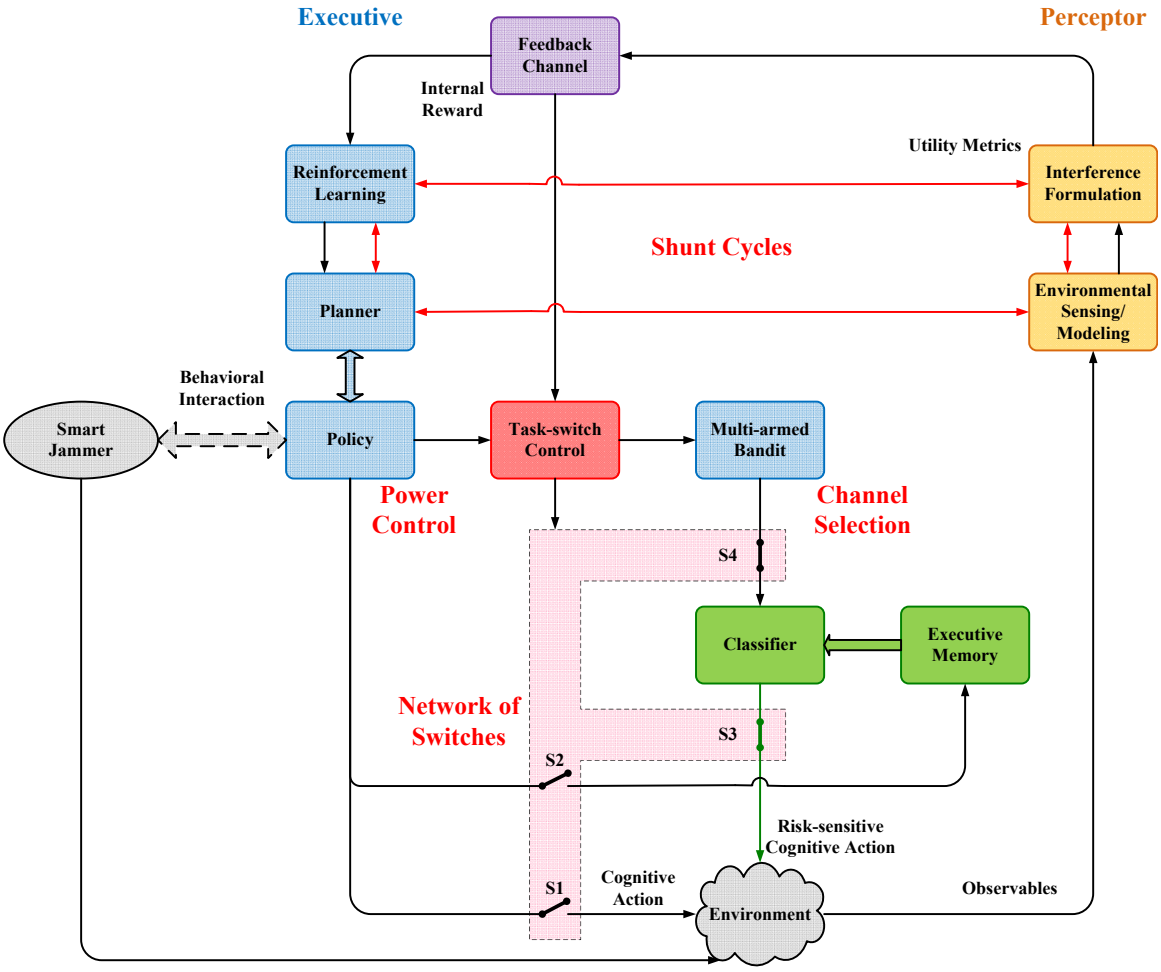

Figure 4.2: Architectural structure of cognitive risk control tailored for anti-jamming V2V communications.

Unlike the cooperative nature of legitimate vehicles, the non-cooperative and adversarial nature of jammer makes it impossible for a legitimate vehicle to benefit from either GPS readings or V2V messages. As a result, radar-ranging method would be the only feasible option for estimating the distance between a legitimate vehicle and the jammer.

As mentioned before, the transmission power of the opponent is yet another key factor for organizing attack/defense. In future CAV networks, both legitimate vehicles and adversarial jammers are considered to be of a certain level of intelligence. By equipping a simple low-cost sensor for physical carrier-sensing (PCS) [164], vehicles will be able to perform energy detection in specific wireless channels. They may also utilize the technique of preamble detection or a combination of both (if prior knowledge is available). With the value of estimated distance between vehicles at hand, transmission specifics like power level can be calculated [165]. This procedure can be carried out by each vehicle independently, including the jammer. Another possible way for the jammer to obtain the transmission power of vehicle V_1 is to conduct eavesdropping [166]. As the transmission specifics

are shared between legitimate vehicles V_1 and V_2 over an open channel, eavesdropping from vehicle V_1 will potentially provide the jammer with all the information needed for launching a jamming attack.

However, due to environmental uncertainties and hardware limitations, the observations are typically imperfect. For example, the power of the jamming signal Q may be perceived inaccurately by vehicle V_1. To that end, let $\mathbf{A}$ denote the error matrix of perceived jamming power from the perspective of vehicle V_1, we have

$$\mathbf{A} = \left(a_{ij}\right)_{N\times N}, \tag{4.1}$$

with

$$a_{ij} = \begin{cases} h, & \text{if} \quad i = j \\ \frac{1-h}{N-1}, & \text{otherwise} \end{cases},$$

where a_{ij} represents the probability that the jamming power perceived by vehicle V_1 is Q_j while the actual jamming power is Q_i, $1 \le i, j \le N$. The accuracy factor of vehicle V_1 is denoted as $h \in [0,1]$. Similarly, assuming that the jammer also has imperfections in its sensing capability, the error matrix of perceived legitimate transmission power from the perspective of jammer can be denoted as

$$\mathbf{B} = \left(b_{ij}\right)_{M\times M}, \tag{4.2}$$

with

$$b_{ij} = \begin{cases} l, & \text{if} \quad i = j \\ \frac{1-l}{M-1}, & \text{otherwise} \end{cases},$$

where b_{ij} represents the probability that the legitimate transmission power perceived by the jammer is P_j while the actual transmission power is P_i, $1 \le i, j \le M$. The accuracy factor of the jammer is denoted by $l \in [0,1]$.

4.4.2 Interference Formulation

Compared with the well-explored cellular channels, V2V channels have their own time-frequency selective fading natures [167]. Typically, the vehicular environments are classified into four scenarios, which are highway, urban, suburban, and rural [168]. Various path-loss models have been proposed to characterize each of those four common scenarios in the literature [169, 170]. In this paper, we consider the traffic environment for an urban scenario, where the road is shared by vehicles, pedestrians, and bicycles with scattering objects (such as street lamps or trees) on the roadside. Following the power law, the path-loss model for such is expressed as [171]

$$PL\left(d\right) = PL_0 + 10w\log_{10}\left(\frac{d}{d_0}\right) + \boldsymbol{X}_\sigma, \quad d \ge d_0 \tag{4.3}$$

where PL_0 is the path loss at a reference distance d_0, w is the path-loss exponent, and $\boldsymbol{X}_\sigma$ is a normally distributed random variable with mean zero and standard deviation σ that characterizes the instantaneous fading component. For a reference distance $d_0 = 10$ m, the validity range is limited to $d \ge 10$ m.

Since the path loss is calculated by taking the difference of the transmission power and the received power in logarithmic scale, we write:

$$PL(d)|_{\mathrm{dB}} = P_{\mathrm{Tx}}|_{\mathrm{dBm}} - P_{\mathrm{Rx}}|_{\mathrm{dBm}}. \tag{4.4}$$

The channel gain of the transmission link between vehicle V_1 and V_2 is formulated as

$$g_V = 10^{-PL(d_V)/10}. \tag{4.5}$$

Likewise, the channel gain of the jamming link between the jammer and vehicle V_2 can be formulated as

$$g_J = 10^{-PL(d_J)/10}. \tag{4.6}$$

As a result, the received signal-to-interference-plus-noise ratio (SINR) at vehicle V_2 will be

$$\beta = \frac{g_V P}{BN_0 + g_J Q}, \tag{4.7}$$

where P and Q represent the transmission power of vehicle V_1 and the jammer, respectively. B is the channel bandwidth and N_0 is the noise power spectral density (PSD). Ideally, the SINR should be maintained at a relatively high level, so that the allocated bandwidth can be fully taken advantage of to improve the overall throughput. Although raising the transmission power of vehicle V_1 will probably increase the received SINR, it will also incur more expenses on the energy budget. Therefore, the utility metric of vehicle V_1 is defined as

$$\mu_V(P_m, Q_n) = \frac{g_V P_m}{BN_0 + g_J Q_n} - c_V P_m, \tag{4.8}$$

where c_V is the transmission cost per unit power of vehicle V_1. Since the purpose of a jammer is to deliberately interfere with the legitimate V2V communication, the utility metric of the jammer can be defined as

$$\mu_J(P_m, Q_n) = -\frac{g_V P_m}{BN_0 + g_J Q_n} - c_J Q_n, \tag{4.9}$$

where c_J is the transmission cost per unit power of the jammer. Taking the error matrices in eqs. (4.1) and (4.2) into consideration, and substituting the channel gains presented in eqs. (4.5) and (4.6), the practical utility functions of vehicle V_1 and the jammer can then be written as

$$\hat{\mu}_V(P_m, Q_n) = \frac{10^{-PL(d_V)/10} P_m}{BN_0 + 10^{-PL(d_J)/10} \sum_{j=1}^{N} a_{nj} Q_j} - c_V P_m, \tag{4.10}$$

and

$$\hat{\mu}_J(P_m, Q_n) = -\frac{10^{-PL(d_V)/10} \sum_{j=1}^{M} b_{mj} P_j}{BN_0 + 10^{-PL(d_J)/10} Q_n} - c_J Q_n, \tag{4.11}$$

respectively. The optimization goals of vehicle V_1 and the jammer over the course of time can therefore be defined as

$$\max_{P^k} \sum_{k=0}^{\infty} \gamma_1^k \hat{\mu}_V \left(P^k, Q^k\right), \quad \text{s.t.} \quad P^k \in \mathbf{P}, \tag{4.12}$$

and

$$\max_{Q^k} \sum_{k=0}^{\infty} \gamma_2^k \hat{\mu}_J \left(P^k, Q^k\right), \quad \text{s.t.} \quad Q^k \in \mathbf{Q}, \tag{4.13}$$

where P^k and Q^k represent the legitimate transmission power and jamming power in cycle k, γ_1 and γ_2 denote the discounting factors that diminish future utilities with $\gamma_1 \in [0,1)$, $\gamma_2 \in [0,1)$, respectively.

Due to the fact that current strategies taken by vehicle V_1 and the jammer will affect each other's future move, those two optimization problems are coupled and hard to solve directly. Furthermore, if more vehicles join the network, eqs. (4.10) and (4.11) and associated formulations need to be revised to account for the influence of additional nodes. In that case, the jamming impact and interference relationship will become much more complicated. Therefore, we resort to the reinforcement learning and view the utilities as internal rewards, which are sent to the executive side via a feedback channel.

4.5 Cognitive Risk Control for Anti-Jamming V2V Communications: The Executive

The executive has a more complex structure and occupies a large portion of the CDS. It is composed of reinforcement learning, planner, policy, task-switch control, MAB, executive memory, and classifier, as shown in Fig. 4.2. The main purpose of executive is to make intelligent decisions, which involves power control and possibly channel selection as well, depending on the specific situation as the decision is being made.

4.5.1 Reinforcement Learning

Based on the internal rewards received from the feedback channel, the value-to-go function of vehicle V_1 at cycle k can be calculated in accordance with [77, 102] and expressed as

$$\boldsymbol{J}_k \left(P^{k-1}\right) = \boldsymbol{J}_{k-1} \left(P^{k-1}\right) + \alpha \left[r_{k-1} \left(P^{k-1}\right) + \gamma_1 \max_{P^*} \boldsymbol{J}_k \left(P^*\right) - \boldsymbol{J}_{k-1} \left(P^{k-1}\right)\right], \tag{4.14}$$

where α is the learning rate, $r_{k-1}\left(P^{k-1}\right) = \hat{\mu}_V^{k-1}\left(P_m, Q_n\right) = \hat{\mu}_V\left(P^{k-1}, Q^{k-1}\right)$ represents the internal reward as a result of the selected power P^{k-1} at the preceding cycle $k-1$. Here, the power P^* represents the greedy action that maximizes the value-to-go function.

4.5.2 Planner and Policy

To find the best possible transmission strategy in the power domain, vehicle V_1 needs to be predictive and therefore look into the future. To that end, the planner along with the policy will generate a set of prospective actions, estimate the hypothesized outcome (i.e., internal rewards) of those prospective actions, update the corresponding value-to-go functions, and also update the policy for generating those actions repeatedly. To be specific, while the planning can be performed in a similar way of reinforcement learning, the main difference is that there is no interaction with environment in the planning stage [116].

Specifically, with the value-to-go function being updated through reinforcement learning, the policy can be updated using the softmax function as follows [172]:

$$\pi_m^k = \frac{\exp\left[\boldsymbol{J}_k\left(P_m\right)/T\right]}{\sum_{m=1}^{M}\exp\left[\boldsymbol{J}_k\left(P_m\right)/T\right]}, \tag{4.15}$$

where T represents the temperature parameter. Based on the updated policy, the next prospective action $P^{k,\omega}$ can be selected in a probabilistic manner. By substituting this prospective action into eq. (4.10), the hypothesized internal reward $r_k\left(P^{k,\omega}\right) = \hat{\mu}_V^k\left(P_m, Q_n\right) = \hat{\mu}_V\left(P^{k,\omega}, Q^{k-1}\right)$ can be calculated. Here, $1 \le \omega \le \Omega$, and Ω represents the total number of prospective actions that are selected in the planning process. For prospective action $P^{k,\omega}$, the value-to-go function is updated in the planning process as follows:

$$\boldsymbol{J}_{k+1}\left(P^{k,\omega}\right) = \boldsymbol{J}_k\left(P^{k,\omega}\right) + \alpha\left[r_k\left(P^{k,\omega}\right) + \gamma_1 \max_{P^*}\boldsymbol{J}_{k+1}\left(P^*\right) - \boldsymbol{J}_k\left(P^{k,\omega}\right)\right]. \tag{4.16}$$

After updating eqs. (4.15) and (4.16) alternately for Ω iterations, we now select the transmission power P^k, also referred to as cognitive action, for the current kth PAC with the following probability:

$$\mathrm{P}\left\{P^k = P_m\right\} = \frac{\exp\left[\boldsymbol{J}_{k+1}\left(P_m\right)/T\right]}{\sum_{m=1}^{M}\exp\left[\boldsymbol{J}_{k+1}\left(P_m\right)/T\right]}. \tag{4.17}$$

However, as mentioned previously, an open and hostile vehicular environment is full of uncertainties. The attack launched by a smart jammer may sometimes be too severe for the victim CAVs to handle. Even through P^k is currently the best transmission power can be found on the present channel, it may still result in a failed V2V communication due to unbearable interference. Therefore, it is a must to introduce task-switch control to assess the risk for the next cycle and make necessary adjustments accordingly, which is discussed in the next subsection.

4.5.3 Task-Switch Control

The task-switch control is responsible for deciding whether channel selection is still needed after the power control has been carried out. It controls the status of a network of switches. Specifically, the usefulness of temporarily selected transmission power P^k is determined by assessing the future risk level it may result in. If P^k is applied to the environment by vehicle V_1 at the end of this PAC, the received SINR at vehicle V_2 would be

$$\beta_{\text{pre}}^{k} = \frac{10^{-PL(d_V)/10} P^{k}}{BN_0 + 10^{-PL(d_J)/10} \sum_{j=1}^{N} a_{nj} Q_j^{k}}. \tag{4.18}$$

To ensure that the received signals can be decoded correctly, the received SINR should be above a certain threshold. This threshold puts a constraint on the interference strength for maintaining V2V communications. If we denote the threshold at cycle k as TSC_k, then the binary risk level can be evaluated by

$$\rho_k = \begin{cases} 0, & \text{if} \quad \beta_{\text{pre}}^{k} \geq \text{TSC}_k \\ 1, & \text{otherwise} \end{cases}. \tag{4.19}$$

In practice, the value of this threshold can be designed by leveraging some prior knowledge or experiences on different V2V types. To be specific, different types of V2V communication will impose different interference requirements. For example, the messages related to cooperative adaptive cruise control (CACC) will have much stricter requirements compared to the data of multimedia streaming or infotainment systems. To accommodate both critical transmissions and personalized services in anti-jamming V2V communications, the threshold that indicates the interference requirement should be adjusted flexibly in accordance with the change of V2V types. Therefore in practice, the exact value of this threshold depends on the specific application of interest.

If ρ_k is 0, it means that the received SINR will meet the requirement and the selected power P^k will reach a good result. In this case, the pair of switches (S1, S2) is closed while that of (S3, S4) is opened, so that the cognitive action can be directly applied to the environment. The action profile can thus be described as $\left\{P^k, \theta^{k-1}\right\}$, where θ^{k-1} means the same channel will be used as it is for the previous $(k-1)$th PAC.

However, if ρ_k turns out to be 1, it implies that the jamming signal is too strong and P^k will not lead to a successful transmission for the current cycle. Since there is no better choice available on the present channel, we have to look for and switch to a better channel for this transmission, which is done by solving an MAB problem, discussed next.

4.5.4 Multi-Armed Bandit

Generally speaking, MAB is a problem where choices are made (that is, "arms" are selected) to maximize the expected long-term payoff [173]. In this paper, the channels available for V2V communication are viewed as the arms. For each selection, a fundamental trade-off has to be made between exploitation and exploration, which means either taking advantage of the option with the highest expected payoff that we currently know of, or trying other options to gain new knowledge for future benefits. Due to its effectiveness and elegant properties, the upper confidence bound (UCB1) algorithm of MAB is adopted for the channel selection in this design [174]. Note that channel selection is performed only if a switching is necessary.

The previous analysis on power control mainly focused on the immediate preceding cycle $k-1$ and the current cycle k, while the analysis on channel selection should take all preceding cycles into consideration. If the binary risk level was $\rho_t = 1$ in cycle t with $0 \leq t \leq k-1$, then the channel selection

would have been performed during that cycle. Let indicator function $I_t(\theta_c)$ represent whether channel θ_c was selected in cycle t, and let θ^t denote the channel that was actually selected; we may then have:

$$I_t(\theta_c) = \begin{cases} 1, & \text{if} \quad \theta^t = \theta_c \\ 0, & \text{otherwise} \end{cases}. \tag{4.20}$$

If channel selection was not needed in that cycle, then θ^t is set to be 0. Accordingly, the total number of channel θ_c being selected in all preceding cycles can be written as

$$L_k(\theta_c) = \sum_{t=0}^{k-1} I_t(\theta_c), \tag{4.21}$$

For each cycle $t > 0$, the MAB-related reward for channel θ_c is defined as

$$r_t(\theta_c) = \begin{cases} B\log_2\left(1+\beta_{\text{pre}}^t\right), & \text{if} \quad \theta^{t-1} = \theta_c \ \text{ and } \ \rho_t = 0 \\ 0, & \text{otherwise} \end{cases}, \tag{4.22}$$

where B is the channel bandwidth as introduced previously, and β_{pre}^t denotes the received SINR at cycle t that is calculated in the same way as in eq. (4.18). We may therefore suggest that one channel can only be rewarded if, only if, it is used in a successful transmission. For normalization, we write:

$$\hat{r}_t(\theta_c) = \frac{r_t(\theta_c)}{r_{\max}(\theta_c)}, \tag{4.23}$$

where $r_{\max}(\theta_c)$ represents the maximum reward that has been achieved. The total normalized reward of using channel θ_c for transmission in all preceding cycles can therefore be expressed as

$$H_k(\theta_c) = \sum_{t=0}^{k-1} \hat{r}_t(\theta_c). \tag{4.24}$$

As a result, the average reward of channel θ_c is

$$\overline{r}_k(\theta_c) = \frac{H_k(\theta_c)}{L_k(\theta_c)}. \tag{4.25}$$

Besides, the total number of channel switching that occurred in the past can be counted with the assistance of task-switch control as follows:

$$s_k = \sum_{t=0}^{k-1} \rho_t. \tag{4.26}$$

The stage is now set for calculating the total expected regret [175], which is a common performance metric for MAB problems, as follows:

$$R_k = \sum_{c:\mu_c<\mu^*} (\mu^* - \mu_c)\,\mathbb{E}\left[L_k(\theta_c)\right] + c_s \sum_{c=1}^{C} \mathbb{E}\left[L_k(\theta_c)\right], \tag{4.27}$$

where μ^* represents the highest expected reward associated with the optimal channel, $\mu^* = \max_{1\le c\le C} \mu_c$, with μ_c being the unknown expected reward for any channel θ_c. $\mathbb{E}$ denotes the expectation operator, and c_s is the unit cost for each channel switching occurred. Therefore, the expected regret is defined as the primary loss due to the fact that the optimal channel is not always selected, plus the additional loss caused by the switching behavior.

Invoking the UCB1 algorithm [151, 174], the upper confidence index for channel θ_c at cycle k can be calculated as

$$\delta_k(\theta_c) = \bar{r}_k(\theta_c) + \sqrt{\frac{2\ln(s_k)}{L_k(\theta_c)}}, \tag{4.28}$$

Then, the channel with the maximum index value will be selected as the desired transmission channel at cycle k, which can be expressed as

$$\hat{\theta}^k = \arg\max_{\theta_c\in\Theta} \delta_k(\theta_c), \tag{4.29}$$

For initialization, each channel will be selected once in order to establish the initial reward values before UCB1 algorithm comes into play.

According to [174], the expected number of times for which channel θ_c is selected during all s_k switches is bounded by

$$\mathbb{E}[L_k(\theta_c)] \le \frac{8\ln(s_k)}{(\mu^*-\mu_c)^2} + 1 + \frac{\pi^2}{3}, \tag{4.30}$$

we then have:

$$\begin{aligned} R_k &\le \sum_{c:\mu_c<\mu^*} \frac{8\ln(s_k)}{\mu^*-\mu_c} + \left(1+\frac{\pi^2}{3}\right)\sum_{c=1}^{C}(\mu^*-\mu_c) \\ &\quad + c_s\left[\sum_{c:\mu_c<\mu^*}\frac{8\ln(s_k)}{(\mu^*-\mu_c)^2} + \left(1+\frac{\pi^2}{3}\right)(C-1)\right] \\ &= \sum_{c:\mu_c<\mu^*}\frac{8(\mu^*-\mu_c+c_s)}{(\mu^*-\mu_c)^2}\ln(s_k) \\ &\quad + \left(1+\frac{\pi^2}{3}\right)\left[\sum_{c=1}^{C}(\mu^*-\mu_c) + c_s(C-1)\right] \\ &\le \sum_{c:\mu_c<\mu^*}\frac{8(\mu^*-\mu_c+c_s)}{(\mu^*-\mu_c)^2}\ln(k) \\ &\quad + \left(1+\frac{\pi^2}{3}\right)\left[\sum_{c=1}^{C}(\mu^*-\mu_c) + c_s(C-1)\right]. \end{aligned} \tag{4.31}$$

It demonstrates the fact that the total expected regret R_k has logarithmic growth. That is, $R_k \sim O(\log k)$. Therefore, adopting this method for channel selection will achieve the optimal regret up to a multiplicative constant, and offers channel $\hat{\theta}^k$ as a replacement for channel θ^{k-1} when encountered with severe jamming attack in the kth PAC.

4.5.5 Executive Memory and Classifier

As discussed previously, whenever the risk level turns out to be $\rho_k = 0$ in the stage of task-switch control, channel selection is not further needed after the power control. In such cases, the action profile $\left\{P^k, \theta^{k-1}\right\}$ about the selected power and associated channel will be stored in the executive memory. Through collecting and accumulating all the past experiences we had, the executive memory will be occupied with enormous historical action profiles, which can be characterized by $f(P, \theta)$ and therefore are of great value for future use.

In the event of a severe attack on the legitimate V2V transmission, the risk level would have become $\rho_k = 1$. In order to response more quickly and effectively, we propose to rely on executive memory as the entity for reselecting transmission power after the channel being switched to $\hat{\theta}^k$. Using the method of *maximum a posteriori* (MAP) estimation [71], we have

$$\hat{P}^k = \arg\max_{P \in \mathbf{P}} f\left(P|\hat{\theta}^k\right), \tag{4.32}$$

which can be calculated as follows:

$$\begin{aligned} \hat{P}^k &= \arg\max_{P \in \mathbf{P}} \frac{f\left(\hat{\theta}^k|P\right) f(P)}{f\left(\hat{\theta}^k\right)} \\ &= \arg\max_{P \in \mathbf{P}} f\left(\hat{\theta}^k|P\right) f(P). \end{aligned} \tag{4.33}$$

Under such circumstances, the action profile at the current cycle k can be denoted as $\left\{\hat{P}^k, \hat{\theta}^k\right\}$. It is said to be risk-sensitive cognitive action as it will bring the foreseeable risk under control by escaping the attack effectively.

After this countermeasure is applied to the environment, meaning that vehicle V_1 carries out its transmission on the new channel with reselected power, the current PAC is completed and the next one begins, which continues on hereafter in a cyclic manner.

4.6 Proposed Algorithm and Implementation Process

Based on previous discussions, the proposed method of CRC for anti-jamming V2V communications is described in Algorithm 2. Besides, the implementation process of the proposed algorithm is illustrated in Fig. 4.3. Due to the non-cooperative relationship, vehicle V_1 and the jammer will update their behavior asynchronously, while every move ever made is still under the influence of its opponent.

As illustrated in Fig. 4.3, for each (perception-action) cycle of vehicle V_1, it starts with sensing/modeling and ends with acting on the environment. Most importantly, there are many iterations performed internally within the stage of "multiple planning" in one PAC. In other words, both sensing and acting (i.e., transmission activities) are only required once for each PAC. Since the entire process of multiple planning is done internally, all those iterations (within the same PAC) can be performed with no intermediate sensing or transmission activities required. In fact, the attribute of efficiency and timeliness was one of the reasons that motivated us to introduce multiple planning in the first

Algorithm 2 Proposed Algorithm for Anti-Jamming V2V Communication in Autonomous Vehicle Networks

Input: legitimate transmission power P_m and jamming power Q_n for each PAC, $1 \leq m \leq M$, $1 \leq n \leq N$
Output: final action profile c_k for each PAC

Initialization:
Value-to-go function $\boldsymbol{J}_0$ and $\boldsymbol{J}_{0,J}$, policy π^0 and π_J^0, risk level $\rho_0 = 0$, executive memory $\mathbf{B}_0 = \varnothing$
Vehicle V_1 selects each transmission channel once to establish the initial values of MAB-related reward
Vehicle V_1 takes an initial action profile $\left\{P^0, \theta^0\right\}$ randomly selected from $\mathbf{P}$ and $\boldsymbol{\Theta}$

for $k = 1$ to Z (number of PACs) **do**
  The jammer:
  Generate and apply action profile $\left\{Q^k, \theta^k\right\}$

  Vehicle V_1:
  Interference formulating:
  Calculate utility $\hat{\mu}_V\left(P^{k-1}, Q^k\right)$
  Learning:
  Update value-to-go function $\boldsymbol{J}_k\left(P^{k-1}\right)$
  Multiple planning:
  for $\omega = 1$ to Ω (number of prospective actions) **do**
    Update policy π^k
    Select prospective action $P^{k,\omega}$
    Calculate hypothesized internal reward $\hat{\mu}_V\left(P^{k,\omega}, Q^k\right)$
    Update value-to-go function $\boldsymbol{J}_{k+1}\left(P^{k,\omega}\right)$
  end for
  Generate pending action profile $\left\{P^k, \theta^{k-1}\right\}$
  Risk assessing:
  Calculate SINR β_{pre}^k
  Calculate risk level ρ_k
  if $\rho_k = 0$ **then**
    Store $\left\{P^k, \theta^{k-1}\right\}$ into executive memory $\mathbf{B}_k$
    Calculate average reward $\overline{r}_k\left(\theta_c\right)$
  else
    Calculate each upper confidence index $\delta_k\left(\theta_c\right)$
    Channel selection:
    Select $\hat{\theta}^k$
    Update counter $L_k\left(\theta_c\right)$ and s_k
    Power reselecting:
    Calculate $\hat{P}^k$
  end if
  Generate final action profile
  $c_k = (1 - \rho_k) \cdot \left\{P^k, \theta^{k-1}\right\} + \rho_k \cdot \left\{\hat{P}^k, \hat{\theta}^k\right\}$
  Apply c_k to the environment

  The jammer:
  Calculate utility $\hat{\mu}_J\left(P^k, Q^k\right)$
  Update value-to-go function $\boldsymbol{J}_{k,J}\left(Q^k\right)$
  Update policy π_J^k
end for

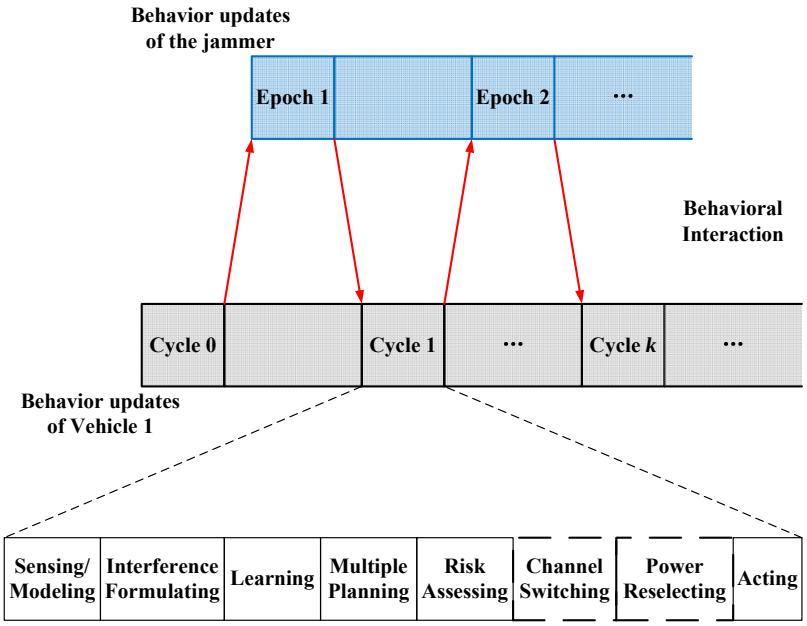

Figure 4.3: Implementation process of the anti-jamming V2V communication on a cyclic basis.

place [63].

Therefore, for each perceived change in the environment, there will be one PAC dedicated to capture, and more importantly, to adapt to the network dynamics in a timely manner. To some extent, it can be viewed that the network is treated as quasi-static within any given PAC, but is continuously adapted to from one PAC to the next.

It should be noted that it is unlikely, and not necessarily, that vehicle V_1 and the jammer make their updates one following the other all the time. Either vehicle V_1 or the jammer could have more accurate sensing or faster response abilities, depending on practical factors like processing resources, battery capacity, hardware limitations, etc. It means that one cycle of vehicle V_1 could be followed by several epochs of the jammer, or the other way around. Nevertheless, either of them can still learn the opponent's behavior at its own pace, on its own, without requiring any prior knowledge about its opponent's strategies or abilities.

4.7 Simulation Results

In this section, simulation results are presented to compare the performance of proposed algorithm for anti-jamming V2V communication with other anti-jamming methods, as shown from Fig. 4.4 to Fig. 4.12.

Specifically, the method of "power control only (with fixed channel)" shows one type of countermeasure, for which power control is adopted in the design while channel switching is not considered. This type of countermeasure has been extensively studied in the literature, such as the algorithms presented in [147, 148, 160]. Another kind of anti-jamming method is to focus on dodging the

attack by frequent channel switching with a constant transmission power, the idea of which has been implemented by the algorithms presented in [149, 150], as shown by the curve of "channel selection only (with fixed power)".

For references of practical interest, the curve of "fixed power, fixed channel" shows the performance of traditional non-secure V2V communication without adaptive features. The curve of "random power, random channel" shows an intuitive countermeasure, in which a legitimate vehicle changes its operation parameters constantly regardless of circumstances. The "proposed method" is compared with all those methods using a number of evaluation metrics. In order to directly show the performance degradation in the case of inaccurate distance estimation, "proposed method (with distance error)" is also presented. In addition, the curve of "no jamming scenario" serves as a benchmark, which shows the performance of proposed method in an ideal scenario where there is no jamming signal at all.

4.7.1 Parameter Settings

According to IEEE 802.11p standard and WAVE specifications [141], the channel bandwidth is set to be 10 MHz in the 5.9 GHz frequency band. The total number of available channels is set to be $C = 4$, being a portion of all 6 service channels allocated for DSRC-based communications. The maximum transmission power is 23 dBm, and the PSD of thermal noise is -174 dBm/Hz with a noise figure of 9 dB [176, 177]. The total number of discrete transmission power for both vehicle V_1 and the jammer is $M = N = 6$. The accuracy factors of vehicle V_1 and the jammer are $h = 0.8$ and $l = 0.9$, respectively. The transmission costs per unit power are $c_V = c_J = 0.2$ [151], and the discounting factors are $\gamma_1 = \gamma_2 = 0.5$. The unit cost for each channel switching is $c_s = 0.3$. The threshold for task-switch control is set to be 3 dB. Without loss of generality, the fourth channel and a transmission power of 19 dBm are used as the fixed settings in related methods.

For the wireless propagation, the path loss at a reference distance $d_0 = 10$ m is $PL_0 = 62$ dB, the path-loss exponent is $w = 1.68$, and the variable $\boldsymbol{X}_\sigma \sim \mathcal{N}\left(0, 1.7^2\right)$ according to [171]. In the simulation, vehicles V_1 and V_2 are assumed to move at 40 km/h, while the jammer is assumed to move at 42 km/h. Initially, the distance between vehicle V_1 and V_2 is $d_V = 25$ m, and the distance between the jammer and vehicle V_2 is $d_J = 30$ m. When inaccurate distance estimation is considered, the inaccurate distances estimated by vehicles V_1 are denoted by $d_V^* = d_V + \alpha_V$ and $d_J^* = d_J + \beta_V$, with estimation errors α_V and β_V being assumed to be Gaussian random variables, $\alpha_V \sim \mathcal{N}\left(0, 2^2\right)$ and $\beta_V \sim \mathcal{N}\left(0, 4^2\right)$, respectively. The jammer is still assumed to have perfect distance estimation as the worst-case scenario.

Besides, the jammer is assumed to be able to intentionally withhold its attack for energy preservation, and the probability for initiating attack is set to be 0.5. The total number of PACs is chosen as 200, while the number of internal iterations within one PAC is 50. The simulation results are averaged over 300 runs.

4.7.2 Performance Comparison

To demonstrate the effectiveness of the proposed method, Figs. 4.4-4.6 have recorded the result for one random simulation run. Specifically, Fig. 4.4 shows the power strategy of vehicle V_1 in the first

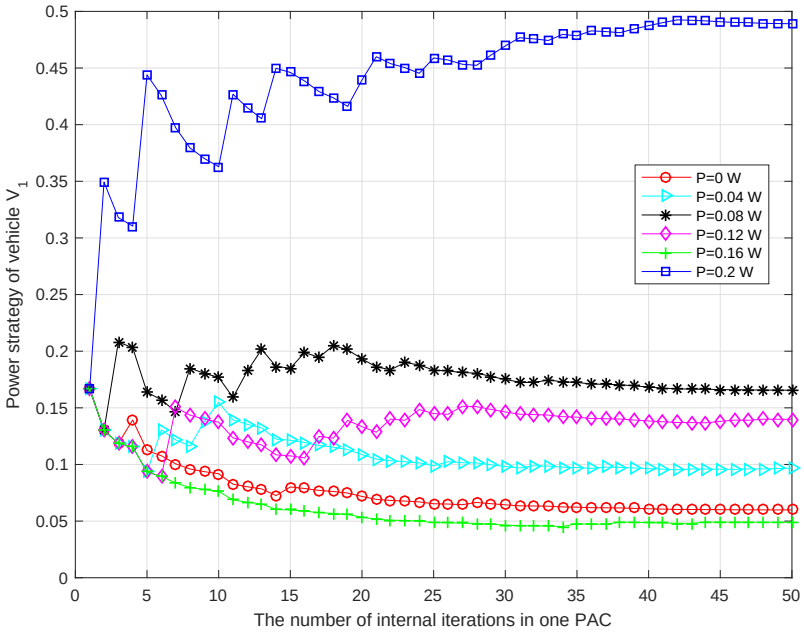

Figure 4.4: The power strategy of vehicle V_1 in one PAC.

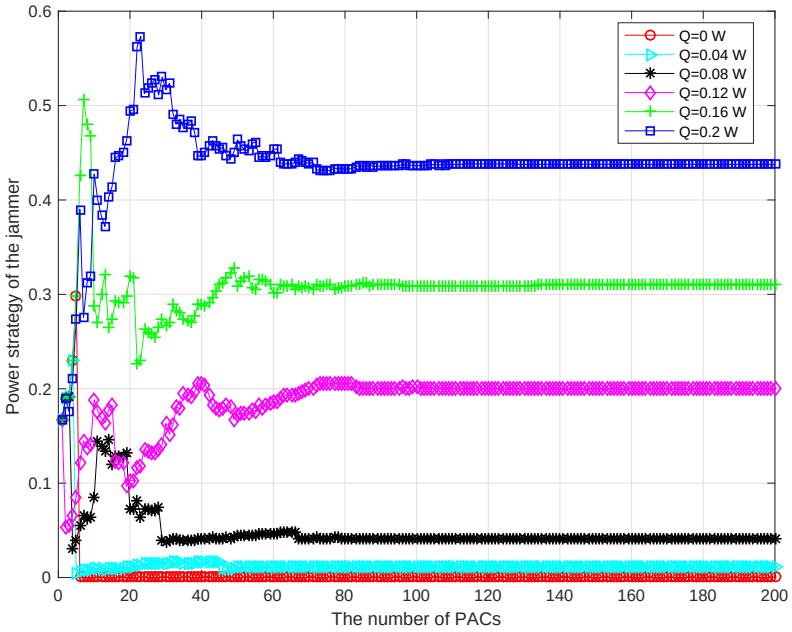

Figure 4.5: The power strategy of jammer over all the PACs.

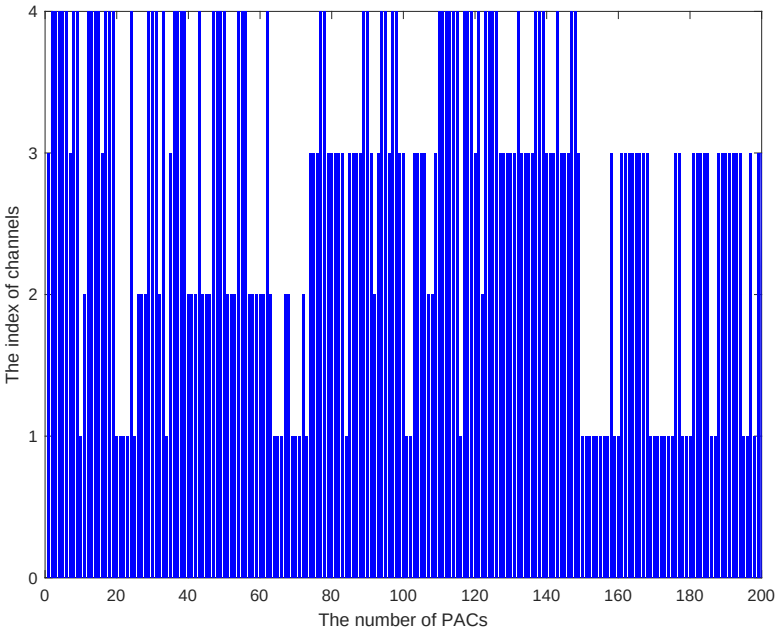

Figure 4.6: The channels used by vehicle V_1 over all the PACs.

PAC, while Fig. 4.5 shows the power strategy of the jammer over all the PACs. It can be seen that the power strategies for both of them will gradually reach a steady state. In the simulated environment, it takes about 40 and 80 iterations for vehicle V_1 and the jammer to converge, respectively. It should be pointed out that there is a significant difference between the iterations for vehicle V_1 and the iterations for the jammer. Although 80 iterations (i.e., epochs for the jammer in Fig. 4.3) seem to be a long period for achieving convergence, it is actually done on the jammer's end, which is not one of our primary concerns; on vehicle V_1's end, each one of those 80 iterations/epochs (for the jammer) corresponds to one PAC (for vehicle V_1), which contains one sensing step, one acting step, and one multiple-planning step that involves 40 internal iterations. Even though 40 is still a large number, it can be processed very fast internally since no interaction with the external environment is needed. Fig. 4.6 shows all the channels used by vehicle V_1 in face of the jamming attack, for which reason multiple channel switching have been performed to maintain reliable V2V communications.

Fig. 4.7 and Fig. 4.8 have shown the utility of vehicle V_1 and the jammer for power control, respectively. It is evident that, in an ideal scenario where there is no attack being launched, vehicle V_1 will have the highest utility while the jammer has its lowest utility. When faced with attacks, the received SINR at vehicle V_2 will decrease, resulting in a deteriorate performance no matter which method is adopted. Under such circumstances, it can be seen that the method of "power control only (with fixed channel)" has similar utility values compared with the proposed method. The reason is that they both can take advantage of power-control procedure, which is empowered by the reinforcement learning and multiple planning processes as described in Section IV. By evaluating and predicting the possible outcomes of different prospective actions, the transmission power will be adjusted in a

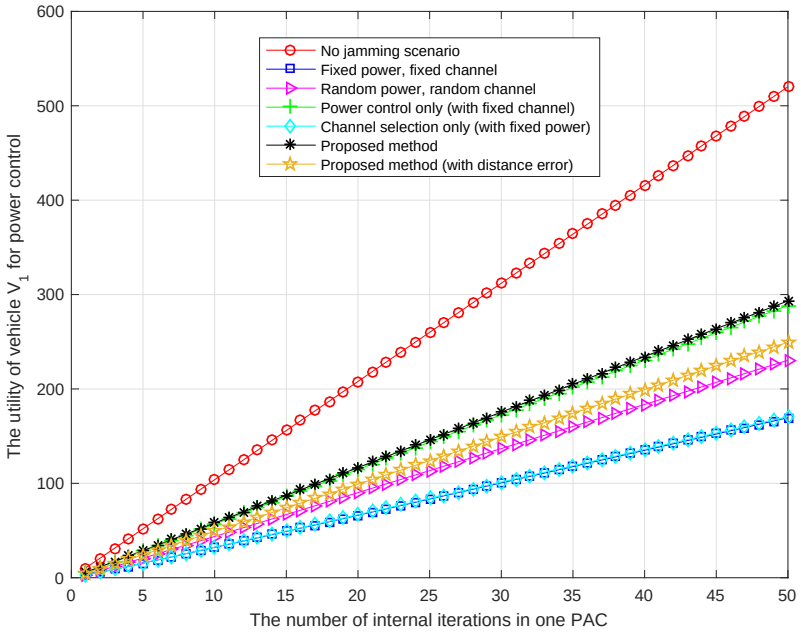

Figure 4.7: The utility of vehicle V_1 for power control.

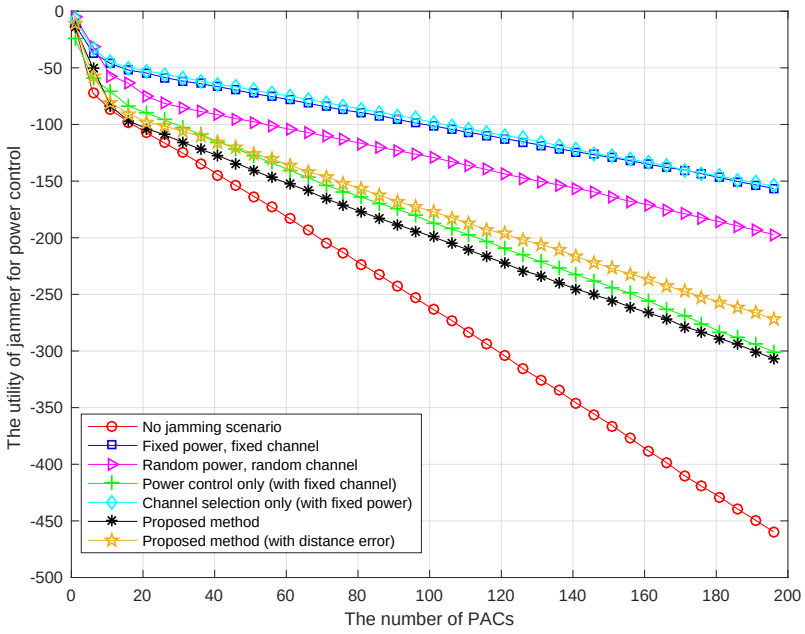

Figure 4.8: The utility of jammer for power control.

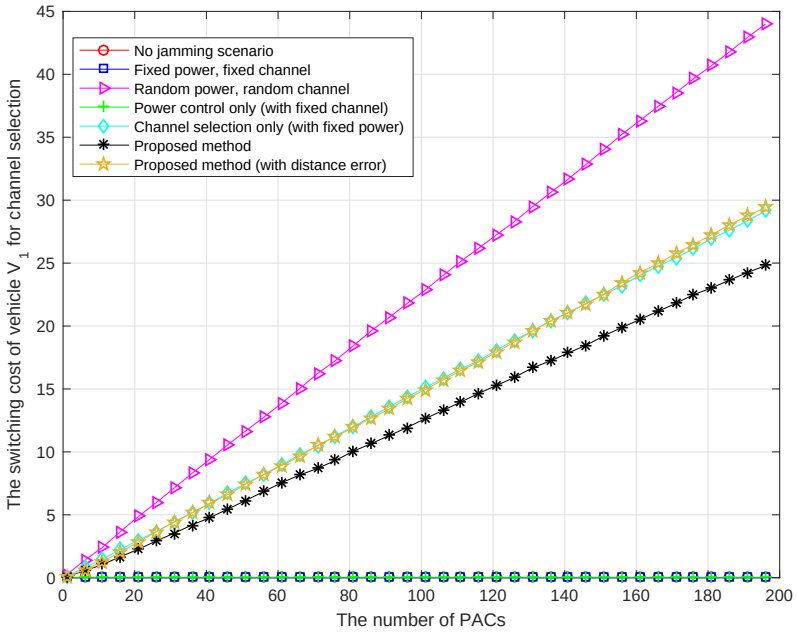

Figure 4.9: The switching cost of vehicle V_1 for channel selection.

cost-effective manner in response to the jammer's actions. From the curve of "proposed method (with distance error)", it can be seen that the performance will degrade slightly in the case of inaccurate distance estimation. Meanwhile, the methods of "channel selection only (with fixed power)" and "fixed power, fixed channel" would result in poor utility for vehicle V_1, due to the lack of adaptive capability in transmission power. The "random power, random channel" method has a moderate performance, as it may accidentally make some good choices in the power domain.

The switching cost of vehicle V_1 for channel selection is depicted in Fig. 4.9. Since the methods of "power control only (with fixed channel)" and "fixed power, fixed channel" always stay on a certain channel, there is no switching cost incurred during the whole time. As for the "no jamming scenario", the risk level would typically be assessed as 0, which means almost no channel switching is ever needed. Therefore, these three curves coincide at the bottom of Fig. 4.9. The method of "random power, random channel" has the highest switching cost, simply because it keeps changing all the time. It can also be seen that the switching cost of "channel selection only (with fixed power)" method is higher than that of the proposed method: for the former method, the only available countermeasure to defend an attack is to switch channels, which means it has no choice but to leave for a new channel whenever the predefined transmission power is deemed not satisfactory; however, for the proposed method, the wrestling between vehicle V_1 and the jammer happens in both power domain and frequency domain, which means that channel selection will only come into play as a backup plan (i.e., a fail-safe) when power control cannot handle the situation. Consequently, the proposed method will reduce unnecessary channel switching, which is particularly important for maintaining a seamless and stable connection in CAV networks. However, this advantage would be neutralized by

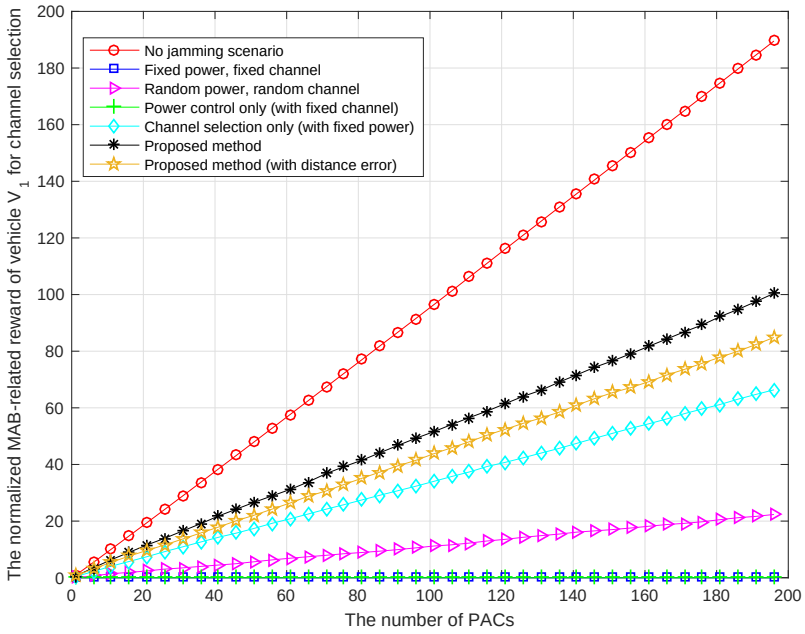

Figure 4.10: The normalized MAB-related reward of vehicle V_1 for channel selection.

the inaccurate estimation of distance, which is shown in "proposed method (with distance error)". As the evaluation for SINR level and channel quality will be negatively affected by an inaccurate distance, more channel switching will incur and the cost will increase.

Fig. 4.10 shows the normalized MAB-related reward of vehicle V_1 for channel selection. Again, being confined to only one channel, the methods of "power control only (with fixed channel)" and "fixed power, fixed channel" will have no such reward. As for the "no jamming scenario", it has the highest normalized reward thanks to the desirable received SINR: while channel switching is rarely needed, the channel in service keeps contributing to successful transmissions. The normalized reward of the proposed method is higher than that of "channel selection only (with fixed power)" method, which is mainly attributed to the difference in the number of switching times. To be specific, for those times when channel switching can be avoided by adjusting the transmission power, the previous channel will be retained for transmission and then rewarded in the proposed method, but not in the "channel selection only (with fixed power)" method as that particular channel would have been abandoned. Same explanation also applies to the "random power, random channel" method. The negative effect of inaccurate distance estimation can again be seen from the curve of "proposed method (with distance error)".

To evaluate different solutions to the channel-selection MAB problem, the overall regret of vehicle V_1 is depicted in Fig. 4.11. Not surprisingly, those two methods that cannot make use of multiple channels will result in "full" regret in terms of channel selection. The "random power, random channel" method has slightly higher regret than "channel selection only (with fixed power)" method due to its randomness, and the "proposed method (with distance error)" has slightly higher regret than the

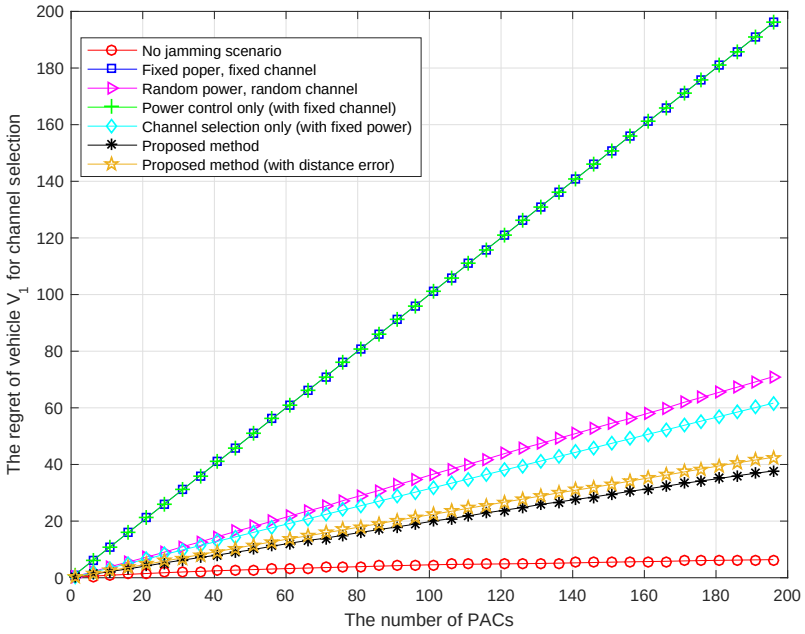

Figure 4.11: The regret of vehicle V_1 for channel selection.

"proposed method" due to inaccurate estimation. Similar to the observations made on Fig. 4.10, the "proposed anti-jamming method" is inferior to the "no jamming scenario" as a direct consequence of incoming attacks, and is superior to the method of "channel selection only (with fixed power)" due to higher normalized MAB-related reward as well as lower switching costs.

Finally, Fig. 4.12 makes a comparison in terms of the maximum achievable throughput, which characterizes the theoretical upper bound for throughput as a result of dynamic behavioral interactions between vehicle V_1 and the jammer, considering a certain bandwidth and thermal noise level. The "no jamming scenario" remains to serve as a benchmark free from any attack damage. It is noteworthy that the maximum achievable throughput of the proposed method is higher than that of other methods. Specifically, the estimation error in distance will cause a performance degradation for the proposed method. The method of "channel selection only (with fixed power)" has a decent throughput, which is maintained at the price of frequent switching and more costs. The method of "random power, random channel" reaches a regular performance as a result of unpredictable behavior. For the remaining two methods, the performance loss is mainly caused at such times when jamming signals appear on the same channel as used by legitimate V2V communications, which again stresses the great importance of adaptive capability in the frequency domain.

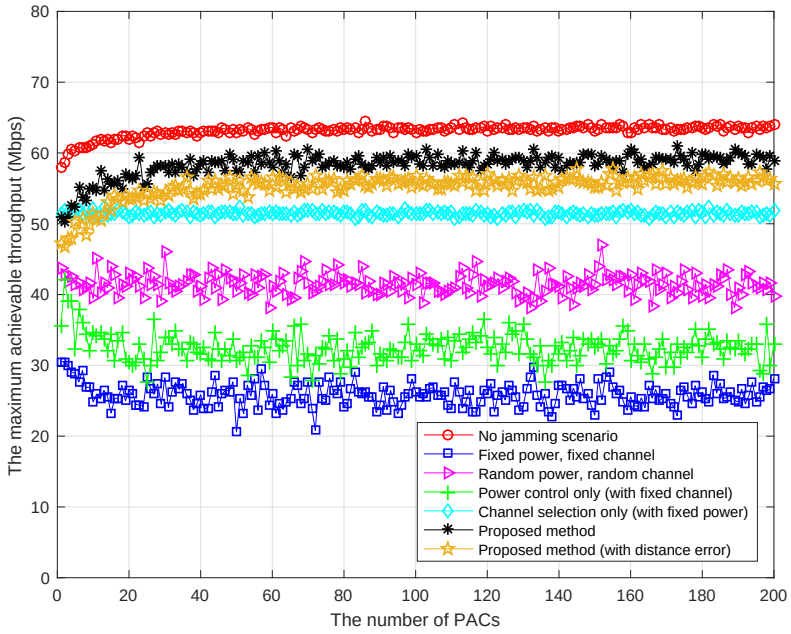

Figure 4.12: The maximum achievable throughput.

4.8 Conclusion

In this paper, we have investigated the anti-jamming V2V communication in CAV networks through power control in conjunction with channel selection. The brain-inspired CDS is applied to study V2V communications, and the general structure of CRC is tailored to analyze and address the jamming problem in CAV networks. For each PAC, the power control is carried out first using reinforcement learning method, the result of which is then examined by the task-switch control. Based on the risk assessment, an MAB problem is formulated to perform the channel-selection process when necessary. Through continuous PACs, the feature of predictive adaptation is realized for the legitimate vehicle in its behavioral interactions with the jammer. Simulation results have shown that the proposed method has desirable performance in terms of several evaluation metrics. In addition to V2V communication systems, assuming the role of a supervisor, CDS would substantially improve the performance of many other vehicle-mounted systems (e.g., vehicular radar system). In future work, we will further investigate the possible marriage of CDS and CAV network in other aspects, and bring out the full capacity of CRC in this promising research field. Some of the future research directions are given as follows:

(i) The impact of inaccurate distance estimation should be further investigated. As the distance variable between on-road vehicles plays an important role in the interference formulation and keeps changing in a dynamic vehicular environment, the real-time accuracy of distance estimation would affect the connectivity and quality of V2V communications in practice, which

deserves more attention.

(ii) As an extension of the previous point, it will be very interesting to study the mutual effect between radar tracking and vehicular communication, both of which can be empowered by cognitive risk control. On one hand, when V2V link is available, the exchanged information will be combined and utilized to improve on-road tracking; on the other hand, tracking accuracy has been demonstrated to have a direct impact on V2V communication performance. This intertwined relationship should be mathematically formulated and analyzed.

(iii) The performance of proposed approach in a large-scale network should be studied. Currently, this approach mainly focuses on a localized area and is only validated for a simple network scenario. With more vehicles joining the network, the jamming/interference condition will become much more complicated, and each individually made decision will impact all other vehicles in the neighborhood. This kind of network extension is inevitable for future ITS systems, and thus, requires dedicated research effort.

(iv) More research activities could be taken to seek new inspirations from the human brain. Relying on the most powerful biological entity that is ever known, there is a great opportunity to advance and upgrade the current design of cognitive anti-jamming V2V communications, among many other engineering applications that is in urgent need for cognitive or intelligent capabilities.

Chapter 5

Coordinated Cognitive Risk Control for Bridging Vehicular Radar and Communication Systems

5.1 Preceding Introduction

Viewing the CAV as a whole, CRC can be utilized across different vehicle-mounted systems for overall improved performance. Though either vehicular radar or the communication system is able to operate independently and CRC can be of service to both of them separately, much more can be gained through developing a bridge that helps the radar system and V2V system benefit from each other. In this chapter, the brand-new notion of C-CRC is introduced. It serves as a cognitive mediator and establishes a mutual-assistance relationship between those two systems.

The scholarly work presented herein builds upon all the research efforts made in previous chapters and takes them one step further.

The publication included in this chapter is:

S. Feng, and S. Haykin, "Coordinated Cognitive Risk Control for Bridging Vehicular Radar and Communication Systems," *IEEE Transactions on Intelligent Transportation Systems*, under review, 2019.

The co-author's contributions to the above work include:

- Technical supervision and financial support of the study presented in this work.
- Manuscript revising and editing.

Abstract

As an essential part of the emerging Internet of Things, connected and autonomous vehicles (CAVs) have the potential to reshape future transportation systems and change the commute style in people's everyday lives. Among many vehicular on-board devices, radar system and vehicle-to-vehicle (V2V) communication system are two important pillars for the realization of CAVs. Focusing on the safety and security aspects of a CAV network, the cognitive dynamic system (CDS) and its special function of cognitive risk control (CRC) have been employed to tackle risk-related issues in previous studies. In this paper, the concept of coordinated CRC (C-CRC) is proposed to serve as a cognitive mediator for bridging vehicular radar and communication systems. By establishing a mutual-assistance relationship, C-CRC provides a new safety mechanism that allows one system to learn from and react to the risks that the other system has encountered. Through continuous perception-action cycles (PACs), the feature of predictive adaptation is realized within each system as well as distributed across both systems. Simulation results have shown that the proposed method has desirable performance in face of motion perturbation and/or jamming attack under various scenarios.

5.2 Introduction

5.2.1 Vehicular Radar and Communication

With the rapid advances in vehicular hardware, machine learning, and data processing techniques, the next generation intelligent transportation system (ITS) is expected to be composed of connected and autonomous vehicles (CAVs) [112, 178]. In addition to a comfortable driving experience, CAVs can provide many other benefits over a wide range, such as improving driving safety, alleviating traffic congestion, increasing usage efficiency of parking spaces, reducing fuel consumption and air pollution, etc. [179].

For CAVs to approach the level of high automation (Level 4) or full automation (Level 5) as stated in SAE standard [139], there are several functional requirements to be fulfilled. The first one is environmental awareness, which relies on vehicle/pedestrian/bicyclist detection as well as accurate distance/velocity estimation for all the targets involved [119, 180]. Second, network connectivity is necessary for CAVs to share their individual information and make intelligent decisions collaboratively, which can be supported by reliable vehicle-to-vehicle (V2V) communications [181]. With well-developed autonomous driving algorithms and sensory inputs from different sources, steering commands such as accelerating/decelerating and lane changing/keeping can finally be made by CAVs in real time.

As a fundamental component of advanced driver-assistance systems (ADAS) [182], vehicular radar is indispensable for tracking on-road targets and achieving environmental awareness. In [183], an autonomous emergency braking (AEB) system based on both radar and camera sensors is developed to protect pedestrians. It helps to avoid accidents by sending out alerts and controlling the automatic brake actuator. A multiple-target tracking design is proposed in [184], where both low-cost radars and advanced radars are considered for detecting obstacles. A collaborative fusion approach that integrates the inputs from mmWave radar and a monocular camera is proposed in [185], which aims at achieving the optimal balance between detection accuracy and computational efficiency.

For CAVs to stay connected, V2V communication is a very straightforward yet challenging approach. Compared with cellular networks, V2V communication has its own characteristics due to high mobility of vehicles and dynamic changes in the surrounding environment [186]. In [187], the benefits of V2V communication on improving time headway in a cooperative adaptive cruise control (CACC) system is studied. In [188], an integrated framework of V2V communication and long-range radar (LRR) is formulated, and a joint vehicular communication-radar system is developed in mmWave band. To solve the problem of radio-resource allocation and platooning control in an LTE-V2V network, a joint optimization problem is formulated in [189], which minimizes the tracking error while guaranteeing the reliability of V2V communication and string stability of vehicle platooning. However, these studies have not paid enough attention to the issue of safety and security, which is a critical issue in CAV networks.

5.2.2 Cognitive Dynamic System and Cognitive Risk Control

While the connected feature of CAVs and the open nature of public roads are generally beneficial for ITS system, they leave the system itself quite vulnerable to malicious activities or malfunctioning units [17]. Both vehicular radar systems and V2V communication systems can be affected by such uncertainties, which will bring serious risk to the CAV network. The security issue has become a hot research topic recently. In [190], an automotive multi-input multi-output (MIMO) radar is designed to detect and handle sensor spoofing attacks in adaptive cruise control (ACC). To combat false data injection (FDI) attacks against a networked radar system, a data fusion algorithm that leverages on the confidence factor of injected data is proposed in [191]. In [192], the effects of security attacks (such as sensor tampering) on V2V channels is investigated, and different countermeasures are discussed for a CACC vehicle stream. Focusing on the safety-messages exchange in ITS applications, [154] investigated the real-time detection method for securing beacons against jamming attacks in vehicular networks. However, the radar and communication systems are studied separately in these works.

Inspired by certain features of the human brain, the cognitive dynamic system (CDS) is a powerful research tool for studying complex engineering applications [59]. For a CAV network, CDS can be employed to improve and coordinate the operation of multiple vehicle-mounted systems. As a special function of CDS, cognitive risk control (CRC) aims at handling the specific situations where a system of interest is operating in the presence of unexpected uncertainty [63]. By taking advantage of accumulated past experiences that are informative to the current situation, CRC actualizes the predictive adaptation feature, which is learned from prefrontal cortex of the human brain [82]. In our previous work, CRC was utilized for transmit-waveform selection in vehicular radar systems [116]; also, it was demonstrated to be effective for anti-jamming V2V communications [193]. This early research laid the foundation for the current work.

Viewing the vehicle as a whole, it is instructive to notice that CRC can be utilized across different vehicle-mounted systems for overall improved performance. Though either the radar or communication system is able to operate independently and CRC can be of service to both of them separately, much more can be gained through developing a bridge that helps radar system and V2V system benefit from each other. However, how to build such a bridge is a brand new and very challenging problem, which is the primary focus of this paper.

5.2.3 Contribution and Organization

The main contributions of this paper are summarized as follows:

(i) The brain-inspired CDS is applied to study CAV networks, and coordinated cognitive risk control (C-CRC) is proposed for bridging vehicular radar and communication systems. By exploiting the information originating from one system that is insightful for its dual system, the possibility of mutual assistance is studied, and a coordinated design on the inter-system level is conceived.

(ii) Compared with existing methods, multiple improvements are made to both radar and communication systems. For vehicular radar, a nonlinear target-tracking model that can take both basic

and expanded forms is adopted, and the cubature Kalman filter (CKF) [194] is employed in the analysis; for V2V communication, the interference formulation is based on tracking results, and practical factors such as vehicle mobility and channel availability are further considered.

(iii) Performance of the proposed method is validated in different scenarios. It is demonstrated that by having C-CRC as a mediator, the tracking accuracy of vehicular radar can be improved with the assistance of available V2V messages, and the efficiency and reliability of V2V communication will be increased with more accurate distance estimations.

Note that part of this work was presented in [195] and [196], and some preliminary results were reported therein. The main differences and new challenges of this work are: 1) For radar systems, a nonlinear model is adopted and CKF is employed for solving the target-tracking problem, which is more practical compared with the linear model and classic Kalman filter presented in [195]. 2) For communication systems, the mobility of involved vehicles is derived from the outcome of the radar system, and the factor of channel availability is considered in the decision-making, both of which were not taken into account in [196]. 3) Most importantly, the brand new notion of C-CRC is introduced and serves as a cognitive mediator for those two systems to work together and benefit from each other, the study of which builds upon all the previous efforts and takes them one step further.

The rest of this paper is organized as follows: Section II briefly describes the system model, Sections III and IV present the design of CRC for cognitive vehicular radar and cognitive vehicular communication, respectively. The functionality of C-CRC is discussed in Section V. Section VI gives an overall description of the proposed design and its implementation process. Section VII discusses the simulation results. Finally, Section VIII concludes this paper.

5.3 System Model

5.3.1 Network Scenario

As illustrated in Fig. 5.1, legitimate vehicles V_1 and V_2 are trying to track the longitudinal motion of an adversarial vehicle, i.e., the jammer. Meanwhile, vehicles V_1 and V_2 are engaged in a link for V2V communication. The jammer is trying to sabotage that communication link; it disturbs vehicle V_2 by sending out jamming signals, the act of which may also be assisted by potential eavesdropping from vehicle V_1.

Specifically, vehicle V_1 is moving forward with velocity v_x^1 and acceleration a_x^1, vehicle V_2 with v_x^2 and a_x^2, and the jammer with v_x^0 and a_x^0, respectively. The longitudinal and lateral distances between vehicle V_1 and the jammer are denoted by d_x^1 and d_y^1, while those between vehicle V_2 and the jammer are denoted by d_x^2 and d_y^2, respectively.

The set of communication channels is denoted as $\mathbf{\Theta} = \{\theta_1, \cdots, \theta_c, \cdots, \theta_C\}, 1 \leq c \leq C$, where $|\mathbf{\Theta}| = C$ is the total number of V2V channels. Due to the dynamic nature of vehicular networks, some of the channels may be unavailable or occupied from time to time. The statistical channel availability is denoted as $\mathbf{\Upsilon} = [\Upsilon_1, \cdots, \Upsilon_c, \cdots, \Upsilon_C]^T$, where variable Υ_c represents the probability of channel θ_c being available. Let parameter $\upsilon_c \in \{0, 1\}$ denote the actual status of channel θ_c with

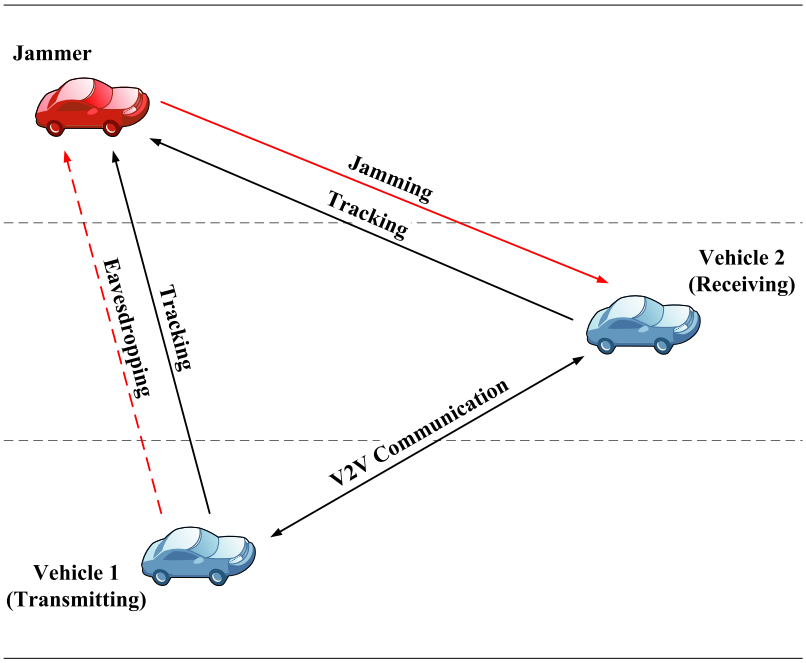

Figure 5.1: Target tracking and anti-jamming communication in a CAV network.

value 0 representing unavailable [151]. It is assumed that vehicle V_1 only selects one channel for transmission at each time step, and only one channel can be targeted by the jammer for the same time step [173].

The transmission-power set of vehicle V_1 can be denoted as $\mathbf{P} = \{P_1, \cdots, P_m, \cdots, P_M\}, 1 \leq m \leq M$, where $|\mathbf{P}| = M$ is the total number of discrete power. Similarly, the transmission-power set of the jammer can be denoted as $\mathbf{Q} = \{Q_1, \cdots, Q_n, \cdots, Q_N\}, 1 \leq n \leq N$, where $|\mathbf{Q}| = N$.

5.3.2 Coordinated Design

Fig. 5.2 has sketched out the basic design of a coordinated vehicular radar and communication system. For each individual system on the bottom, the perception-action cycle (PAC) is performed within the system itself for generating and updating actions [59]. Built upon the two pillars, a new building block called the cognitive mediator is developed in this design.

Generally speaking, the cognitive mediator aims at facilitating the interaction between those two pillar systems and guiding them to find their respective solutions in a collaborative way. With the support of a cognitive mediator, the partition between radar and communication systems is broken, which is of great importance when the vehicle is facing perturbations or under attack. In such cases, the risks that could damage one system are not only detected and taken care of within that particular system, they will also raise an alarm for the other system and certain measures will be taken in this second system to maintain its performance. In other words, the cognitive mediator will provide a new safety mechanism, which allows one system to learn from and react to the risks that the other system has encountered.

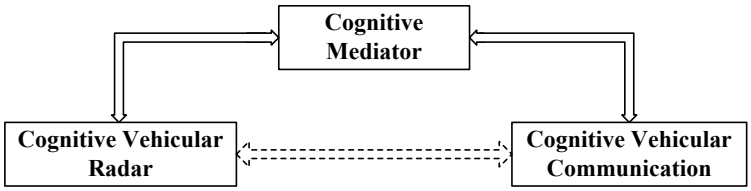

Figure 5.2: The basic design of a coordinated vehicular radar and communication system.

In this paper, the newly developed C-CRC will take the role of a cognitive mediator. More detailed discussions will be provided after regular CRC for cognitive vehicular radar and cognitive vehicular communication are presented in the next two sections, respectively.

5.4 System I: Cognitive Vehicular Radar

5.4.1 Perceptor with Nonlinear and Expandable Formulation

Different from previous work on cognitive vehicular radar [116, 195], the model formulated for target tracking in this paper is a nonlinear (and more practical) model, which cannot be solved by a classic Kalman filter. Therefore, as a good candidate for applications that require the use of nonlinear filtering under Gaussian assumption, CKF is adopted in the analysis [194]. Besides, depending on how much information is available, the filtering is formulated to alternate between basic and expanded forms.

5.4.1.1 Basic Nonlinear Formulation

If vehicle V_1 is tracking the jammer independently, the underlying state vector at time step k (i.e., in the kth PAC) can be expressed as

$$\boldsymbol{x}_k = \left[v_{x,k}^1, a_{x,k}^1, d_{x,k}^1, v_{x,k}^0, a_{x,k}^0\right]^T.$$

In such cases, the basic form of state equation that describes system evolvement is formulated as follows:

$$\boldsymbol{x}_{k+1} = \mathbf{F}_{k+1,k}\boldsymbol{x}_k + \boldsymbol{\Gamma}_{k+1,k}u_k + \boldsymbol{w}_k, \tag{5.1}$$

with

$$\mathbf{F}_{k+1,k} = \begin{bmatrix} 1 & \delta & 0 & 0 & 0 \\ 0 & 1 & 0 & 0 & 0 \\ \delta & \delta^2/2 & 1 & -\delta & -\delta^2/2 \\ 0 & 0 & 0 & 1 & \delta \\ 0 & 0 & 0 & 0 & 1 \end{bmatrix}, \boldsymbol{\Gamma}_{k+1,k} = \begin{bmatrix} \delta \\ 0 \\ \delta^2/2 \\ 0 \\ 0 \end{bmatrix}.$$

Here, $\boldsymbol{w}_k = \boldsymbol{\Psi}_{k+1,k}\hat{\boldsymbol{w}}_k$, and

$$\boldsymbol{\Psi}_{k+1,k} = \begin{bmatrix} 0 & \delta^2/2 & 0 & 0 & 0 \\ 0 & \delta & 0 & 0 & 0 \\ 0 & \delta^3/6 & 0 & 0 & -\delta^3/6 \\ 0 & 0 & 0 & 0 & \delta^2/2 \\ 0 & 0 & 0 & 0 & \delta \end{bmatrix}.$$

In the state equation, the transition matrix is denoted as $\mathbf{F}_{k+1,k}$. Variable u_k represents the acceleration/deceleration due to known forces acting on vehicle V_1, and matrix $\boldsymbol{\Gamma}_{k+1,k}$ describes how u_k will affect the evolvement of state dynamics. Moreover, $\boldsymbol{w}_k$ denotes the additive process noise with $\hat{\boldsymbol{w}}_k$ being Gaussian $\hat{\boldsymbol{w}}_k \sim \mathcal{N}\left(0, \hat{\mathbf{Q}}_{w,k}\right)$, and matrix $\boldsymbol{\Psi}_{k+1,k}$ describes how stochastic changes will affect the system. The symbol δ denotes a small time period used for discretization.

Since $\hat{\boldsymbol{w}}_k$ is assumed to be zero-mean Gaussian, the covariance matrix of process noise $\boldsymbol{w}_k$ is expressed as

$$\begin{aligned} \mathbf{Q}_{w,k} &= \boldsymbol{\Psi}_{k+1,k}\hat{\mathbf{Q}}_{w,k}\boldsymbol{\Psi}_{k+1,k}^T \\ &= \begin{bmatrix} \delta^4/4 & \delta^3/2 & \delta^5/12 & 0 & 0 \\ \delta^3/2 & \delta^2 & \delta^4/6 & 0 & 0 \\ \delta^5/12 & \delta^4/6 & \delta^6/18 & -\delta^5/12 & -\delta^4/6 \\ 0 & 0 & -\delta^5/12 & \delta^4/4 & \delta^3/2 \\ 0 & 0 & -\delta^4/6 & \delta^3/2 & \delta^2 \end{bmatrix} \hat{\mathbf{Q}}_{w,k}. \end{aligned}$$

The first matrix on the right-hand side can be denoted as $\mathbf{R}$ for future use.

With data collected from on-board sensors, the range and range rate of the jammer can be measured by vehicle V_1. Hence, the measurement vector is expressed as

$$\boldsymbol{z} = [r_1, \dot{r_1}]^T,$$

where the range is $r_1 = \sqrt{\left(d_x^1\right)^2 + \left(d_y^1\right)^2}$, and range rate $\dot{r_1}$ is the first-order derivative of r_1. Consequently, the measurement equation can be expressed as

$$\boldsymbol{z}_k = \mathbf{b}\left(\boldsymbol{x}_k\right) + \boldsymbol{v}_k = \left[\sqrt{\left(\boldsymbol{x}_k\left[3\right]\right)^2 + \left(d_y^1\right)^2}, \frac{\boldsymbol{x}_k\left[1\right] + \delta\boldsymbol{x}_k\left[2\right] - \boldsymbol{x}_k\left[4\right] - \delta\boldsymbol{x}_k\left[5\right] + \delta u_k}{\sqrt{\left(\boldsymbol{x}_k\left[3\right]\right)^2 + \left(d_y^1\right)^2}}\right]^T + \boldsymbol{v}_k, \tag{5.2}$$

where $\boldsymbol{v}_k$ is the measurement noise whose covariance matrix is denoted as $\mathbf{Q}_{v,k}$.

For a linear frequency modulated (LFM) waveform with Guassian amplitude modulation, the measurement noise covariance matrix can be expressed as [131]

$$\mathbf{Q}_{v,k}\left(\zeta_{k-1}\right) = \begin{bmatrix} \frac{c^2\lambda^2}{2\eta} & -\frac{c^2 b\lambda^2}{2\pi f_c \eta} \\ -\frac{c^2 b\lambda^2}{2\pi f_c \eta} & \frac{c^2}{(2\pi f_c)^2\eta}\left(\frac{1}{2\lambda^2} + 2b^2\lambda^2\right) \end{bmatrix}, \tag{5.3}$$

where vector $\zeta_{k-1} = [\lambda_{k-1}, b_{k-1}]^T$ denotes the transmit waveform generated at time step $k-1$, with λ

and b denote pulse length and frequency sweep rate, respectively. Moreover, constant c is the speed of light, f_c is the carrier frequency, and η denotes the received signal-to-noise ratio (SNR), which is calculated as

$$\eta = \left(\frac{r_0}{r_1}\right)^4, \tag{5.4}$$

where r_0 represents the range at which 0dB SNR is obtained.

5.4.1.2 Expanded Nonlinear Formulation

Whenever the V2V link between vehicles V_1 and V_2 is connected, tracking information (about the jammer) obtained by vehicle V_2 can be shared with and exploited by vehicle V_1. In such cases, the state vector can be expanded and expressed as

$$\boldsymbol{x}_k^* = \left[\boldsymbol{x}_k^T, v_{x,k}^2, a_{x,k}^2, d_{x,k}^2\right]^T = \left[v_{x,k}^1, a_{x,k}^1, d_{x,k}^1, v_{x,k}^0, a_{x,k}^0, v_{x,k}^2, a_{x,k}^2, d_{x,k}^2\right]^T,$$

the expanded form of state equation will be rewritten as

$$\boldsymbol{x}_{k+1}^* = \mathbf{F}_{k+1,k}^* \boldsymbol{x}_k^* + \boldsymbol{\Gamma}_{k+1,k}^* \boldsymbol{u}_k^* + \boldsymbol{w}_k^*, \tag{5.5}$$

with

$$\mathbf{F}_{k+1,k}^* = \left(\begin{array}{c|c} \mathbf{F}_{k+1,k} & \mathbf{O} \\ \hline \mathbf{A} & \mathbf{B} \end{array}\right), \boldsymbol{\Gamma}_{k+1,k}^* = \left(\begin{array}{c|c} \boldsymbol{\Gamma}_{k+1,k} & \mathbf{O} \\ \hline \mathbf{O} & \mathbf{C} \end{array}\right),$$

$$\boldsymbol{\Psi}_{k+1,k}^* = \left(\begin{array}{c|c} \boldsymbol{\Psi}_{k+1,k} & \mathbf{O} \\ \hline \mathbf{D} & \mathbf{E} \end{array}\right),$$

where

$$\mathbf{A} = \begin{bmatrix} 0 & 0 & 0 & 0 & 0 \\ 0 & 0 & 0 & 0 & 0 \\ 0 & 0 & 0 & -\delta & -\delta^2/2 \end{bmatrix}, \mathbf{B} = \begin{bmatrix} 1 & \delta & 0 \\ 0 & 1 & 0 \\ \delta & \delta^2/2 & 0 \end{bmatrix},$$

$$\mathbf{C} = \begin{bmatrix} \delta \\ 0 \\ \delta^2/2 \end{bmatrix}, \mathbf{D} = \begin{bmatrix} 0 & 0 & 0 & 0 & 0 \\ 0 & 0 & 0 & 0 & 0 \\ 0 & 0 & 0 & 0 & -\delta^3/6 \end{bmatrix}, \mathbf{E} = \begin{bmatrix} 0 & \delta^2/2 & 0 \\ 0 & \delta & 0 \\ 0 & \delta^3/6 & 0 \end{bmatrix},$$

and $\mathbf{O}$ represents null matrices with corresponding dimensions. In addition, vector $\boldsymbol{u}_k^* = [u_k, \bar{u}_k]^T$, with $\bar{u}_k$ being a known variable to vehicle V_2. Since the process noise is now $\boldsymbol{w}_k^* = \boldsymbol{\Psi}_{k+1,k}^* \hat{\boldsymbol{w}}_k$, its covariance matrix can be expressed as

$$\mathbf{Q}_{w,k}^* = \boldsymbol{\Psi}_{k+1,k}^* \hat{\mathbf{Q}}_{w,k} \left(\boldsymbol{\Psi}_{k+1,k}^*\right)^T = \left(\begin{array}{c|c} \mathbf{R} & \mathbf{F} \\ \hline \mathbf{G} & \mathbf{H} \end{array}\right) \hat{\mathbf{Q}}_{w,k},$$

where

$$\mathbf{F} = \begin{bmatrix} 0 & 0 & 0 \\ 0 & 0 & 0 \\ 0 & 0 & \delta^6/36 \\ 0 & 0 & -\delta^5/12 \\ 0 & 0 & -\delta^4/6 \end{bmatrix}, \mathbf{G} = \begin{bmatrix} 0 & 0 & 0 & 0 & 0 \\ 0 & 0 & 0 & 0 & 0 \\ 0 & 0 & \delta^6/36 & -\delta^5/12 & -\delta^4/6 \end{bmatrix},$$

$$\mathbf{H} = \begin{bmatrix} \delta^4/4 & \delta^3/2 & \delta^5/12 \\ \delta^3/2 & \delta^2 & \delta^4/6 \\ \delta^5/12 & \delta^4/6 & \delta^6/18 \end{bmatrix},$$

and matrix $\mathbf{R}$ has been introduced earlier.

Meanwhile, the measurement equation should also be expanded to account for additional information received from vehicle V_2 through V2V communications. Moreover, the longitudinal distance between vehicles V_1 and V_2 can be retrieved from GPS or odometer readings due to their cooperative attribute [197]. As a result, the new measurement vector will be

$$z^* = \left[z^T, r_2, \dot{r_2}, r_3\right]^T = \left[r_1, \dot{r_1}, r_2, \dot{r_2}, r_3\right]^T,$$

where $r_2 = \sqrt{\left(d_x^2\right)^2 + \left(d_y^2\right)^2}$ is the range between vehicle V_2 and the jammer, range rate $\dot{r_2}$ is the first-order derivative of r_2, and r_3 is the range between vehicles V_1 and V_2.

Therefore, the expanded measurement equation can be expressed as

$$\begin{aligned} z_k^* = \mathbf{b}^*\left(\boldsymbol{x}_k^*\right) + \boldsymbol{v}_k^* = \Bigg[& \sqrt{\left(\boldsymbol{x}_k^*[3]\right)^2 + \left(d_y^1\right)^2}, \frac{\boldsymbol{x}_k^*[1] + \delta\boldsymbol{x}_k^*[2] - \boldsymbol{x}_k^*[4] - \delta\boldsymbol{x}_k^*[5] + \delta u_k}{\sqrt{\left(\boldsymbol{x}_k^*[3]\right)^2 + \left(d_y^1\right)^2}}, \\ & \sqrt{\left(\boldsymbol{x}_k^*[8]\right)^2 + \left(d_y^2\right)^2}, \frac{-\boldsymbol{x}_k^*[4] - \delta\boldsymbol{x}_k^*[5] + \boldsymbol{x}_k^*[6] + \delta\boldsymbol{x}_k^*[7] + \delta u_k^*}{\sqrt{\left(\boldsymbol{x}_k^*[8]\right)^2 + \left(d_y^2\right)^2}}, \sqrt{\left(\boldsymbol{x}_k^*[8] - \boldsymbol{x}_k^*[3]\right)^2 + \left(d_y^1 - d_y^2\right)^2} \Bigg]^T + \boldsymbol{v}_k^*, \end{aligned} \tag{5.6}$$

where $\boldsymbol{v}_k^*$ is the measurement noise, whose covariance matrix can be expressed as

$$\mathbf{Q}_{v,k}^*\left(\zeta_{k-1}\right) = \operatorname{diag}\left[\mathbf{Q}_{v,k}\left(\zeta_{k-1}\right), \bar{\mathbf{Q}}_{v,k}\left(\zeta_{k-1}\right), \iota\right], \tag{5.7}$$

where the new block matrix $\bar{\mathbf{Q}}_{v,k}\left(\zeta_{k-1}\right)$ is based on the SNR level $\bar{\eta}$ experienced by vehicle V_2, and parameter ι accounts for the imperfection in distance readings.

5.4.1.3 Cubature Kalman Filtering

No matter which kind of state-measurement formulation is taken, a set of computational steps well developed for CKF can now be carried out recursively, as described in [71, 194]. Recognizing that

the state equation is linear and the measurement equation is nonlinear, the Kalman gain can be computed as

$$\mathbf{G}_k = \mathbf{P}_{xz,n|n-1}\mathbf{P}^{-1}_{zz,n|n-1}, \tag{5.8}$$

where $\mathbf{P}_{xz,n|n-1}$ is the cross-covariance matrix of state $\boldsymbol{x}_k$ and measurement $\boldsymbol{z}_k$, expressed as

$$\mathbf{P}_{xz,n|n-1} = \int_{\mathbb{R}} \boldsymbol{x}_k \mathbf{b}^T(\boldsymbol{x}_k)\, \mathcal{N}\left(\boldsymbol{x}_k; \hat{\boldsymbol{x}}_{k|k-1}, \mathbf{P}_{k|k-1}\right) d\boldsymbol{x}_k - \hat{\boldsymbol{x}}_{k|k-1}\hat{\boldsymbol{z}}^T_{k|k-1}, \tag{5.9}$$

and $\mathbf{P}_{zz,n|n-1}$ is the innovations covariance matrix:

$$\mathbf{P}_{zz,n|n-1} = \int_{\mathbb{R}} \mathbf{b}(\boldsymbol{x}_k)\mathbf{b}^T(\boldsymbol{x}_k)\, \mathcal{N}\left(\boldsymbol{x}_k; \hat{\boldsymbol{x}}_{k|k-1}, \mathbf{P}_{k|k-1}\right) d\boldsymbol{x}_k - \hat{\boldsymbol{z}}_{k|k-1}\hat{\boldsymbol{z}}^T_{k|k-1} + \mathbf{Q}_{v,k}. \tag{5.10}$$

Here, $\mathbb{R}$ denotes the entire space where state $\boldsymbol{x}_k$ resides, and $\hat{\boldsymbol{z}}_{k|k-1}$ is the predicted estimate of measurement $\boldsymbol{z}_k$ given the sequence of previous measurements:

$$\hat{\boldsymbol{z}}_{k|k-1} = \int_{\mathbb{R}} \mathbf{b}(\boldsymbol{x}_k)\, \mathcal{N}\left(\boldsymbol{x}_k; \hat{\boldsymbol{x}}_{k|k-1}, \mathbf{P}_{k|k-1}\right) d\boldsymbol{x}_k. \tag{5.11}$$

Upon receipt of the new measurement $\boldsymbol{z}_k$, the filtered estimate of the state is calculated as

$$\hat{\boldsymbol{x}}_{k|k} = \hat{\boldsymbol{x}}_{k|k-1} + \mathbf{G}_k\left(\boldsymbol{z}_k - \hat{\boldsymbol{z}}_{k|k-1}\right), \tag{5.12}$$

and the covariance matrix of the filtered state-estimation error is calculated as

$$\mathbf{P}_{k|k} = \mathbf{P}_{k|k-1} - \mathbf{G}_k\mathbf{P}_{zz,n|n-1}\mathbf{G}^T_k. \tag{5.13}$$

Then, we may express the predicted estimate of the state as

$$\hat{\boldsymbol{x}}_{k+1|k} = \mathbf{F}_{k+1,k}\hat{\boldsymbol{x}}_{k|k} + \boldsymbol{\Gamma}_{k+1,k}u_k, \tag{5.14}$$

and the prediction-error covariance matrix as

$$\mathbf{P}_{k+1|k} = \mathbf{F}_{k+1,k}\mathbf{P}_{k|k}\mathbf{F}^T_{k+1,k} + \mathbf{Q}_{w,k}. \tag{5.15}$$

The recursive computation of CKF can move forward systematically and be repeated through all the PACs as required[1].

Relying on CKF, the entropic state of the perceptor at time step k can be computed as follows:

$$H^{o/*}_k = \left|\mathbf{P}^{o/*}_{k|k}\right|, \tag{5.16}$$

where $|\cdot|$ takes the determinant of a matrix.

[1]For brevity, superscript $(*)$ is omitted in CKF from eq. (5.8) through eq. (5.15) for the case of expanded formulation, bearing in mind that the same procedure can be applied to both basic and expanded formulations. Hereafter, superscript $(o/*)$ will be used if a notation applies to both forms of nonlinear filtering formulation.

5.4.2 Feedback Channel and Task-Switch Control-A (TSC-A)

Being a key component of CDS, the feedback channel connects the perceptor to the executive. Generally speaking, the entropic state of the perceptor reflects to which extent the filtered estimate is dispersed. Therefore, the internal reward is designed to reveal whether the previously selected transmit-waveform is making tracking performance better. To be exact, the internal reward can be expressed as

$$r_k^{o/*} = \frac{H_{k-1}^{o/*} - H_k^{o/*}}{H_k^{o/*}}. \tag{5.17}$$

Unfortunately, vehicular networks in practice are full of uncertainties, which will lead to undesired system behavior if no proper control is implemented. For instance, an abrupt move of the jammer (whether intentional or not), severe weather conditions, or a poorly maintained road will inevitably affect the dynamics of the original system evolvement.

To study the impact of such perturbations, a distraction vector, denoted as $\boldsymbol{m}_k$ or $\boldsymbol{m}_k^*$ (depending on the current filtering formulation), is introduced. The system evolvement then follows the equation below:

$$\boldsymbol{x}_{k+1}^{o/*} = \mathbf{F}_{k+1,k}^{o/*}\boldsymbol{x}_k^{o/*} + \boldsymbol{\Gamma}_{k+1,k}^{o/*}\boldsymbol{u}_k^{o/*} + \boldsymbol{m}_k^{o/*} + \boldsymbol{w}_k^{o/*}. \tag{5.18}$$

Naturally, the occurrence of $\boldsymbol{m}_k^{o/*}$ makes the state estimation obtained in the original model less accurate. With no prior knowledge about when the perturbations will occur or disappear, cognitive vehicular radar should have built-in capabilities to evaluate and handle the risk involved. To this end, a mechanism called task-switch control (denoted as TSC-A in this paper) is developed to implement CRC, which relies on the following formula:

$$\rho_k^{o/*} = \begin{cases} 0, & \text{if } \sum_{i=\max(1,k-L+1)}^{k} \left|\min\left[0, \operatorname{sgn}\left(r_i^{o/*}\right)\right]\right| < \beta \\ 1, & \text{otherwise} \end{cases}, \tag{5.19}$$

where $\rho_k^{o/*}$ represents the switching indicator, $\operatorname{sgn}(\cdot)$ is the sign function, $r_k^{o/*}$ is the internal reward, L is the length of a counting window, and β denotes a predefined threshold.

When the original system equation is working smoothly (be it basic or expanded), the switching indicator $\rho_k^{o/*}$ would take value 0; however, if $\rho_k^{o/*} = 1$, it indicates that the transmit-waveforms selected in the past few cycles are inadequate for overcoming the perturbations. Based on the specific value that $\rho_k^{o/*}$ takes, the executive is restructured and will choose different transmit-waveform parameters accordingly.

5.4.3 Executive for Waveform Selection and Possible Reselection

5.4.3.1 Waveform Selection

As the first building block in the executive, reinforcement learning updates the value-to-go function recursively with internal rewards:

$$\boldsymbol{J}_{k-1}(c) \leftarrow \boldsymbol{J}_{k-1}(c) + \alpha \left[r_k^{o/*} + \gamma \sum_{c_k} \pi_k(c_{k-1}, c_k) \boldsymbol{J}_k(c) - \boldsymbol{J}_{k-1}(c) \right], \tag{5.20}$$

where α is the learning-rate parameter, $\gamma \in [0,1)$ is the discount factor, and $\pi(c_{k-1}, c_k)$ represents the policy. Besides, c_{k-1} is the immediate past action (i.e., ζ_{k-1}), and c_k is the action to be selected at the current time step.

Next, the procedure of planning is performed for multiple times at each time step. Specifically, the jth prospective action $\zeta_k^j = \left[\lambda_k^j, b_k^j\right]^T$ would result in a measurement noise covariance matrix $\mathbf{Q}_{v,k+1}^{o/*,j}\left(\zeta_k^j\right)$, based on which the hypothesized innovations covariance matrix can be calculated as

$$\mathbf{P}_{zz,n+1|n}^j = \int_{\mathbb{R}} \mathbf{b}(\boldsymbol{x}_{k+1}) \mathbf{b}^T(\boldsymbol{x}_{k+1}) \mathcal{N}\left(\boldsymbol{x}_{k+1}; \hat{\boldsymbol{x}}_{k+1|k}, \mathbf{P}_{k+1|k}\right) d\boldsymbol{x}_{k+1} - \hat{\boldsymbol{z}}_{k+1|k} \hat{\boldsymbol{z}}_{k+1|k}^T + \mathbf{Q}_{v,k+1}^j, \tag{5.21}$$

the hypothesized Kalman gain can be expressed as

$$\mathbf{G}_{k+1}^j = \mathbf{P}_{xz,n+1|n} \left(\mathbf{P}_{zz,n+1|n}^j\right)^{-1}, \tag{5.22}$$

and the hypothesized filtering-error covariance matrix as

$$\mathbf{P}_{k+1|k+1}^j = \mathbf{P}_{k+1|k} - \mathbf{G}_{k+1}^j \mathbf{P}_{zz,n+1|n} \left(\mathbf{G}_{k+1}^j\right)^T. \tag{5.23}$$

Invoking eqs. (5.16) and (5.17), the hypothesized internal reward can be computed, which is then used to update the value-to-go function $\boldsymbol{J}_k(c)$. After all prospective actions are examined, the one that maximizes the value-to-go function will be selected as the cognitive action:

$$c_k = \arg\max_c \boldsymbol{J}_k(c), \tag{5.24}$$

which is a potential choice for the transmit-waveform parameter to be used in vehicular radar.

5.4.3.2 Possible Reselection

The cognitive action just obtained does not necessarily represent the end of transmit-waveform selection, rather, a reselection process will be activated if the indicator $\rho_k^{o/*}$ of TSC-A takes value 1. If $\rho_k^{o/*} = 0$, the cognitive action c_k already obtained can be directly used to reconfigure the radar transmitter; otherwise, a new module consisting of an executive memory and a classifier is further needed to bring the risk under control [63].

The executive memory is an adaptive library occupied by abundant and informative past experi-

ences. Each time a cognitive action is selected and applied in the perturbation-free situation, it is also stored in the executive memory for future reference. When the reselection of a transmit-waveform is needed, the executive memory will put forth a set of prospective past experiences, which are utilized by the classifier as follows:

$$c_k^* = \arg\min_{c \in \hat{\mathbb{B}}} dis\,(c_k, c)\,, \tag{5.25}$$

where $\hat{\mathbb{B}}$ is the set of prospective past experiences provided by the executive memory, and c_k^* represents the risk-sensitive cognitive action as the final choice for transmit-waveform. Operator $dis\,(\cdot)$ denotes the calculation of Euclidean distance in a grid reflecting transmit-waveform vector ζ. Action c_k^* is then applied to the environment for target tracking instead of c_k at the current time step, which is followed by the next PAC of cognitive vehicular radar system.

5.5 System II: Cognitive Vehicular Communication

To tackle potential attacks launched by the jammer and stay connected to other vehicles within a CAV network, vehicle V_1 should be able to make adjustments in its V2V transmission specifics when necessary. Since the accuracy of distance estimation will significantly affect the decision-making in V2V communication, tracking information gathered from vehicular radar is well exploited by the communication counterpart in this paper, which is different from previous work on cognitive vehicular communication [193, 196]. In addition to the practical consideration of vehicle mobility, the factor of wireless channel availability is also taken into account and analyzed.

5.5.1 Environmental Sensing and Interference Formulation

By equipping a low-cost sensor for physical carrier-sensing (PCS) [164], CAVs will be able to perform energy detection and learn the transmission power of their opponents. However, due to hardware limitations, the observations are typically imperfect. The power of the jamming signal Q may be perceived inaccurately by vehicle V_1. Let $\bar{\mathbf{A}}$ denote the error matrix of perceived jamming power from the perspective of vehicle V_1, we have

$$\bar{\mathbf{A}} = \left(a_{ij}\right)_{N\times N}, \tag{5.26}$$

with

$$a_{ij} = \begin{cases} h, & \text{if} \quad i = j \\ \frac{1-h}{N-1}, & \text{otherwise} \end{cases},$$

where a_{ij} represents the probability that the jamming power perceived by vehicle V_1 is Q_j while the actual jamming power is Q_i, $1 \le i, j \le N$. The accuracy factor of vehicle V_1 is denoted as $h \in [0,1]$. Similarly, the error matrix of perceived legitimate transmission power for the jammer can be denoted as

$$\bar{\mathbf{B}} = \left(b_{ij}\right)_{M\times M}, \tag{5.27}$$

with

$$b_{ij} = \begin{cases} l, & \text{if} \quad i = j \\ \frac{1-l}{M-1}, & \text{otherwise} \end{cases},$$

where b_{ij} represents the probability that the legitimate transmission power perceived by the jammer is P_j while the actual transmission power is P_i, $1 \leq i, j \leq M$. The accuracy factor of the jammer is denoted as $l \in [0,1]$.

To characterize the wireless channels between vehicles, a well-developed path-loss model for an urban V2V scenario is adopted in this paper [171]:

$$PL(r_3) = PL_0 + 10w\log_{10}\left(\frac{d}{d_0}\right) + \boldsymbol{X}_\sigma, \quad r_3 \geq d_0 \tag{5.28}$$

where PL_0 is the path loss at a reference distance d_0, d is the range between two involved vehicles, w is the path-loss exponent, and $\boldsymbol{X}_\sigma$ is a normally distributed random variable with mean zero and standard deviation σ.

Therefore, the channel gain of the transmission link between vehicles V_1 and V_2 can be expressed as

$$g_V = 10^{-PL(d_V)/10}, \tag{5.29}$$

and the channel gain of the jamming link between the jammer and vehicle V_2 can be expressed as

$$g_J = 10^{-PL(d_J)/10}, \tag{5.30}$$

where d_V denotes the range between vehicles V_1 and V_2, and d_J denotes the range between the jammer and vehicle V_2, both from vehicle V_1's perspective. Under different circumstances, the values of d_V and d_J are computed in different ways, which will be explained in detail later on.

Assuming that the legitimate vehicle V_1 is transmitting on channel θ_c, the received signal-to-interference-plus-noise ratio (SINR) at vehicle V_2 will be

$$\beta = \frac{g_V P}{BN_0 + g_J Q}, \tag{5.31}$$

where P and Q represent the transmission power of vehicle V_1 and the jammer, respectively. B is the channel bandwidth and N_0 is the noise power spectral density (PSD). Taking account of the error matrices and substituting the channel gains, the utility metric of vehicle V_1 can be expressed as

$$\hat{\mu}_V(P_m, Q_n) = \frac{\upsilon_c 10^{-PL(d_V)/10} P_m}{BN_0 + 10^{-PL(d_J)/10} \sum_{j=1}^{N} a_{nj} Q_j} - c_V P_m, \tag{5.32}$$

where υ_c is the availability status of channel θ_c, and c_V is the transmission cost per unit power for vehicle V_1. Since the purpose of a jammer is to deliberately interfere with the legitimate V2V communication, the utility metric of the jammer can be expressed as

$$\hat{\mu}_J(P_m, Q_n) = -\frac{\upsilon_c 10^{-PL(d_V)/10} \sum_{j=1}^{M} b_{mj} P_j}{BN_0 + 10^{-PL(d_J)/10} Q_n} - c_J Q_n, \tag{5.33}$$

where c_J is the transmission cost per unit power for the jammer.

5.5.2 Power Selection and Task-Switch Control-B (TSC-B)

For each PAC, the utility metrics are viewed as internal rewards and used to select the next transmission power, which would alleviate the negative impact of jamming attacks. To this end, reinforcement learning and multiple planning are carried out for power selection as the first line of defense.

In the kth PAC, the value-to-go function of reinforcement learning can be calculated as

$$\boldsymbol{J}_k\left(P^{k-1}\right) = \boldsymbol{J}_{k-1}\left(P^{k-1}\right) + \alpha\left[r_{k-1}\left(P^{k-1}\right) + \gamma_1 \max_{P^*} \boldsymbol{J}_k\left(P^*\right) - \boldsymbol{J}_{k-1}\left(P^{k-1}\right)\right], \tag{5.34}$$

where P^{k-1} is the transmission power used in the preceding cycle, α is the learning rate, $r_{k-1}\left(P^{k-1}\right) = \hat{\mu}_V\left(P^{k-1}, Q^{k-1}\right)$ represents the internal reward as a result of using power P^{k-1}. The power P^* represents the greedy action that maximizes the value-to-go function.

The policy can then be updated using the softmax function:

$$\pi_m^k = \frac{\exp\left[\boldsymbol{J}_k\left(P_m\right)/T\right]}{\sum_{m=1}^{M} \exp\left[\boldsymbol{J}_k\left(P_m\right)/T\right]}, \tag{5.35}$$

where T represents the temperature parameter.

Next, the planning will be performed for multiple times in a predictive fashion. Different from the reinforcement learning that is based on actual internal reward and only performed once in each PAC, the planning is based on hypothesized internal reward and can be performed repeatedly to improve the prediction accuracy.

The procedure of each planning step is as follows: first, a prospective action $P^{k,\omega}$ can be selected probabilistically according to the policy π^k, its hypothesized internal reward $r_k\left(P^{k,\omega}\right)$ is then calculated using eq. (5.32), the value-to-go function is updated using eq. (5.34), and the policy is updated using eq. (5.35).

After both reinforcement learning and multiple planning are completed, a new transmission power P^k will be selected, which is called the cognitive action in the vehicular communication system and is subject to approval by task-switch control (denoted as TSC-B in this paper). The reason for seeking approval is that the effort made in finding an updated transmission power does not guarantee the selected power will be satisfactory. The legitimate transmissions can still be severely distorted or even buried in jamming signals coming from the opponent.

Under such circumstances, the battlefield must be expanded from the power domain to the spectrum domain and bring in channel selection as the second line of defense. This treatment is inspired by the biophysical switching mechanism of the human brain, in which certain pathways necessary to generate appropriate responses (in face of sensory stimuli) are activated selectively [198].

If the selected power P^k were to be applied by vehicle V_1 to the environment, the received SINR at vehicle V_2 would be

$$\beta_{\text{pre}}^k = \frac{\upsilon_c 10^{-PL(d_V)/10} P^k}{BN_0 + 10^{-PL(d_J)/10} \sum_{j=1}^{N} a_{nj} Q_j^k}. \tag{5.36}$$

Note that any transmission on a preoccupied or unavailable channel (i.e., $\upsilon_c = 0$) would be of no use.

The TSC-B is performed by comparing the predicted SINR β_{pre}^{k} with a predefined threshold, which ensures that the received signals can be decoded correctly. Denote the threshold at cycle k as TSC_k, a binary risk level can be evaluated by

$$\rho_k = \begin{cases} 0, & \text{if} \quad \beta_{\text{pre}}^{k} \geq \text{TSC}_k \\ 1, & \text{otherwise} \end{cases}. \tag{5.37}$$

In practice, the value of this threshold can be designed by leveraging some prior knowledge or experiences on different V2V types.

If the risk level ρ_k is evaluated as 0, then the selected power $\boldsymbol{P}^k$ is deemed to be satisfactory and can be applied to the environment directly on the same channel; however, if ρ_k turns out to be 1, meaning a high risk, then it indicates that the process of power selection has not eliminated potential risk caused by the jammer or the availability of previous transmission channel has expired, either of which calls for the additional process of channel selection (and power reselection) to be implemented.

5.5.3 Possible Channel Selection and Power Reselection

In this paper, the channel selection is formulated as a multi-armed bandit (MAB) problem and solved by the upper confidence bound (UCB1) algorithm [174]. Each V2V communication channel for vehicle V_1 is viewed as an arm. For every PAC that involves channel selection, the channel with the highest index as defined in the UCB1 algorithm will be selected and switched to.

Let indicator function $I_t(\theta_c)$ represent whether channel θ_c was selected in a previous cycle t with $0 \leq t \leq k-1$, and let θ^t denote the channel that was actually selected in that cycle ($\theta^t = 0$ if selection was not needed). We have:

$$I_t(\theta_c) = \begin{cases} 1, & \text{if} \quad \theta^t = \theta_c \\ 0, & \text{otherwise} \end{cases}. \tag{5.38}$$

Then, the total number of channels θ_c being selected in all preceding cycles can be written as

$$L_k(\theta_c) = \sum_{t=0}^{k-1} I_t(\theta_c). \tag{5.39}$$

For each cycle $t > 0$, the MAB-related reward for channel θ_c is defined as

$$r_t(\theta_c) = \begin{cases} B\log_2\left(1+\beta_{\text{pre}}^{t}\right), & \text{if} \quad \theta^{t-1} = \theta_c \ \text{ and } \ \rho_t = 0 \\ 0, & \text{otherwise} \end{cases}, \tag{5.40}$$

where β_{pre}^{t} denotes the received SINR at cycle t. After normalization, the total reward of using channel θ_c for transmission can be written as

$$H_k(\theta_c) = \sum_{t=0}^{k-1} \hat{r}_t(\theta_c). \tag{5.41}$$

As a result, the average reward of channel θ_c will be

$$\overline{r}_k(\theta_c) = \frac{H_k(\theta_c)}{L_k(\theta_c)}. \tag{5.42}$$

Besides, the total number of channel switches that occurred in the past can be counted as follows:

$$s_k = \sum_{t=0}^{k-1} \rho_t. \tag{5.43}$$

As a common performance metric for MAB problems, the total expected regret can be calculated as follows [175]:

$$R_k = \sum_{c:\mu_c<\mu^*} (\mu^* - \mu_c)\,\mathbb{E}[L_k(\theta_c)] + c_s \sum_{c=1}^{C} \mathbb{E}[L_k(\theta_c)], \tag{5.44}$$

where μ^* represents the highest expected reward associated with the optimal channel, $\mu^* = \max_{1\le c\le C} \mu_c$, with μ_c being the unknown expected reward for any channel θ_c. $\mathbb{E}$ denotes the expectation operator, and c_s is the unit cost for each channel switching that occurred.

Invoking the UCB1 algorithm, the upper confidence index for channel θ_c at cycle k can now be calculated as

$$\delta_k(\theta_c) = \overline{r}_k(\theta_c) + \sqrt{\frac{2\ln(s_k)}{L_k(\theta_c)}}, \tag{5.45}$$

which is the sum of average reward and the so-called confidence width. Based on this index, the desired transmission channel can be selected as follows:

$$\hat{\theta}^k = \arg\max_{\theta_c \in \Theta} \delta_k(\theta_c). \tag{5.46}$$

While channel switching offers a great opportunity in the spectrum domain to escape attacks, it consumes time and computational resources to be accomplished. In order to respond more quickly and efficiently, we propose to use an executive memory in the communication system for reselecting transmission power after the channel being switched to $\hat{\theta}^k$ rather than starting power selection all over again.

Essentially, the executive memory is a storage filled with all the historical actions about selected power and its associated channel whenever $\rho_t = 0$. Through collecting and accumulating past experiences, the executive memory can be characterized by $f(P,\theta)$ and will be utilized if $\rho_k = 1$ for the current PAC. In this case, using the method of *maximum a posteriori* (MAP) estimation [71], we have

$$\hat{P}^k = \arg\max_{P\in\mathbf{P}} f\left(P|\hat{\theta}^k\right), \tag{5.47}$$

where $\hat{P}^k$ represents the reselected transmission power after the channel has been switched. It can be calculated as

$$\hat{P}^k = \arg\max_{P\in\mathbf{P}} \frac{f\left(\hat{\theta}^k|P\right) f(P)}{f\left(\hat{\theta}^k\right)} = \arg\max_{P\in\mathbf{P}} f\left(\hat{\theta}^k|P\right) f(P), \tag{5.48}$$

where $f(\theta|P)$ and $f(P)$ can be obtained from the constructed executive memory.

Consequently, the action profile consisting of a new power and a new channel at the current PAC can be denoted as $\left\{\hat{P}^k, \hat{\theta}^k\right\}$. It is called a risk-sensitive cognitive action in vehicular communication systems as it will bring the foreseeable risk under control by avoiding the jamming attack effectively.

5.6 The Mediator: Coordinated Cognitive Risk Control (C-CRC)

The previous two sections have discussed vehicular tracking and V2V communication systems implemented with regular CRC. It is noteworthy that the risk-sensitive cognitive action (in both radar and communication systems) will have two distinctive features after all this effort: 1) consistently ahead of the measurement updates by one cycle due to the predictive nature of multiple planning, and 2) bypassing the influence of uncertainty and bringing risk under control due to the adaptive nature of executive memory. Hence, we speak of the important feature of predictive adaptation, as inspired by the prefrontal cortex of human brain [82].

Obviously, the mechanism of task-switch control plays a key role in both vehicular radar and communication systems. In this section, a cognitive mediator in the form of C-CRC is discussed. It helps to establish a mutual-assistance relationship, which is beyond a simple connection and brings those two pillar systems much closer.

5.6.1 The Effect of TSC-B on Cognitive Vehicular Radar

As discussed in Section IV.B, if the anticipated SINR is higher than the threshold used in TSC-B, then the pending transmission power would lead to a successful transmission and will be put into use; otherwise, an extra means of channel switching has to be taken and a new transmission power will be found on the new channel. That is, TSC-B will decide whether the anti-jamming defense only takes place in the power domain or it is extended to the frequency domain as well.

On a related matter, it should be pointed out that TSC-B in the communication system is also a very useful indicator for guiding the operation of vehicular radar systems. In addition to the specific content of V2V messages that a vehicular communication system shares with the radar system, the operational mode of a vehicular radar can actually be adjusted according to the status of TSC-B.

As explained earlier, whenever the evaluation result of risk level ρ_k in TSC-B turns out to be zero, it means that no channel switching is further needed and the transmission will be carried out on the same channel. In this case, assuming that the vehicular channel characteristic is symmetric within a certain range [199], the tracking data gathered by vehicles V_2 can be shared through V2V links and utilized by vehicle V_1. Specifically, additional variables for the motion dynamics of vehicle V_2 and the jammer will be incorporated in the perceptor of the vehicular radar system, which now takes the

expanded nonlinear formulation of filtering with state $\boldsymbol{x}_k^*$ and measurement $\boldsymbol{z}_k^*$ at time step k. That is, the updating and predicting procedures in CKF will now be based on the two-vehicle model, meaning that vehicle V_2 is also participating in the target tracking. With more real-time information about the jammer coming from different sources, the tracking results will be more accurate. For example, after the tracking is done, the range between vehicle V_2 and the jammer will be estimated as

$$r_{2\text{est},k} = \sqrt{\left(\boldsymbol{x}_k^*[8]\right)^2 + \left(d_y^2\right)^2}, \tag{5.49}$$

which is of particular interest when it comes to the communication system.

On the other hand, if the risk level ρ_k in TSC-B is positive for some cycles, it indicates that the transmission channel would have to be changed in the V2V communication. In this case, the wireless connection will be interrupted for a short while and additional tracking data from vehicle V_2 will be inaccessible temporarily. Therefore, the updating and predicting procedures in CKF will degenerate to rely on the one-vehicle model. It means that state $\boldsymbol{x}_k^*$ and measurement $\boldsymbol{z}_k^*$ are reduced to $\boldsymbol{x}_k$ and $\boldsymbol{z}_k$, respectively, and vehicle V_1 is currently on its own for tracking the jammer. This time around, the estimated range between vehicle V_2 and the jammer will have to be based on previous estimations and be calculated as

$$r_{2\text{est},K} = \sqrt{\left(\boldsymbol{x}_k^*[8] + s_{V2,\text{est}} - s_{J,\text{est}}\right)^2 + \left(d_y^2\right)^2}, \tag{5.50}$$

where k represents a past cycle in which V2V was disconnected, K is the current cycle,

$$s_{V2,\text{est}} = (K-k)\,\boldsymbol{x}_k^*[6]\,\delta + \frac{1}{2}(K-k)^2\,\boldsymbol{x}_k^*[7]\,\delta^2$$

is the estimated distance traveled by vehicle V_2 during the disconnection period,

$$s_{J,\text{est}} = \sum_{i=k}^{K} \boldsymbol{x}_i[4]\,\delta$$

is the estimated distance traveled by the jammer, and $(K-k)\,\delta$ represents the time period since V2V was disconnected. Similarly, since the measurement r_3 is also unavailable during V2V disconnection, the estimated range between vehicles V_1 and V_2 can be expressed as

$$r_{3\text{est},K} = \sqrt{\left(\boldsymbol{x}_k^*[8] - \boldsymbol{x}_k^*[3] + s_{V2,\text{est}} - s_{V1,\text{est}}\right)^2 + \left(d_y^1 - d_y^2\right)^2}, \tag{5.51}$$

where

$$s_{V1,\text{est}} = \sum_{i=k}^{K} \boldsymbol{x}_i[1]\,\delta$$

is the distance traveled by vehicle V_1 during this period. Without external assistance, vehicle V_1 will perform tracking independently until the V2V links are reestablished on a new channel in the following cycles.

To sum up, the CKF in vehicular radar will either take the two-vehicle model or one-vehicle model in its nonlinear formulation, depending on the result of TSC-B and current availability of

V2V connections. In so doing, the tracking accuracy of the radar system can be improved whenever additional information becomes available.

5.6.2 The Effect of TSC-A on Cognitive Vehicular Communication

Just like the way that TSC-B is responsible for determining whether channel selection and power reselection are needed after a pending transmission power is picked out in the communication system, TSC-A decides whether a reselection of the transmit-waveform is needed after a pending one is picked out in the radar system. As discussed in Section III.B, TSC-A is designed to detect whether the selected transmit-waveform parameter of vehicular radar is working properly in the current situation. If the answer is positive, then the cognitive action already generated will suffice; otherwise, that action will be suspended and extra means are taken to come up with a risk-sensitive cognitive action. In such a way, TSC-A regulates the selection process of the transmit-waveform parameters in the vehicular radar system.

In addition to that, the evaluation of TSC-A also has important implications and impacts on vehicular communication. The reason behind this is that the distance variables, which have been filtered in the radar system on a cyclic basis, also serve as key inputs for the communication system. As different operating circumstances of a vehicular radar will result in different degrees of accuracy, the intermediate values of distance in a CKF should be carefully chosen for evaluating the signal strength of wireless transmissions.

To be specific, if the evaluation result of switching indicator $\rho_k^{o/*}$ in TSC-A is zero, it indicates that the vehicular radar is now working in a desirable condition, and therefore, the tracking outputs will be trustworthy. In this case, the radar system will be guided to pass on the predicted distance between vehicles to the communication system, so that the decisions made on the transmission power and/or channel will be suitable for the new distances as anticipated. That is, the distance variable(s) from the predicted estimate of the state $\hat{\boldsymbol{x}}_{k+1|k}$ or $\hat{\boldsymbol{x}}^*_{k+1|k}$, as expressed in eq. (5.14), will be used to calculate the ranges discussed in the previous subsection. Here, the feature of predictive adaptation has shown its practical value once again, which is now distributed across both systems.

On the other hand, if the switching indicator of TSC-A is evaluated to be positive, it implies that the radar system is currently going through a perturbed phase. During this phase, the tracking outcome would be less accurate, so that more conservative treatment should be considered. In this case, the radar system will be guided to pass on the updated distance between vehicles to the communication system. That is, the distance variable(s) from a filtered estimate of the state $\hat{\boldsymbol{x}}_{k|k}$ or $\hat{\boldsymbol{x}}^*_{k|k}$, as expressed in eq. (5.12), will be used instead. Since the updated distance has already taken both measurements and preceding predictions into consideration, but not yet gone though the current prediction, it is more reliable than a predicted distance in the presence of perturbations.

Going back to the aforementioned distances of d_J and d_V between the vehicles, it is now clear that they will be best estimated when the status of both vehicular radar and communication systems are taken into consideration. Specifically, TSC-A determines whether predicted distance or updated distance should be used; TSC-B decides whether eq. (5.49) or eq. (5.50) should be used for distance d_J, and whether measurement r_3 or eq. (5.51) should be used for distance d_V.

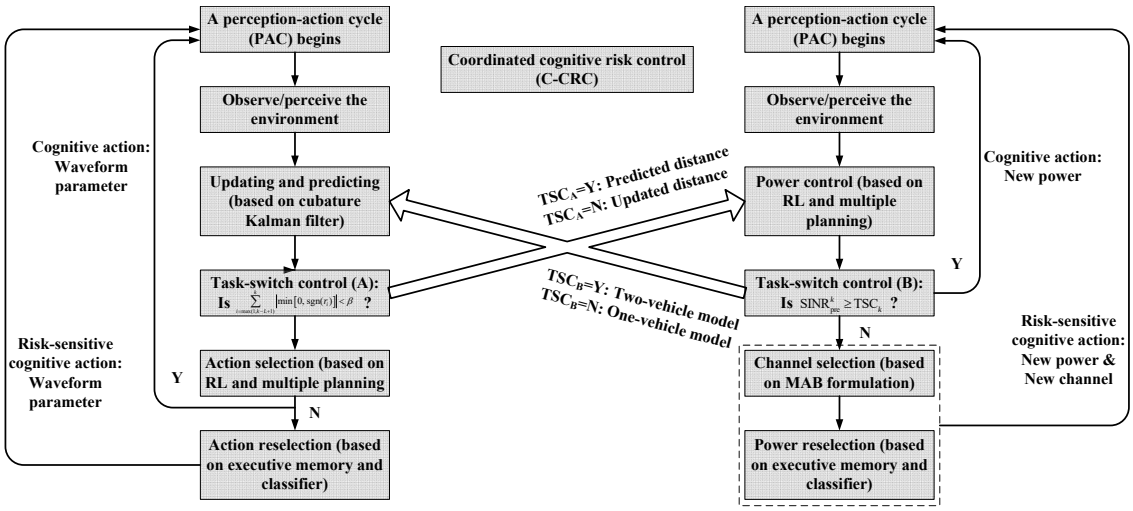

Figure 5.3: Implementation process of the proposed design for bridging vehicular radar and communication systems.

In short, when the evaluation result in TSC-A of the radar system is desirable, the interference formulation of vehicular communication should take the predicted distance between vehicles as input; otherwise, the updated distance is taken as input instead. In so doing, the communication system will further improve its performance over what it would have achieved by just implementing CRC locally.

5.7 Proposed Design and Implementation Process

Based on previous discussions, the proposed design for bridging vehicular radar and communication systems is described in Algorithm 3[2]. Besides, the implementation process of the proposed design is illustrated in Fig. 5.3. The left-hand side of Fig. 5.3 depicts the flowchart for cognitive vehicular radar, while the right-hand side of Fig. 5.3 is meant for cognitive vehicular communication. The mediator, C-CRC, sits in the middle and facilitates the mutual assistance, which helps make adjustments to one system according to the other. The effect of TSC-A on the communication system is illustrated by the upper-right pointing arrow, and the effect of TSC-B on the radar system is illustrated by the upper-left pointing arrow.

For simplicity, the procedure described in Algorithm 3 shows how this coordinated design would work if one PAC in the radar system is followed by one PAC in the communication system. It should be pointed out that the operating pace of vehicular radar is not necessarily the same as that of vehicular communication for any given vehicle. The PACs in a radar system could go faster and result in more frequent filtering estimations, or, the PACs in a communication system may be more efficient and lead to extra information exchanges. In either case, the implementation process within each system will remain the same; each individual system passes on the result of its own task-switch control the second it has been evaluated, but only checks the evaluation result from the other system when it

[2]For clarity, superscript/subscript R and C are added in some notations to differentiate the radar system and communication system, respectively.

is needed. That is, both systems will still be operating at their own paces without the requirement of inter-system synchrony. In terms of the implementation steps in Algorithm 3, it means that Line 3 through Line 16 might be repeated for several times before it moves on to Line 36 through Line 49, or the other way around, depending on which system is updated more frequently in practice.

Algorithm 3 Proposed Algorithm for Bridging Vehicular Radar and Communication Systems

Input: Radar observables $\boldsymbol{z}_k^{o/*}$, $k = 1, 2, \cdots, Z$, legitimate transmission power P_m and jamming power Q_n for each PAC, $1 \leq m \leq M$, $1 \leq n \leq N$

Output: Radar action-profile $[\lambda_k, b_k]^T$, and communication action-profile $\left\{P^k, \theta^k\right\}$

Initialization:

$\boldsymbol{x}_0^*$, $\hat{\boldsymbol{x}}_{1|0}^*$, $\mathbf{P}_{1|0}^*$, $\rho_{0,\mathrm{R}}^{o/*} = 0$, $\boldsymbol{J}_0^{\mathrm{R}}$, π_{R}^0, $\hat{\mathbf{B}}_{0,\mathrm{R}} = \varnothing$

An initial transmit-waveform action $[\lambda_0, b_0]^T$ in vehicular radar is randomly selected and applied

$\boldsymbol{J}_0^{\mathrm{C}}$, $\boldsymbol{J}_{0,J}^{\mathrm{C}}$, π_{C}^0 and $\pi_{J,\mathrm{C}}^0$, $\rho_{0,\mathrm{C}} = 0$, $\mathbf{B}_{0,\mathrm{C}} = \varnothing$

An initial power/channel action $\left\{P^0, \theta^0\right\}$ in V2V communication is randomly selected and applied

---

1: **for** $k = 1$ to Z (number of PACs) **do**
2: **System I: Cognitive Vehicular Radar**
3: Take observable $\boldsymbol{z}_k^{o/*}$
4: **if** $\rho_{k-1,\mathrm{C}} = 0$ **then**
5: Perform CKF with $\boldsymbol{x}_k^*$ and $\boldsymbol{z}_k^*$
6: **else**
7: Perform CKF with $\boldsymbol{x}_k$ and $\boldsymbol{z}_k$
8: **end if**
9: Calculate $H_k^{o/*}$, $r_k^{o/*}$, $\rho_{k,\mathrm{R}}^{o/*}$
10: Update $\boldsymbol{J}_k^{\mathrm{R}}$, π_{R}^k
11: Select $c_{k,\mathrm{R}}^p$
12: **if** $\rho_{k,\mathrm{R}}^{o/*} = 1$ **then**
13: Select $c_{k,\mathrm{R}}^*$
14: **end if**
15: Generate radar action-profile
$c_{k,\mathrm{R}} = \left(1 - \rho_{k,\mathrm{R}}^{o/*}\right) \cdot c_{k,\mathrm{R}}^p + \rho_{k,\mathrm{R}}^{o/*} \cdot c_{k,\mathrm{R}}^*$
16: Apply $c_{k,\mathrm{R}} \triangleq [\lambda_k, b_k]^T$ to the environment

---

17: **The Mediator: Coordinated Cognitive Risk Control**
18: **if** $\rho_{k,\mathrm{R}}^{o/*} = 0$ **then**
19: **if** $\rho_{k-1,\mathrm{C}} = 0$ **then**
20: Calculate $r_{2\mathrm{est}}$ with $\hat{\boldsymbol{x}}_{k+1|k}^*$
21: Take r_3 as $r_{3\mathrm{est}}$
22: **else**
23: Calculate $r_{2\mathrm{est}}$ with $\hat{\boldsymbol{x}}_{k+1|k}$

Calculate $r_{3\text{est}}$ with $\hat{\boldsymbol{x}}_{k+1|k}$
end if
else
if $\rho_{k-1,\mathrm{C}} = 0$ **then**
Calculate $r_{2\text{est}}$ with $\hat{\boldsymbol{x}}^*_{k|k}$
Take r_3 as $r_{3\text{est}}$
else
Calculate $r_{2\text{est}}$ with $\hat{\boldsymbol{x}}_{k|k}$
Calculate $r_{3\text{est}}$ with $\hat{\boldsymbol{x}}_{k|k}$
end if
end if

System II: Cognitive Vehicular Communication
Action profile $\left\{Q^k, \theta^k\right\}$ is generated and applied by the jammer
Calculate $\hat{\mu}_V\left(P^{k-1}, Q^k\right)$
Update $\boldsymbol{J}_k^{\mathrm{C}}$, π_{C}^k
Generate pending action profile $\left\{\bar{P}^k, \theta^{k-1}\right\}$
Calculate β_{pre}^k, $\rho_{k,\mathrm{C}}$
if $\rho_{k,\mathrm{C}} = 1$ **then**
Calculate $\delta_k\left(\theta_c\right)$
Select $\hat{\theta}^k$
Update $L_k\left(\theta_c\right)$, s_k
Calculate $\hat{P}^k$
end if
Generate communication action-profile
$c_{k,\mathrm{C}} = \left(1-\rho_{k,\mathrm{C}}\right) \cdot \left\{\bar{P}^k, \theta^{k-1}\right\} + \rho_{k,\mathrm{C}} \cdot \left\{\hat{P}^k, \hat{\theta}^k\right\}$
Apply $c_{k,\mathrm{C}} \triangleq \left\{P^k, \theta^k\right\}$ to the environment
$\hat{\mu}_J\left(P^k, Q^k\right)$ is calculated, $\boldsymbol{J}_{k,J}^{\mathrm{C}}$ and $\pi_{J,\mathrm{C}}^k$ are updated
end for

5.8 Simulation Results

In this section, simulation results are presented and discussed to demonstrate the performance of the proposed design, shown as "C-CRC". The performance of several existing algorithms is also provided for comparison. For transmit-waveform selection in radar tracking, the curve of "FTW" shows a vehicular radar with fixed transmit-waveform, "Q" represents the algorithm based on traditional Q-learning as described in [77], and "Tpye 1 CRC only" shows the existing CRC-based tracking algorithm proposed in [116]. For anti-jamming vehicular communications, the curve of "Fixed" strategy shows the result for vehicle V_1 staying on a fixed channel and transmitting with a constant power, "Random" strategy represents that vehicle V_1 will keep changing both channel and power randomly as an intuitive countermeasure, and "Tpye 2 CRC only" shows the existing CRC-based

anti-jamming algorithm proposed in [193].

In the simulations, we consider four different cases, each of which represents a scenario that CAVs may encounter in a practical environment. Case 1 stands for the most ideal scenario, where there is no motion perturbation or jamming attack at all. Case 2 represents that the jammer is changing its movement abruptly without launching a jamming attack, while Case 3 represents that the jammer is moving normally but starts to attack the legitimate V2V link. Case 4 shows the worst scenario, where the jammer is misbehaving in motion and attacking the V2V system at the same time.

5.8.1 Parameter Settings

As depicted in Fig. 5.1, the vehicles are assumed to be moving in adjacent lanes with $d_y^1 = 6\text{m}$ and $d_y^2 = 3\text{m}$. The carrier frequency of vehicular radar is $f_c = 77\text{GHz}$. Linear frequency modulation is adopted with both up-sweep and down-sweep chirps, with

$$\{\lambda \in [10e\text{-}6, 300e\text{-}6], b \in [-300e8, 300e8]\},$$

and grid step-size $\Delta\lambda = 10e\text{-}6$ and $\Delta b = 20e8$. The reference range is set to be $r_0 = 1\text{km}$. The learning rate is $\alpha = 0.1$, discount factor is $\gamma = 0.5$, and the threshold for TSC-A is $\beta = 3$.

The true value of the initial state in the expanded nonlinear formulation of CKF is set to be

$$\boldsymbol{x}_0^* = \left[\boldsymbol{x}_0^T, 65\text{km/h}, 2\text{m/s}^2, 300\text{m}\right]^T,$$

with the estimation of initial state and covariance matrix as

$$\hat{\boldsymbol{x}}_{1|0}^* = \left[\hat{\boldsymbol{x}}_{1|0}^T, 60\text{km/h}, 0\text{m/s}^2, 400\text{m}\right]^T,$$

$$\mathbf{P}_{1|0}^* = \text{diag}\left(\left[10^3, 1, 10^3, 10^3, 1, 10^3, 1, 10^3\right]\right).$$

Here,

$$\boldsymbol{x}_0 = \left[70\text{km/h}, 2.5\text{m/s}^2, 200\text{m}, 80\text{km/h}, 3\text{m/s}^2\right]^T,$$

$$\hat{\boldsymbol{x}}_{1|0} = \left[65\text{km/h}, 0\text{m/s}^2, 250\text{m}, 75\text{km/h}, 0\ \text{m/s}^2\right]^T,$$

are the true value and estimation of initial state in the basic nonlinear formulation, respectively, with the initial covariance matrix as

$$\mathbf{P}_{1|0} = \text{diag}\left(\left[10^3, 1, 10^3, 10^3, 1\right]\right).$$

Moreover, the distraction vector is expressed as $\boldsymbol{m}_k \sim \mathcal{N}\left(0, \mathbf{Q}_{m,k}\right)$ with $\mathbf{Q}_{m,k} = \text{diag}\left(\left[1, 1, 10^2, 1, 1\right]\right)$, or $\boldsymbol{m}_k^* \sim \mathcal{N}\left(0, \mathbf{Q}_{m,k}^*\right)$ with $\mathbf{Q}_{m,k}^* = \text{diag}\left(\left[1, 1, 10^2, 1, 1, 1, 10^2\right]\right)$, depending on the current filtering formulation. The motion perturbation starts at 2.1s and ends at 3s. The total number of PACs in the vehicular radar is chosen as 100.

According to the IEEE 802.11p standard, the channel bandwidth is set to be $B = 10$ MHz in the

5.9 GHz frequency band. The total number of V2V channels is set to be $C = 4$, being a portion of all 6 service channels allocated for DSRC-based communications [142]. The transmission-power set is the same for both vehicle V_1 and the jammer, with $M = N = 6$ and the maximum transmission power being 23 dBm [176]. The PSD of thermal noise is -174 dBm/Hz with a noise figure of 9 dB. The transmission cost per unit power is $c_V = c_J = 0.2$ [151], and the discounting factor is $\gamma_1 = \gamma_2 = 0.5$. The threshold for TSC-B is set to be 3 dB. The statistical channel availability is assumed to be $\boldsymbol{\Upsilon} = [0.8, 0.8, 0.8, 0.8]^T$ unless stated otherwise.

For wireless propagation, the path loss at a reference distance $d_0 = 10$ m is $PL_0 = 62$ dB, the path-loss exponent is $w = 1.68$, and the variable $\boldsymbol{X}_\sigma \sim \mathcal{N}\left(0, 1.7^2\right)$ according to [171]. Besides, the jammer is assumed to be able to intentionally withhold its attack for energy preservation, and the probability of initiating an attack is set to be 0.5. The total number of PACs in vehicular communication is also chosen as 100, while the number of planning steps (i.e., internal iterations) within each PAC is 50.

5.8.2 Results and Discussions

5.8.2.1 Cognitive Vehicular Radar

For tracking performance, the metric of root mean-square error (RMSE) is used to evaluate different algorithms [71]. For example, the RMSE for velocity v_x^0 is defined as

$$\text{RMSE}\left(v_x^0\right) = \sqrt{\frac{1}{S}\sum_{n=1}^{S}\left(v_{x,k}^0 - \hat{v}_{x,k}^0\right)^2}, \tag{5.52}$$

where $v_{x,k}^0$ and $\hat{v}_{x,k}^0$ represent the true and filtered velocity for the jammer, respectively.

Fig. 5.4 and Fig. 5.5 have shown the RMSE of longitudinal distance d_x^1 and the jammer's velocity v_x^0, respectively, in Case 4. It is obvious that the accuracy of all algorithms will be affected after the perturbation occurs. Specifically, the fixed setting "FTW" and Q-learning based algorithm "Q" will have a severe performance decrease, since there is no built-in mechanism to deal with unexpected events. The "Tpye 1 CRC only" method is relatively more robust due to the possible reselection of transmit-waveform parameter when faced with perturbations. It is noteworthy that the proposed "C-CRC" method outperforms the other three algorithms in tracking accuracy. The performance gain is mainly achieved through utilizing the additional information obtained from V2V links. With the assistance of V2V communication (whenever it is available), the underlying state of the tracking problem can be formulated more thoroughly in a nonlinear fashion, and the measurements from another source will offer new insights on the jammer's dynamics. Compared with the "Tpye 1 CRC only" method, the proposed method will be less affected by the perturbation in terms of having lower RMSE at peak point as well as faster recovery from the deviation.

Table 5.1 and Table 5.2 present the highest RMSE of longitudinal distance d_x^1 and the jammer's velocity v_x^0, respectively, in all four cases. It can be seen that the results for Case 1 and Case 3 are desirable and quite similar, since there is no malfunctioning or misbehaving in target motions. Also, the results for Case 2 and Case 4 are similar yet much worse, due to the unexpected presence of kinematic perturbations. In any case, the "C-CRC" method will have the most desirable performance.

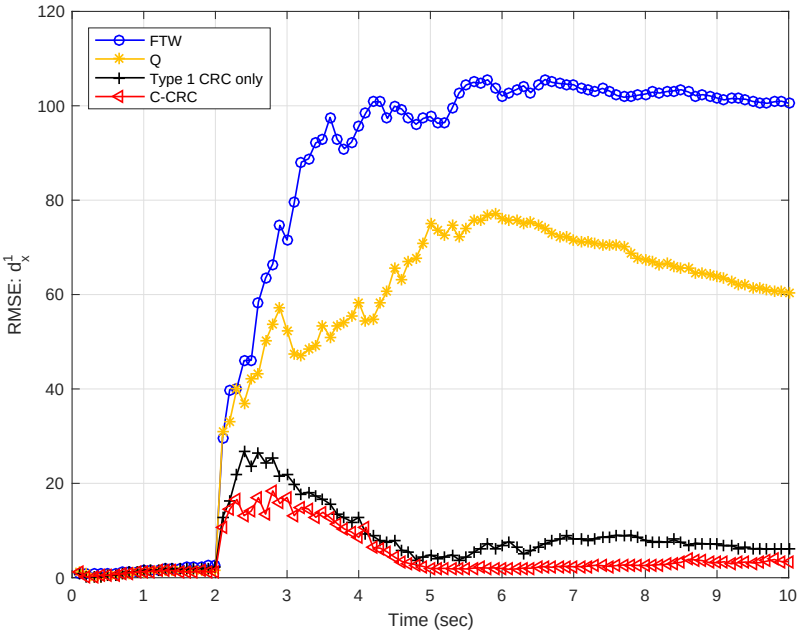

Figure 5.4: RMSE of the longitudinal distance d_x^1 (in Case 4).

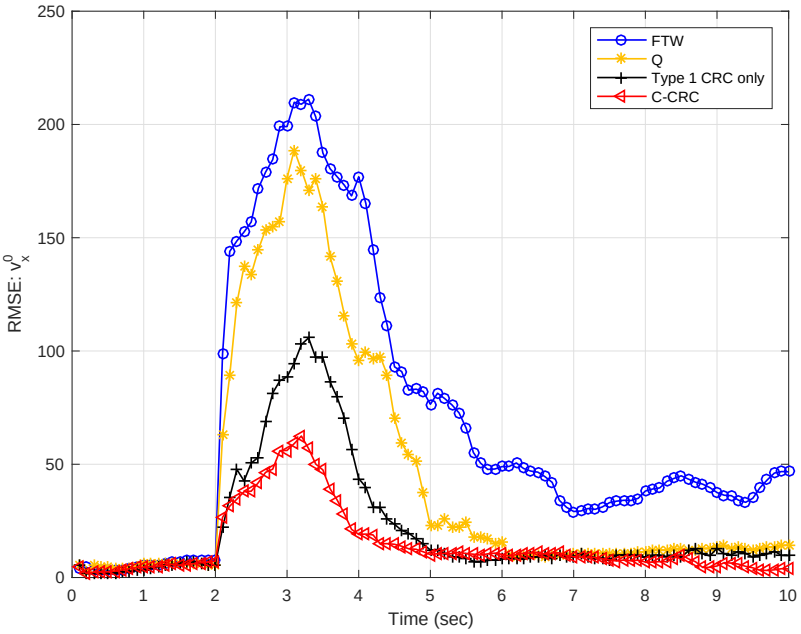

Figure 5.5: RMSE for the velocity of the jammer v_x^0 (in Case 4).

Table 5.1: The highest RMSE of the longitudinal distance d_x^1

Case # \ Algorithm	FTW	Q	Type 1 CRC only	C-CRC
Case 1	0.43	0.27	0.17	0.14
Case 2	102.31	78.91	24.45	13.65
Case 3	0.37	0.33	0.25	0.18
Case 4	105.52	77.19	26.74	18.41

Table 5.2: The highest RMSE of the velocity of the jammer v_x^0

Case # \ Algorithm	FTW	Q	Type 1 CRC only	C-CRC
Case 1	0.91	0.92	0.72	0.53
Case 2	215.10	193.04	100.26	33.52
Case 3	1.02	0.90	0.71	0.69
Case 4	211.14	188.74	105.78	62.46

It is noticeable that the performance of "C-CRC" in Case 4 is slightly worse than that in Case 2, since the V2V link that "C-CRC" usually takes additional information from is currently under the negative impact of jamming attack.

5.8.2.2 Cognitive Vehicular Communication

In terms of the communication performance, Fig. 5.6 has shown the utility of vehicle V_1 (i.e., user utility) and that of the jammer (i.e., jammer utility) for power selection, while Fig. 5.7 has shown the regret of vehicle V_1 for channel selection, all in Case 4. The "Fixed" strategy will not perform well in such an adversarial scenario since it has no adaptive ability in either the power domain or spectrum domain. The "Random" strategy has an ordinary performance, since its randomness and unpredictable behavior will be able to defend or avoid the jamming attack occasionally. The "Tpye 2 CRC only" method is more robust as it is able to perform both power selection and channel selection for adaptation. Compared with these strategies, the "C-CRC" method will result in the highest user utility, the lowest jammer utility, and the lowest regret. The reason is that "C-CRC" is capable of modifying the distance inputs according to the current status of both tracking and communication systems, thanks to cognitive mediator's involvement and regulations.

Table 5.3 and Table 5.4 show user utility and jammer utility, respectively, for power selection in all four cases. No matter which algorithm it is, the results for Case 2 are slightly worse than that for Case 1, due to inaccurate distance estimations caused by motion perturbation. More importantly, the results for Case 3 are much worse than that for Case 2. It verifies that the communication

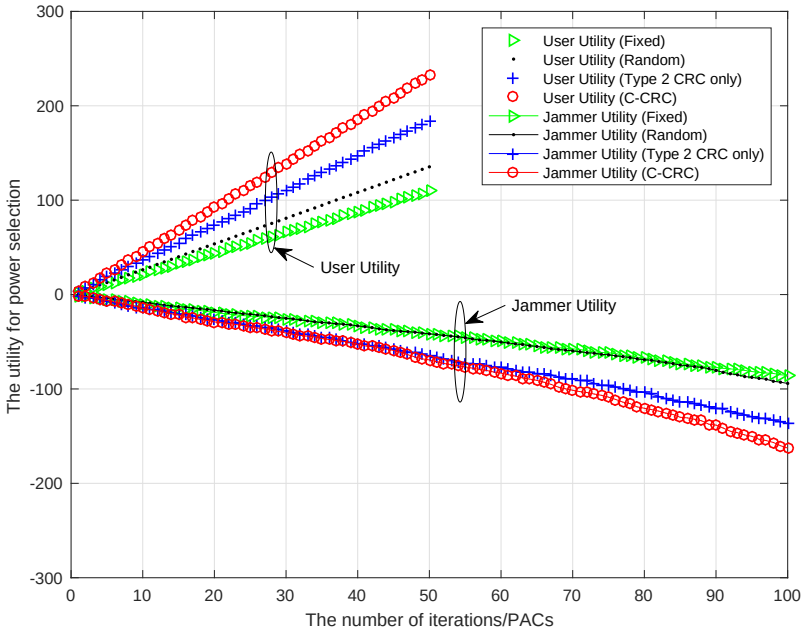

Figure 5.6: The utility of vehicle V_1 and the jammer for power selection (in Case 4).

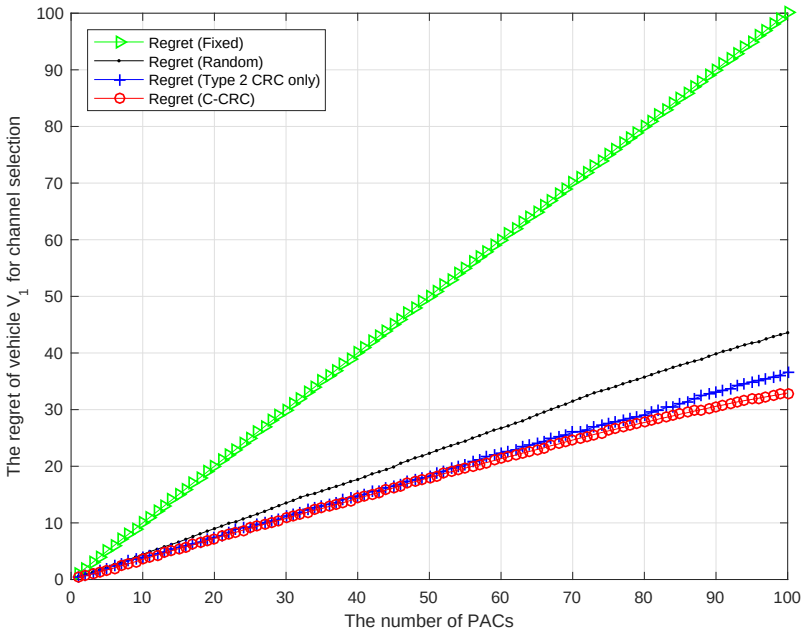

Figure 5.7: The regret of vehicle V_1 for channel selection (in Case 4).

Table 5.3: The utility of vehicle V_1 for power selection

Case # \ Algorithm	Fixed	Random	Type 2 CRC only	C-CRC
Case 1	231.05	243.52	277.15	293.39
Case 2	209.65	221.59	255.86	281.12
Case 3	112.62	145.66	188.56	235.46
Case 4	109.63	135.32	184.50	232.31

Table 5.4: The utility of the jammer for power selection

Case # \ Algorithm	Fixed	Random	Type 2 CRC only	C-CRC
Case 1	-187.49	-202.57	-245.18	-279.62
Case 2	-162.61	-188.22	-213.56	-254.26
Case 3	-100.09	-119.76	-156.47	-172.88
Case 4	-85.60	-94.14	-136.45	-162.61

Table 5.5: The total regret of vehicle V_1 for channel selection

Case # \ Algorithm	Fixed	Random	Type 2 CRC only	C-CRC
Case 1	100	42.40	22.42	19.25
Case 2	100	42.74	27.55	25.33
Case 3	100	42.26	30.72	27.54
Case 4	100	43.59	36.63	32.94

performance will be affected to a greater extent by the occurrence of a jamming attack than the input of inaccurate distance estimations. In addition, the results for Case 4 are slightly worse than that for Case 3, which demonstrates that inaccurate distance estimations on top of a jamming attack will make V2V communications even harder. In any case, the "C-CRC" method still maintains the most desirable performance compared with the rest.

Table 5.5 shows the total regret of vehicle V_1 for channel selection in all four cases. It is obvious that the "Fixed" strategy will have "full" regret as no channel switching can be made, and the "Random" strategy will have a steady regret as it has the same behavior pattern in each case. The observations we can make for "Tpye 2 CRC only" and "C-CRC" methods echo with what we have learned from Table 5.3 and Table 5.4.

Table 5.6: The effect of channel availability on power selection (for the proposed "C-CRC" method in Case 4)

Metrics / Channel Availability	User Utility	Jammer Utility
$[1,1,1,1]^T$	302.76	-196.21
$[0.8,0.8,0.8,0.8]^T$	232.31	-162.61
$[0.6,0.6,0.6,0.6]^T$	171.30	-134.77
$[0.8,0.7,0.6,0.5]^T$	192.37	-139.54

Table 5.7: The effect of channel availability on channel selection (for the proposed "C-CRC" method in Case 4)

Metrics / Channel Availability	Total Regret	MAB Reward	Switching Cost
$[1,1,1,1]^T$	24.95	63.43	4.98
$[0.8,0.8,0.8,0.8]^T$	32.94	38.77	5.91
$[0.6,0.6,0.6,0.6]^T$	37.67	21.29	9.96
$[0.8,0.7,0.6,0.5]^T$	34.65	30.89	7.14

Furthermore, Table 5.6 and Table 5.7 show the effect of channel availability on power selection and channel selection, respectively, for the proposed "C-CRC" method in Case 4. It can be seen that, with less spectrum opportunity, user utility will decrease and jammer utility will increase in power selection. Also, vehicle V_1 will have higher regret, lower MAB-related reward, and more switching costs in channel selection. It indicates that for a crowed vehicular network where many vehicles have to share wireless resources, the V2V performance would deteriorate, which is another interesting and practical problem that requires further attention and research effort.

5.9 Conclusion

In this paper, the brain-inspired CDS has been applied to study the radar tracking and anti-jamming communication in a CAV network. Serving as a cognitive mediator, C-CRC is proposed for bridging vehicular radar and communication systems. By establishing a mutual-assistance relationship that is beyond simple connection, C-CRC provides a new safety mechanism that allows one system to learn from and react to the risks that the other system has encountered. Through continuous PACs, the feature of predictive adaptation is realized within each system as well as distributed across both

systems. Simulation results have shown that the proposed method has desirable performance in the face of motion perturbation and/or jamming attacks under various scenarios. In future work, we will further investigate the security issues in a large-scale adversarial CAV network, and bring out the full capacity of C-CRC in this promising research field.

Chapter 6

Conclusion

6.1 Contributions

This thesis is the first of its kind in the sense that, for the first time two distinctive topics of CDS and CAVs are studied together, the essence of which has brought a fantastic "chemical reaction" between these two topics and led to new ways of thinking. To reiterate, the main contributions made in each chapter of this thesis can be summarized below.

6.1.1 Contributions Made in Chapter 2

The main contributions of Chapter 2 can be summarized as follows:

(i) A new class of future vehicles, namely the RACE (risk-sensitive, autonomous, connected, and electric) vehicles, is envisioned to cope with uncertain attacks and potential threats.

(ii) The safety, security and privacy issues in CAV networks are identified, and the CDS is introduced as the supervisor of RACE vehicles for improving and coordinating multiple vehicle-mounted systems.

(iii) A special function of CDS, namely CRC, is described in the presence of uncertain threats. The future directions and research challenges ahead are also presented.

To the best of the author's knowledge, this is the first theoretical work that integrates the research tool of CDS with the engineering application of CAVs.

6.1.2 Contributions Made in Chapter 3

The main contributions of Chapter 3 can be summarized as follows:

(i) The architectural structure of CRC within CDS is investigated and tailored for CVR systems. Our model is based on what we know about the mechanisms that the nervous system uses to guide the organism in behavior. The theoretical originality and importance of this model rests

mainly on the application to risk control of the predictive adaptation feature of the prefrontal cortex.

(ii) An algorithm for transmit-waveform selection in CVR systems is proposed based on CRC. In these systems, the transmit waveforms employed by the executive side of the CVR are regarded as the cognitive actions, which are continuously updated and improved under the influence of PACs. In addition, a smooth transition of the transmit waveform from one PAC to the next is guaranteed by taking localized attention mechanism into account, which will prolong the lifespan of radar hardware as well.

(iii) The first experimental demonstration of CRC is presented in the application of CVR systems. It is demonstrated that this new design will be able to achieve a performance comparable to other existing designs in the absence of uncertainty, and more importantly, to make a significant improvement in the performance even when faced with unexpected disturbances or adverse events.

To the best of the author's knowledge, the scholarly work presented herein is the first experimental work of CRC being applied to a practical vehicular system.

6.1.3 Contributions Made in Chapter 4

The main contributions of Chapter 4 can be summarized as follows:

(i) The brain-inspired CDS is applied to study V2V communications, and CRC is tailored for addressing the jamming problem in CAV networks. The novelty of this design rests mainly on the application to risk control of the predictive-adaptation property of human brain, which modern neuroscience attributes to the prefrontal cortex.

(ii) A new method based on CRC is designed for anti-jamming V2V communication in CAV networks. The power control is carried out first using reinforcement learning methods, the result of which is then examined by a module called task-switch control. Based on the risk assessment, an MAB problem is called upon to perform the channel-selection process when it is needed.

(iii) Performance of the proposed method is validated using a number of evaluation metrics. It is demonstrated that a network of switches will be able to coordinate the operations of power control and channel selection, in such a way that unnecessary operations are avoided while maintaining a desirable throughput.

To the best of the author's knowledge, the scholarly work presented herein is the first experimental work on V2V communication that involves anti-jamming, power control, and channel selection at the same time.

6.1.4 Contributions Made in Chapter 5

The main contributions of Chapter 5 can be summarized as follows:

(i) The brain-inspired CDS is applied to study CAV networks, and C-CRC is proposed for bridging vehicular radar and communication systems. By exploiting the information originating from one system that is insightful for its dual system, the possibility of mutual assistance is studied, and a coordinated design on the inter-system level is conceived.

(ii) Compared with existing methods, multiple improvements are made to both radar and communication systems. For vehicular radar, a nonlinear target-tracking model that can take both basic and expanded forms is adopted, and the CKF is employed in the analysis; for V2V communication, the interference formulation is based on tracking results, and practical factors such as vehicle mobility and channel availability are further considered.

(iii) Performance of the proposed method is validated in different scenarios. It is demonstrated that by having C-CRC as a mediator, the tracking accuracy of vehicular radar can be improved with the assistance of available V2V messages, and the efficiency and reliability of V2V communication will be increased with more accurate distance estimations.

The scholarly work presented herein builds upon all the research efforts made in previous chapters and takes them one step further.

6.2 Limitations

There are a number of limitations pertaining to the current research, especially when considering the application of the methods developed in this research to practical transportation implementation. Specifically, the following limitations may affect the applicable scenarios and deserve extra attention.

6.2.1 Network Scale is Small

As briefly mentioned in previous chapters, the scale of vehicular networks under this study is relatively small. From Chapter 3 to Chapter 5, only a portion of the entire CAV network as illustrated in Chapter 2 is considered, and only two or three vehicles are considered in each analysis. In practice, it is very likely that multiple targets need to be tracked, and many vehicles may try to communicate with each other at the same time. The detection/tracking formulation and interference topology will be more complicated when there is a large number of vehicles and other road users coexisting in the network. In such circumstances, the effect of a complex and large-scale network needs to be accounted for, which is left out in the current work.

6.2.2 System Models are Simplified

The system models adopted in Chapters 3-5 are simplified from the vehicular environment in a realistic world. Some of the practical factors are not considered in the study. For example, vehicles driving at different velocities will result in Doppler shift, which has a negative effect on the connectivity and reliability of V2V communications due to synchronization losses in the receivers. Also, the Doppler shift can either degrade or enhance radar performance depending upon how it affects the detection

and tracking processes. In addition, some special scenarios or extreme situations should be studied independently, such as on-off ramps of a highway or tunnels, the unique characteristics of which will impact both vehicular radar and communication systems. The implications of these practical factors can be further investigated.

6.2.3 A Design Gap Remains

As identified in Chapter 2, CDS can be of use for designing a variety of vehicle-mounted systems, including cognitive vehicular system, communication system, lighting system, etc., with the first two being carefully studied in this thesis. However, there is still a gap between vehicle-mounted systems and ADAS systems. The former mainly aims at obtaining accurate real-time information from sensory inputs, while the latter emphasizes on higher-level services or functions they can provide to the human driver to facilitate driving tasks. While some ADAS services can be directly built upon the output of vehicle-mounted systems, such as blind spot detection, a majority of ADAS systems require further processing and most likely involve multiple vehicle-mounted systems. How to offer such ADAS services based on the obtained information is a non-trivial problem.

6.3 Future Directions

During this research, some directions of future work have already been discussed. Viewing from the entire research project towards the end, we can identify the following topics as some of the most challenging and promising directions.

6.3.1 Extending to Large-Scale and Heterogeneous Networks

One of the drawbacks and limitations of this thesis is that the network scale considered in most sections is not large. Though it might be a sensible way to start working in a brand new area, it certainly is not enough if we want to apply those proposed methods in future transportation systems. Specifically, a large-scale and heterogeneous network should be considered, which preferably consists of multiple ground CAVs (some of which might be malicious or misbehaving), intelligent drones, satellites, pedestrians, infrastructures, and all kinds of other road users and roadside units. The vehicular radar system will perform multi-target tracking using methods such as interacting multiple model (IMM), and the vehicular communication system will take aggregated jamming signals and mutual interference into account while considering the heterogeneous feature of different entities. The effort put in this path will bring the current work closer to its application in a complex vehicular environment.

6.3.2 Leveraging Recent Advances in Artificial Intelligence

It is truly amazing how much progress has been made in the area of artificial intelligence and machine learning in the past few years. Among others, deep Boltzmann machine, CNN, RNN, long short-term memory (LSTM), DRL, and autoencoder have been extensively used to develop various algorithms for

CAVs. Generally, the intelligence required for CAVs can be viewed as a specialized subfield of artificial intelligence, the proper use of which will undoubtedly accelerate the development pace of CAVs. For example, recent advances in computer vision-based methods have been constantly increasing the level of perception accuracy on an annual basis, and DRL-based methods are getting better and better on the control side by finding the optimal decisions in various situations efficiently. There is much to be gained from taking advantage of the achievements of artificial intelligence.

6.3.3 Upgrading to a Multi-Layered Hierarchical CDS

The CDS adopted in this thesis has a single-layered structure for every building block. Although the structure so defined is powerful enough for some of the practical applications, there is a great potential of going beyond the information capacity of a single-layered CDS. From a neuroscience perspective, if we were to examine the neocortical structure of the mammalian brain, we would find the existence of six-layered laminar structure within every region of the cortex (including both the perceptor part and the executive part) [200]. Furthermore, there are 32 separate neocortical areas that are implicated in visual processing, which can be organized into 10 hierarchical levels; for the somatosensory-motor hierarchy, it has 9 levels of intertwined cortical processing with at least 13 areas involved [201]. It is within the deep hierarchical structure formed by many cortical regions with six-layered laminar structure that the real computational power of the brain is harnessed. As a brain-inspired model, it is therefore logical for the CDS to be structurally expanded in a manner similar to the brain. It may be referred to as a multi-layered hierarchical CDS, or equally we speak of deep learning rooted in the CDS framework. Through introducing a new generation of multi-layered hierarchical CDS, the basic principles of cognition, namely PAC, memory, attention, and intelligence will be enhanced enormously, which may open the gate leading to a higher level of cognitive capability for many engineering applications including CAVs.

Bibliography

[1] Robert Hult, Gabriel R Campos, Erik Steinmetz, Lars Hammarstrand, Paolo Falcone, and Henk Wymeersch. "Coordination of cooperative autonomous vehicles: Toward safer and more efficient road transportation". In: *IEEE Signal Processing Magazine* 33.6 (2016), pp. 74–84 (cit. on p. 1).

[2] Eshed Ohn-Bar and Mohan Manubhai Trivedi. "Looking at humans in the age of self-driving and highly automated vehicles". In: *IEEE Transactions on Intelligent Vehicles* 1.1 (2016), pp. 90–104 (cit. on p. 1).

[3] Joshua E Siegel, Dylan C Erb, and Sanjay E Sarma. "A survey of the connected vehicle landscape–Architectures, enabling technologies, applications, and development areas". In: *IEEE Transactions on Intelligent Transportation Systems* 19.8 (2017), pp. 2391–2406 (cit. on p. 1).

[4] Philip Koopman and Michael Wagner. "Autonomous vehicle safety: An interdisciplinary challenge". In: *IEEE Intelligent Transportation Systems Magazine* 9.1 (2017-Spring), pp. 90–96 (cit. on p. 1).

[5] Marco Brilli Alessandra Pieroni Noemi Scarpato. "Industry 4.0 Revolution in Autonomous and Connected Vehicle A Non-Conventional Approach to Manage Big Data". In: *Journal of Theoretical and Applied Information Technology* 96.1 (2018-01) (cit. on p. 1).

[6] Juan Antonio Guerrero-Ibanez, Sherali Zeadally, and Juan Contreras-Castillo. "Integration challenges of intelligent transportation systems with connected vehicle, cloud computing, and Internet of Things technologies". In: *IEEE Wireless Communications* 22.6 (2015), pp. 122–128 (cit. on p. 1).

[7] Steven E Shladover. "Connected and automated vehicle systems: Introduction and overview". In: *Journal of Intelligent Transportation Systems* 22.3 (2018), pp. 190–200 (cit. on p. 1).

[8] Society of Motor Manufacturers and Traders. *Connected and Autonomous Vehicles: SMMT Position Paper*. 2017-02, pp. 1–46 (cit. on p. 1).

[9] Federal Highway Administration. *Environmental Justice Considerations for Connected and Automated Vehicles*. Washington, DC: U.S. Department of Transportation, 2016-12, pp. 1–5 (cit. on pp. 1, 2).

[10] J. Siegel, D. Erb, and S. Sarma. "Algorithms and Architectures: A Case Study in When, Where and How to Connect Vehicles". In: *IEEE Intelligent Transportation Systems Magazine* 10.1 (2018-Spring), pp. 74–87. ISSN: 1939-1390 (cit. on p. 1).

[11] Hanif Ullah, Nithya Gopalakrishnan Nair, Adrian Moore, Chris Nugent, Paul Muschamp, and Maria Cuevas. "5G Communication: An Overview of Vehicle-to-Everything, Drones, and Healthcare Use-Cases". In: *IEEE Access* 7 (2019), pp. 37251–37268 (cit. on p. 1).

[12] Sam Toglaw, Moayad Aloqaily, and Ala Abu Alkheir. "Connected, Autonomous and Electric Vehicles: The Optimum Value for a Successful Business Model". In: *2018 Fifth International Conference on Internet of Things: Systems, Management and Security*. IEEE. 2018, pp. 303–308 (cit. on p. 2).

[13] R. Oorni and A. Goulart. "In-Vehicle Emergency Call Services: eCall and Beyond". In: *IEEE Communications Magazine* 55.1 (2017-01), pp. 159–165 (cit. on p. 2).

[14] Kang Miao Tan, Vigna K. Ramachandaramurthy, and Jia Ying Yong. "Integration of electric vehicles in smart grid: A review on vehicle to grid technologies and optimization techniques". In: *Renewable and Sustainable Energy Reviews* 53 (2016), pp. 720–732. ISSN: 1364-0321. DOI: https://doi.org/10.1016/j.rser.2015.09.012 (cit. on p. 2).

[15] S. Bitam, A. Mellouk, and S. Zeadally. "VANET-cloud: a generic cloud computing model for vehicular Ad Hoc networks". In: *IEEE Wireless Communications* 22.1 (2015-02), pp. 96–102 (cit. on p. 2).

[16] Elisabeth Uhlemann. "Initial steps toward a cellular vehicle-to-everything standard [connected vehicles]". In: *IEEE Vehicular Technology Magazine* 12.1 (2017-02), pp. 14–19 (cit. on p. 2).

[17] S. Parkinson, P. Ward, K. Wilson, and J. Miller. "Cyber Threats Facing Autonomous and Connected Vehicles: Future Challenges". In: *IEEE Trans. Intell. Transp. Syst.* 18.11 (2017-11), pp. 2898–2915 (cit. on pp. 3, 26, 42, 71, 100).

[18] Herndon Green. "Radio-Controlled Automobile". In: *Radio News* 7.6 (1925-11), pp. 592–656 (cit. on p. 3).

[19] T. Luettel, M. Himmelsbach, and H. J. Wuensche. "Autonomous Ground Vehicles—Concepts and a Path to the Future". In: *Proc. IEEE* 100.Special Centennial Issue (2012-05), pp. 1831–1839. ISSN: 0018-9219. DOI: 10.1109/JPROC.2012.2189803 (cit. on pp. 3, 41, 71).

[20] Mohamed Elbanhawi, Milan Simic, and Reza Jazar. "In the passenger seat: Investigating ride comfort measures in autonomous cars". In: *IEEE Intelligent Transportation Systems Magazine* 7.3 (2015), pp. 4–17 (cit. on p. 3).

[21] National Highway Traffic Safety Administration. *Preliminary statement of policy concerning automated vehicles*. Washington, DC: U.S. Department of Transportation, 2013-05, pp. 1–14 (cit. on p. 3).

[22] SAE International. *Taxonomy and Definitions for Terms Related to Driving Automation Systems for On-Road Motor Vehicles*. SAE Standard J3016, 2018-06, pp. 1–35. DOI: https://doi.org/10.4271/J3016_201806. URL: https://doi.org/10.4271/J3016_201806 (cit. on p. 3).

[23] Harold M Morrison, Albert F Welch, and Eugene A Hanysz. "Automatic highway and driver aid developments". In: *SAE Transactions* 69 (1961), pp. 31–53 (cit. on p. 4).

[24] Sebastian Thrun, Mike Montemerlo, Hendrik Dahlkamp, David Stavens, Andrei Aron, James Diebel, Philip Fong, John Gale, Morgan Halpenny, Gabriel Hoffmann, et al. "Stanley: The robot that won the DARPA Grand Challenge". In: *Journal of field Robotics* 23.9 (2006), pp. 661–692 (cit. on p. 4).

[25] CB Insights. *46 Corporations Working On Autonomous Vehicles*. Accessed: 2019-06-25. 2018-09. URL: https://www.cbinsights.com/research/autonomous-driverless-vehicles-corporations-list/ (visited on 2018-09-04) (cit. on pp. 4, 6).

[26] Lyudmyla Novosilska. *Top Technology Companies Driving the Connected Car Revolution*. Accessed: 2019-06-25. 2018-11. URL: https://igniteoutsourcing.com/automotive/connected-car-companies/ (visited on 2018-11-29) (cit. on p. 4).

[27] Sebastian Thrun. *What we're driving at*. Accessed: 2019-06-25. 2010-10. URL: https://googleblog.blogspot.com/2010/10/what-were-driving-at.html (visited on 2010-10-09) (cit. on p. 4).

[28] Philip E Ross. "The Audi A8: The world's first production car to achieve level 3 autonomy". In: *IEEE Spectrum* (2017) (cit. on p. 5).

[29] Navigant Research Leaderboard Report. *Automated Driving Vehicles: Assessment of Strategy and Execution for 20 Companies Developing Automated Driving Systems*. Accessed: 2019-06-25. 2019-01. URL: https://www.navigantresearch.com/reports/navigant-research-leaderboard-automated-driving-vehicles (visited on 2019-01-01) (cit. on p. 6).

[30] Elisabeth Behrmann David Welch. *Who's Winning the Self-Driving Car Race?* Accessed: 2019-06-25. 2018-10. URL: https://www.bloomberg.com/news/features/2018-05-07/who-s-winning-the-self-driving-car-race (visited on 2018-10-04) (cit. on p. 6).

[31] Mariusz Bojarski, Davide Del Testa, Daniel Dworakowski, Bernhard Firner, Beat Flepp, Prasoon Goyal, Lawrence D Jackel, Mathew Monfort, Urs Muller, Jiakai Zhang, et al. "End to end learning for self-driving cars". In: *arXiv preprint arXiv:1604.07316* (2016) (cit. on p. 7).

[32] Yuchi Tian, Kexin Pei, Suman Jana, and Baishakhi Ray. "Deeptest: Automated testing of deep-neural-network-driven autonomous cars". In: *Proceedings of the 40th international conference on software engineering*. ACM. 2018, pp. 303–314 (cit. on p. 7).

[33] Weishan Dong, Jian Li, Renjie Yao, Changsheng Li, Ting Yuan, and Lanjun Wang. "Characterizing driving styles with deep learning". In: *arXiv preprint arXiv:1607.03611* (2016) (cit. on p. 7).

[34] Ashesh Jain, Amir R Zamir, Silvio Savarese, and Ashutosh Saxena. "Structural-RNN: Deep learning on spatio-temporal graphs". In: *Proceedings of the IEEE Conference on Computer Vision and Pattern Recognition*. 2016, pp. 5308–5317 (cit. on p. 7).

[35] Timothy P Lillicrap, Jonathan J Hunt, Alexander Pritzel, Nicolas Heess, Tom Erez, Yuval Tassa, David Silver, and Daan Wierstra. "Continuous control with deep reinforcement learning". In: *arXiv preprint arXiv:1509.02971* (2015) (cit. on p. 7).

[36] Volodymyr Mnih, Koray Kavukcuoglu, David Silver, Andrei A Rusu, Joel Veness, Marc G Bellemare, Alex Graves, Martin Riedmiller, Andreas K Fidjeland, Georg Ostrovski, et al. "Human-level control through deep reinforcement learning". In: *Nature* 518.7540 (2015), p. 529 (cit. on p. 7).

[37] Max Jaderberg, Volodymyr Mnih, Wojciech Marian Czarnecki, Tom Schaul, Joel Z Leibo, David Silver, and Koray Kavukcuoglu. "Reinforcement learning with unsupervised auxiliary tasks". In: *arXiv preprint arXiv:1611.05397* (2016) (cit. on p. 7).

[38] Chenyi Chen, Ari Seff, Alain Kornhauser, and Jianxiong Xiao. "Deepdriving: Learning affordance for direct perception in autonomous driving". In: *Proceedings of the IEEE International Conference on Computer Vision*. 2015, pp. 2722–2730 (cit. on p. 7).

[39] Ahmad El Sallab, Mohammed Abdou, Etienne Perot, and Senthil Yogamani. "End-to-end deep reinforcement learning for lane keeping assist". In: *arXiv preprint arXiv:1612.04340* (2016) (cit. on p. 7).

[40] Shai Shalev-Shwartz and Amnon Shashua. "On the sample complexity of end-to-end training vs. semantic abstraction training". In: *arXiv preprint arXiv:1604.06915* (2016) (cit. on p. 7).

[41] Ahmad EL Sallab, Mohammed Abdou, Etienne Perot, and Senthil Yogamani. "Deep reinforcement learning framework for autonomous driving". In: *Electronic Imaging* 2017.19 (2017), pp. 70–76 (cit. on p. 7).

[42] Wade Genders and Saiedeh Razavi. "Using a deep reinforcement learning agent for traffic signal control". In: *arXiv preprint arXiv:1611.01142* (2016) (cit. on p. 7).

[43] Anders Lindgren and Fang Chen. "State of the art analysis: An overview of advanced driver assistance systems (ADAS) and possible human factors issues". In: *Human factors and economics aspects on safety* (2006), pp. 38–50 (cit. on p. 7).

[44] Klaus Bengler, Klaus Dietmayer, Berthold Farber, Markus Maurer, Christoph Stiller, and Hermann Winner. "Three decades of driver assistance systems: Review and future perspectives". In: *IEEE Intelligent Transportation Systems Magazine* 6.4 (2014), pp. 6–22 (cit. on p. 7).

[45] Clara Marina Martinez, Mira Heucke, Fei-Yue Wang, Bo Gao, and Dongpu Cao. "Driving style recognition for intelligent vehicle control and advanced driver assistance: A survey". In: *IEEE Transactions on Intelligent Transportation Systems* 19.3 (2017), pp. 666–676 (cit. on p. 7).

[46] The Economist. *Look, no hands.* Accessed: 2019-06-25. 2012-08. URL: https://www.economist.com/technology-quarterly/2012/08/30/look-no-hands (visited on 2012-08-30) (cit. on p. 8).

[47] Juan Guerrero-Ibanez, Sherali Zeadally, and Juan Contreras-Castillo. "Sensor technologies for intelligent transportation systems". In: *Sensors* 18.4 (2018), p. 1212 (cit. on p. 8).

[48] Muhammad Ayaz, Mohammad Ammad-uddin, Imran Baig, et al. "Wireless sensor's civil applications, prototypes, and future integration possibilities: A review". In: *IEEE Sensors Journal* 18.1 (2017), pp. 4–30 (cit. on p. 8).

[49] World Health Organization. *Road traffic injuries.* Accessed: 2019-06-25. 2018-12. URL: https://www.who.int/en/news-room/fact-sheets/detail/road-traffic-injuries (visited on 2018-12-07) (cit. on p. 9).

[50] NHTSA's National Center for Statistics and Analysis. *2017 Fatal Motor Vehicle Crashes: Overview—Traffic Safety Facts Research Note (DOT HS 812 603).* Washington, DC: U.S. Department of Transportation, 2018-10, pp. 1–7 (cit. on p. 9).

[51] NHTSA's National Center for Statistics and Analysis. *2015 Motor Vehicle Crashes: Overview—Traffic Safety Facts Research Note (DOT HS 812 318).* Washington, DC: U.S. Department of Transportation, 2016-08, pp. 1–9 (cit. on p. 9).

[52] National Highway Traffic Safety Administration. *Critical Reasons for Crashes Investigated in the National Motor Vehicle Crash Causation Survey.* Washington, DC: U.S. Department of Transportation, 2015-02, pp. 1–2 (cit. on p. 9).

[53] NHTSA's National Center for Statistics and Analysis. *Alcohol-Impaired Driving—Traffic Safety Facts 2017 Data (DOT HS 812 630).* Washington, DC: U.S. Department of Transportation, 2018-11, pp. 1–8 (cit. on p. 9).

[54] Centers for Disease Control and Prevention. *Impaired Driving: Get the Facts.* Accessed: 2019-06-25. 2019-03. URL: https://www.cdc.gov/motorvehiclesafety/impaired_driving/impaired-drv_factsheet.html (visited on 2019-03-22) (cit. on p. 9).

[55] NHTSA's National Center for Statistics and Analysis. *A Brief Statistical Summary: Drug Involvement of Fatally Injured Drivers—Traffic Safety Facts: Crash and Stats (DOT HS 811 415).* Washington, DC: U.S. Department of Transportation, 2010-11, pp. 1–3 (cit. on p. 9).

[56] European Commission, Directorate-General Mobility and Transport, Unit C2-Road Safety. *Road safety in the European Union—Trends, Statistics and Main Challenges.* Luxembourg: Publications Office of the European Union, 2018-04, pp. 1–28 (cit. on p. 9).

[57] Office of Regulatory Analysis and Evaluation, NHTSA's National Center for Statistics and Analysis. *Preliminary Regulatory Impact Analysis: FMVSS No. 150, Vehicle-to-Vehicle Communication Technology for Light Vehicles.* Washington, DC: U.S. Department of Transportation, 2016-11, pp. 1–375 (cit. on p. 9).

[58] Dominik Wee Michele Bertoncello. *Ten ways autonomous driving could redefine the automotive world*. Accessed: 2019-06-25. 2015-06. URL: https://www.mckinsey.com/industries/automotive-and-assembly/our-insights/ten-ways-autonomous-driving-could-redefine-the-automotive-world (visited on 2015-06-01) (cit. on p. 9).

[59] S. Haykin. *Cognitive Dynamic Systems: Perception-Action Cycle, Radar and Radio*. Cambridge University Press, 2012 (cit. on pp. 10, 11, 17, 18, 29, 41, 72, 75, 100, 102).

[60] S. Haykin. "Cognitive dynamic systems [Point of view]". In: *Proc. IEEE* 94.11 (2006-11), pp. 1910–1911 (cit. on pp. 10, 41).

[61] S. Haykin. "Cognitive dynamic systems: Radar, control, and radio [Point of view]". In: *Proceedings of the IEEE* 100.7 (2012), pp. 2095–2103 (cit. on p. 10).

[62] S. Haykin and J. M. Fuster. "On Cognitive Dynamic Systems: Cognitive Neuroscience and Engineering Learning From Each Other". In: *Proc. IEEE* 102.4 (2014-04), pp. 608–628 (cit. on pp. 10, 72).

[63] S. Haykin, J. M. Fuster, D. Findlay, and S. Feng. "Cognitive Risk Control for Physical Systems". In: *IEEE Access* 5 (2017-07), pp. 14664–14679. DOI: 10.1109/ACCESS.2017.2726439 (cit. on pp. 10, 12, 25, 31, 41, 56, 72, 86, 100, 109).

[64] S. Haykin. "Artificial Intelligence Integrated with Cognitive Dynamic System for Cybersecurity". In: *IEEE Trans. Cogn. Commun. Netw.* (in press, 2019), pp. 1–20 (cit. on p. 10).

[65] J. M. Fuster. *Cortex and Mind: Unifying Cognition*. Oxford University Press, 2003 (cit. on pp. 10, 41, 72).

[66] J. M. Fuster. "Prefrontal Cortex in Decision-Making: The Perception-Action Cycle". In: *Decision Neuroscience*. Academic Press, 2017, pp. 95–105 (cit. on pp. 10, 73).

[67] Joaquin M Fuster. *Cortical Memory*. Accessed: 2019-06-25. 2007-04. URL: http://www.scholarpedia.org/article/Cortical_memory#Executive_Memory (visited on 2007-04-16) (cit. on pp. 11, 14).

[68] J. Kim, J. Lee, J. Kim, and J. Yun. "M2M Service Platforms: Survey, Issues, and Enabling Technologies". In: *IEEE Commun. Surveys Tuts.* 16.1 (2014-First), pp. 61–76 (cit. on p. 12).

[69] CP Robert. *The Bayesian Choice*. Springer-Verlag, New York, 2001 (cit. on p. 12).

[70] Y. C. Ho and R. C. K. Lee. "A Bayesian Approach to Problems in Stochastic Estimation and Control". In: *IEEE Transactions on Automatic Control* AC-9 (1964-10), pp. 333–339 (cit. on p. 12).

[71] S. Haykin. *Neural Networks and Learning Machines*. 3rd edition. Prentice-Hall, 2009 (cit. on pp. 12, 18, 46, 47, 58, 84, 106, 114, 122).

[72] Joaquin Fuster. *The Prefrontal Cortex*. Academic Press, 2015 (cit. on p. 13).

[73] Goren Gordon, David M Kaplan, Benjamin Lankow, et al. "Toward an integrated approach to perception and action: Conference report and future directions". In: *Frontiers in Systems Neuroscience* 5 (2011-04), pp. 1–6 (cit. on p. 13).

[74] Daniel Y Little and Friedrich T Sommer. "Learning and exploration in action-perception loops". In: *Frontiers in Neural Circuits* (2013-03), pp. 1–19 (cit. on p. 13).

[75] Claude Elwood Shannon. "A mathematical theory of communication". In: *Bell System Technical Journal* 27.3 (1948), pp. 379–423 (cit. on p. 13).

[76] Thomas M Cover and Joy A Thomas. *Elements of Information Theory*. John Wiley & Sons, 2012 (cit. on pp. 13, 47).

[77] Richard S Sutton and Andrew G Barto. *Reinforcement Learning: An Introduction*. 2nd edition. MIT Press Cambridge, 2018 (cit. on pp. 13, 50, 52, 57, 79, 120).

[78] Earl K Miller and Jonathan D Cohen. "An integrative theory of prefrontal cortex function". In: *Annual Review of Neuroscience* 24.1 (2001), pp. 167–202 (cit. on p. 14).

[79] S. Haykin. "The Cognitive Dynamic System for Risk Control [Point of View]". In: *Proceedings of the IEEE* 105.8 (2017-08), pp. 1470–1473 (cit. on p. 14).

[80] Joaquin M Fuster. "Network memory". In: *Trends in Neurosciences* 20.10 (1997), pp. 451–459 (cit. on p. 14).

[81] Joaquin M Fuster. "Prefrontal neurons in networks of executive memory". In: *Brain Research Bulletin* 52.5 (2000), pp. 331–336 (cit. on p. 14).

[82] J. M. Fuster. "The Prefrontal Cortex Makes the Brain a Preadaptive System". In: *Proc. IEEE* 102.4 (2014-04), pp. 417–426. ISSN: 0018-9219. DOI: 10.1109/JPROC.2014.2306250 (cit. on pp. 15, 25, 53, 100, 115).

[83] S. Haykin. "Cognitive radio: Brain-empowered wireless communications". In: *IEEE J. Sel. Areas Commun.* 23.2 (2005-02), pp. 201–220 (cit. on pp. 16, 17, 41).

[84] S. Haykin. "Cognitive radar: A way of the future". In: *IEEE Signal Process. Mag.* 23.1 (2006-01), pp. 30–40 (cit. on pp. 16–18, 41).

[85] J. Mitola and G. Q. Maguire. "Cognitive radio: Making software radios more personal". In: *IEEE Pers. Commun.* 6.4 (1999-08), pp. 13–18 (cit. on p. 17).

[86] Joseph Mitola. "Cognitive Radio: An Integrated Agent Architecture for Software Defined Radio". In: *Ph. D. Dissertation, Royal Institute of Technology (KTH)* (2000) (cit. on p. 17).

[87] Ian F Akyildiz, Won-Yeol Lee, Mehmet C Vuran, and Shantidev Mohanty. "NeXt generation/dynamic spectrum access/cognitive radio wireless networks: A survey". In: *Computer Networks* 50.13 (2006-09), pp. 2127–2159 (cit. on p. 17).

[88] Y. Liang, K. Chen, G. Y. Li, and P. Mahonen. "Cognitive radio networking and communications: An overview". In: *IEEE Transactions on Vehicular Technology* 60.7 (2011-09), pp. 3386–3407 (cit. on p. 17).

[89] Q. Wu, G. Ding, J. Wang, and Y. D. Yao. "Spatial-Temporal Opportunity Detection for Spectrum-Heterogeneous Cognitive Radio Networks: Two-Dimensional Sensing". In: *IEEE Trans. Wireless Commun.* 12.2 (2013-02), pp. 516–526 (cit. on pp. 17, 41).

[90] Y. Xu, A. Anpalagan, Q. Wu, et al. "Decision-Theoretic Distributed Channel Selection for Opportunistic Spectrum Access: Strategies, Challenges and Solutions". In: *IEEE Commun. Surveys Tuts.* 15.4 (2013-Fourth), pp. 1689–1713 (cit. on p. 17).

[91] A. Ali and W. Hamouda. "Advances on Spectrum Sensing for Cognitive Radio Networks: Theory and Applications". In: *IEEE Communications Surveys Tutorials* 19.2 (2017-Secondquarter), pp. 1277–1304 (cit. on p. 17).

[92] M. El Tanab and W. Hamouda. "Resource Allocation for Underlay Cognitive Radio Networks: A Survey". In: *IEEE Communications Surveys Tutorials* 19.2 (2017-Secondquarter), pp. 1249–1276 (cit. on p. 17).

[93] S. Haykin, D. J. Thomson, and J. H. Reed. "Spectrum Sensing for Cognitive Radio". In: *Proceedings of the IEEE* 97.5 (2009-05), pp. 849–877 (cit. on p. 17).

[94] P. Setoodeh and S. Haykin. "Robust transmit power control for cognitive radio". In: *Proc. IEEE* 97.5 (2009-05), pp. 915–939 (cit. on p. 17).

[95] F. Khozeimeh and S. Haykin. "Brain-Inspired Dynamic Spectrum Management for Cognitive Radio Ad Hoc Networks". In: *IEEE Transactions on Wireless Communications* 11.10 (2012-10), pp. 3509–3517 (cit. on p. 17).

[96] S. Haykin and P. Setoodeh. "Cognitive radio networks: The spectrum supply chain paradigm". In: *IEEE Transactions on Cognitive Communications and Networking* 1.1 (2015), pp. 3–28 (cit. on p. 17).

[97] S. Haykin, P. Setoodeh, S. Feng, and D. Findlay. "Cognitive Dynamic System as the Brain of Complex Networks". In: *IEEE Journal on Selected Areas in Communications* 34.10 (2016-10), pp. 2791–2800 (cit. on p. 17).

[98] Yaakov Bar-Shalom, X Rong Li, and Thiagalingam Kirubarajan. *Estimation with applications to tracking and navigation: Theory algorithms and software*. John Wiley & Sons, 2004 (cit. on p. 18).

[99] M. S. Greco, F. Gini, P. Stinco, and K. Bell. "Cognitive Radars: On the Road to Reality: Progress Thus Far and Possibilities for the Future". In: *IEEE Signal Processing Magazine* 35.4 (2018-07), pp. 112–125 (cit. on p. 18).

[100] P. Stinco, M. S. Greco, F. Gini, and B. Himed. "ComRadE: Cognitive Passive Tracking in Symbiotic IEEE 802.22 Systems". In: *IEEE Transactions on Aerospace and Electronic Systems* 53.2 (2017-04), pp. 1023–1034 (cit. on p. 18).

[101] S. Haykin, A. Zia, Y. Xue, and I. Arasaratnam. "Control theoretic approach to tracking radar: First step towards cognition". In: *Digital Signal Processing* 21.5 (2011-09), pp. 576–585 (cit. on p. 18).

[102] S. Haykin, M. Fatemi, P. Setoodeh, and Y. Xue. "Cognitive control". In: *Proc. IEEE* 100.12 (2012-12), pp. 3156–3169 (cit. on pp. 18, 79).

[103] S. Haykin, Y. Xue, and P. Setoodeh. "Cognitive Radar: Step Toward Bridging the Gap Between Neuroscience and Engineering". In: *Proc. IEEE* 100.11 (2012-11), pp. 3102–3130. ISSN: 0018-9219. DOI: 10.1109/JPROC.2012.2203089 (cit. on pp. 18, 42, 51).

[104] Nobuo Suga. "Cortical computational maps for auditory imaging". In: *Neural Networks* 3.1 (1990), pp. 3–21 (cit. on p. 18).

[105] Jeanette A Thomas, Cynthia F Moss, and Marianne Vater. *Echolocation in bats and dolphins*. University of Chicago Press, 2004 (cit. on p. 18).

[106] Andrea Zanella, Nicola Bui, Angelo Castellani, Lorenzo Vangelista, and Michele Zorzi. "Internet of things for smart cities". In: *IEEE Internet of Things Journal* 1.1 (2014-02), pp. 22–32 (cit. on p. 25).

[107] J. Contreras-Castillo, S. Zeadally, and J. A. Guerrero-Ibañez. "Internet of Vehicles: Architecture, Protocols, and Security". In: *IEEE Internet of Things Journal* 5.5 (2018-10), pp. 3701–3709 (cit. on p. 25).

[108] B. Paden, M. Čáp, S. Z. Yong, D. Yershov, and E. Frazzoli. "A Survey of Motion Planning and Control Techniques for Self-Driving Urban Vehicles". In: *IEEE Trans. Intell. Veh.* 1.1 (2016-03), pp. 33–55. ISSN: 2379-8858. DOI: 10.1109/TIV.2016.2578706 (cit. on pp. 25, 41).

[109] C. Bila, F. Sivrikaya, M. A. Khan, and S. Albayrak. "Vehicles of the Future: A Survey of Research on Safety Issues". In: *IEEE Trans. Intell. Transp. Syst.* 18.5 (2017-05), pp. 1046–1065. ISSN: 1524-9050. DOI: 10.1109/TITS.2016.2600300 (cit. on pp. 25, 41).

[110] Boyang Li, Mithat C Kisacikoglu, Chen Liu, Navjot Singh, and Melike Erol-Kantarci. "Big data analytics for electric vehicle integration in green smart cities". In: *IEEE Communications Magazine* 55.11 (2017-11), pp. 19–25 (cit. on p. 25).

[111] Canadian Automated Vehicles Centre of Excellence [CAVCOE]. "Preparing for Autonomous Vehicles in Canada: A White Paper Prepared for the Government of Canada". In: (2015-12) (cit. on p. 25).

[112] G. Ding, Q. Wu, L. Zhang, Y. Lin, T. A. Tsiftsis, and Y. D. Yao. "An amateur drone surveillance system based on the cognitive Internet of Things". In: *IEEE Commun. Mag.* 56.1 (2018-01), pp. 29–35 (cit. on pp. 26, 41, 71, 99).

[113] Luliang Jia, Yuhua Xu, Youming Sun, Shuo Feng, and Alagan Anpalagan. "Stackelberg game approaches for anti-jamming defence in wireless networks". In: *IEEE Wireless Communications* 25.6 (2018-12), pp. 120–128 (cit. on p. 26).

[114] S. Karnouskos and F. Kerschbaum. "Privacy and Integrity Considerations in Hyperconnected Autonomous Vehicles". In: *Proc. IEEE* 106.1 (2018-01), pp. 160–170 (cit. on pp. 26, 42).

[115] Nikos Komninos, Eleni Philippou, and Andreas Pitsillides. "Survey in smart grid and smart home security: Issues, challenges and countermeasures". In: *IEEE Communications Surveys & Tutorials* 16.4 (2014-04), pp. 1933–1954 (cit. on p. 27).

[116] S. Feng and S. Haykin. "Cognitive Risk Control for Transmit-Waveform Selection in Vehicular Radar Systems". In: *IEEE Transactions on Vehicular Technology* 67.10 (2018-10), pp. 9542–9556 (cit. on pp. 33, 72, 80, 100, 103, 120).

[117] T. J. O'Shea, K. Karra, and T. C. Clancy. "Learning to communicate: Channel auto-encoders, domain specific regularizers, and attention". In: *Proc. IEEE ISSPIT* (2016-12), pp. 223–228 (cit. on p. 41).

[118] Timothy J. O'Shea and T. Charles Clancy. "Deep reinforcement learning radio control and signal detection with KeRLym, a Gym RL agent". In: *arXiv* (2016). URL: `http://arxiv.org/abs/1605.09221` (cit. on p. 41).

[119] Q. Wu et al. "Cognitive Internet of Things: A new paradigm beyond connection". In: *IEEE Internet Things J.* 1.2 (2014-04), pp. 129–143 (cit. on pp. 41, 99).

[120] M. Chen, M. Mozaffari, W. Saad, C. Yin, M. Debbah, and C. S. Hong. "Caching in the Sky: Proactive Deployment of Cache-Enabled Unmanned Aerial Vehicles for Optimized Quality-of-Experience". In: *IEEE J. Sel. Areas Commun.* 35.5 (2017-05), pp. 1046–1061 (cit. on p. 41).

[121] Mingzhe Chen, Ursula Challita, Walid Saad, Changchuan Yin, and Merouane Debbah. "Machine Learning for Wireless Networks with Artificial Intelligence: A Tutorial on Neural Networks". In: *arXiv* (2017). URL: `http://arxiv.org/abs/1710.02913` (cit. on p. 41).

[122] G. Bresson, Z. Alsayed, L. Yu, and S. Glaser. "Simultaneous Localization and Mapping: A Survey of Current Trends in Autonomous Driving". In: *IEEE Trans. Intell. Veh.* 2.3 (2017-09), pp. 194–220. ISSN: 2379-8858. DOI: `10.1109/TIV.2017.2749181` (cit. on pp. 41, 71).

[123] M. Bojarski et al. "End to End Learning for Self-Driving Cars". In: *arXiv* (2016). URL: `http://arxiv.org/abs/1604.07316` (cit. on p. 41).

[124] K. Jo, J. Kim, D. Kim, C. Jang, and M. Sunwoo. "Development of autonomous car—Part II: A case study on the implementation of an autonomous driving system based on distributed architecture". In: *IEEE Trans. Ind. Electron.* 62.8 (2015-08), pp. 5119–5132 (cit. on p. 41).

[125] Simone Pettigrew. "Why public health should embrace the autonomous car". In: *Aust. N. Z. J. Public Health* 41.1 (2017-02), pp. 5–7 (cit. on p. 41).

[126] Daniel Watzenig and Martin Horn. *Automated Driving: Safer and More Efficient Future Driving*. Springer, 2017 (cit. on p. 42).

[127] S. M. Patole, M. Torlak, D. Wang, and M. Ali. "Automotive radars: A review of signal processing techniques". In: *IEEE Signal Process. Mag.* 34.2 (2017-03), pp. 22–35. ISSN: 1053-5888. DOI: `10.1109/MSP.2016.2628914` (cit. on p. 42).

[128] J. Hasch, E. Topak, R. Schnabel, T. Zwick, R. Weigel, and C. Waldschmidt. "Millimeter-wave technology for automotive radar sensors in the 77 GHz frequency band". In: *IEEE Trans. Microw. Theory Techn.* 60.3 (2012-03), pp. 845–860. ISSN: 0018-9480. DOI: `10.1109/TMTT.2011.2178427` (cit. on p. 42).

[129] Paul J TH Venhovens and Karl Naab. "Vehicle dynamics estimation using Kalman filters". In: *Vehicle Syst. Dyn.* 32.2–3 (1999-02), pp. 171–184 (cit. on p. 43).

[130] Moustapha Doumiati, Ali Charara, Alessandro Victorino, and Daniel Lechner. *Vehicle Dynamics Estimation using Kalman Filtering: Experimental Validation*. John Wiley & Sons, 2012 (cit. on p. 43).

[131] D. J. Kershaw and R. J. Evans. "Optimal waveform selection for tracking systems". In: *IEEE Trans. Inf. Theory* 40.5 (1994-09), pp. 1536–1550. ISSN: 0018-9448. DOI: 10.1109/18.333866 (cit. on pp. 45, 104).

[132] Chris Chatfield. *Introduction to Multivariate Analysis*. Routledge, 2018 (cit. on p. 47).

[133] M. Fatemi and S. Haykin. "Cognitive control: Theory and application". In: *IEEE Access* 2 (2014-06), pp. 698–710 (cit. on pp. 47, 48, 50, 57).

[134] Marc C Kennedy and Anthony O'Hagan. "Bayesian calibration of computer models". In: *J. Royal Stat. Soc. Series B Stat. Methodol.* 63.3 (2001-01), pp. 425–464 (cit. on p. 48).

[135] Sundeep Samson, James A Reneke, and Margaret M Wiecek. "A review of different perspectives on uncertainty and risk and an alternative modeling paradigm". In: *Reliab. Eng. Syst. Safety* 94.2 (2009-02), pp. 558–567 (cit. on p. 49).

[136] S. Theodoridis and K. Koutroumbas. *Pattern Recognition*. 4th edition. Elsevier Science, 2008. ISBN: 9780080949123 (cit. on p. 52).

[137] H. Menouar, I. Guvenc, K. Akkaya, A. S. Uluagac, A. Kadri, and A. Tuncer. "UAV-Enabled Intelligent Transportation Systems for the Smart City: Applications and Challenges". In: *IEEE Commun. Mag.* 55.3 (2017-03), pp. 22–28 (cit. on p. 71).

[138] N. Zhang, S. Zhang, P. Yang, O. Alhussein, W. Zhuang, and X. Shen. "Software Defined Space-Air-Ground Integrated Vehicular Networks: Challenges and Solutions". In: *IEEE Commun. Mag.* 55.7 (2017-07), pp. 101–109 (cit. on p. 71).

[139] SAE International. *Taxonomy and Definitions for Terms Related to On-Road Motor Vehicle Automated Driving Systems*. SAE Standard J3016, 2018, pp. 1–35. DOI: DOI:10.4271/J3016_201401 (cit. on pp. 71, 99).

[140] W. Shi, H. Zhou, J. Li, W. Xu, N. Zhang, and X. Shen. "Drone Assisted Vehicular Networks: Architecture, Challenges and Opportunities". In: *IEEE Network* 32.3 (2018-05), pp. 130–137 (cit. on p. 71).

[141] IEEE. "IEEE Standard for Local and Metropolitan Area Networks - Part 11: Wireless LAN Medium Access Control (MAC) and Physical Layer (PHY) Specifications Amendment 6: Wireless Access in Vehicular Environments". In: *IEEE Std 802.11p-2010* (2010-07), pp. 1–51 (cit. on pp. 71, 87).

[142] John B Kenney. "Dedicated short-range communications (DSRC) standards in the United States". In: *Proc. IEEE* 99.7 (2011-07), pp. 1162–1182 (cit. on pp. 71, 122).

[143] 3GPP. "Technical Specification Group Radio Access Network: Study on LTE-based V2X Services (Release 14)". In: *3GPP Technical Report, TR 36.885 V14.0.0* (2010-07), pp. 1–217 (cit. on p. 71).

[144] 3GPP. "Technical Specification Group Services and System Aspects: Study on enhancement of 3GPP Support for 5G V2X Services (Release 16)". In: *3GPP Technical Report, TR 22.886 V16.0.0* (2018-06), pp. 1–67 (cit. on p. 71).

[145] C. Bila, F. Sivrikaya, M. A. Khan, and S. Albayrak. "Vehicles of the Future: A Survey of Research on Safety Issues". In: *IEEE Trans. Intell. Transp. Syst.* 18.5 (2017-05), pp. 1046–1065 (cit. on p. 71).

[146] O. Puñal, C. Pereira, A. Aguiar, and J. Gross. "Experimental Characterization and Modeling of RF Jamming Attacks on VANETs". In: *IEEE Trans. Veh. Technol.* 64.2 (2015-02), pp. 524–540 (cit. on p. 71).

[147] D. Yang, G. Xue, J. Zhang, A. Richa, and X. Fang. "Coping with a Smart Jammer in Wireless Networks: A Stackelberg Game Approach". In: *IEEE Trans. Wireless Commun.* 12.8 (2013-08), pp. 4038–4047 (cit. on pp. 72, 86).

[148] S. D'Oro, E. Ekici, and S. Palazzo. "Optimal Power Allocation and Scheduling Under Jamming Attacks". In: *IEEE/ACM Trans. Netw.* 25.3 (2017-06), pp. 1310–1323 (cit. on pp. 72, 86).

[149] X. Liu, Y. Xu, L. Jia, Q. Wu, and A. Anpalagan. "Anti-Jamming Communications Using Spectrum Waterfall: A Deep Reinforcement Learning Approach". In: *IEEE Commun. Lett.* 22.5 (2018-05), pp. 998–1001 (cit. on pp. 72, 87).

[150] P. Zhou and T. Jiang. "Toward Optimal Adaptive Wireless Communications in Unknown Environments". In: *IEEE Trans. Wireless Commun.* 15.5 (2016-05), pp. 3655–3667 (cit. on pp. 72, 87).

[151] L. Jia, Y. Xu, Y. Sun, S. Feng, L. Yu, and A. Anpalagan. "A Multi-Domain Anti-Jamming Defense Scheme in Heterogeneous Wireless Networks". In: *IEEE Access* 6 (2018-06), pp. 40177–40188 (cit. on pp. 72, 83, 87, 102, 122).

[152] Liang Xiao, Yan Chen, W Sabrina Lin, and KJ Ray Liu. "Indirect reciprocity security game for large-scale wireless networks". In: *IEEE Trans. Inf. Forensics Security* 7.4 (2012-08), pp. 1368–1380 (cit. on p. 72).

[153] Nan Zhang, Wei Yu, Xinwen Fu, and Sajal K Das. "Maintaining defender's reputation in anomaly detection against insider attacks". In: *IEEE Trans. Syst. Man, Cybern. B, Cybern.* 40.3 (2010-06), pp. 597–611 (cit. on p. 72).

[154] A. Benslimane and H. Nguyen-Minh. "Jamming Attack Model and Detection Method for Beacons Under Multichannel Operation in Vehicular Networks". In: *IEEE Trans. Veh. Technol.* 66.7 (2017-07), pp. 6475–6488 (cit. on pp. 72, 100).

[155] H. Sedjelmaci, S. M. Senouci, and N. Ansari. "Intrusion Detection and Ejection Framework Against Lethal Attacks in UAV-Aided Networks: A Bayesian Game-Theoretic Methodology". In: *IEEE Trans. Intell. Transp. Syst.* 18.5 (2017-05), pp. 1143–1153 (cit. on p. 72).

[156] I. K. Azogu, M. T. Ferreira, J. A. Larcom, and H. Liu. "A new anti-jamming strategy for VANET metrics-directed security defense". In: *IEEE GLOBECOM*. 2013-12, pp. 1344–1349 (cit. on p. 72).

[157] P. Gu, C. Hua, R. Khatoun, Y. Wu, and A. Serhrouchni. "Cooperative Anti-Jamming Relaying for Control Channel Jamming in Vehicular Networks". In: *IEEE GLOBECOM*. 2017-12, pp. 1–6 (cit. on p. 72).

[158] X. Lu, D. Xu, L. Xiao, L. Wang, and W. Zhuang. "Anti-Jamming Communication Game for UAV-Aided VANETs". In: *IEEE GLOBECOM*. 2017-12, pp. 1–6 (cit. on p. 72).

[159] L. Xiao, X. Lu, D. Xu, Y. Tang, L. Wang, and W. Zhuang. "UAV Relay in VANETs Against Smart Jamming With Reinforcement Learning". In: *IEEE Trans. Veh. Technol.* 67.5 (2018-05), pp. 4087–4097 (cit. on p. 72).

[160] Y. Xu et al. "A One-Leader Multi-Follower Bayesian-Stackelberg Game for Anti-Jamming Transmission in UAV Communication Networks". In: *IEEE Access* 6 (2018-04), pp. 21697–21709 (cit. on pp. 72, 86).

[161] Hua Qin, Yang Peng, and Wensheng Zhang. "Vehicles on RFID: Error-cognitive vehicle localization in GPS-less environments". In: *IEEE Trans. Veh. Technol.* 66.11 (2017-11), pp. 9943–9957 (cit. on p. 75).

[162] Nabil M Drawil, Haitham M Amar, and Otman A Basir. "GPS localization accuracy classification: A context-based approach". In: *IEEE Trans. Intell. Transp. Syst.* 14.1 (2013-03), pp. 262–273 (cit. on p. 75).

[163] Quoc Duy Vo and Pradipta De. "A survey of fingerprint-based outdoor localization". In: *IEEE Commun. Surveys Tuts.* 18.1 (2016-01), pp. 491–506 (cit. on p. 75).

[164] Hui Ma, Rajiv Vijayakumar, Sumit Roy, and Jing Zhu. "Optimizing 802.11 wireless mesh networks based on physical carrier sensing". In: *IEEE/ACM Trans. Netw* 17.5 (2009-10), pp. 1550–1563 (cit. on pp. 76, 110).

[165] Dejun Yang, Guoliang Xue, Jin Zhang, Andrea Richa, and Xi Fang. "Coping with a smart jammer in wireless networks: A Stackelberg game approach". In: *IEEE Trans. Wireless Commun.* 12.8 (2013-08), pp. 4038–4047 (cit. on p. 76).

[166] Yulong Zou, Jia Zhu, Liuqing Yang, Ying-Chang Liang, and Yu-Dong Yao. "Securing physical-layer communications for cognitive radio networks". In: *IEEE Commun. Mag.* 53.9 (2015-09), pp. 48–54 (cit. on p. 76).

[167] C. F. Mecklenbrauker et al. "Vehicular Channel Characterization and Its Implications for Wireless System Design and Performance". In: *Proc. IEEE* 99.7 (2011-07), pp. 1189–1212 (cit. on p. 77).

[168] Christoph F Mecklenbrauker, Andreas F Molisch, Johan Karedal, Fredrik Tufvesson, Alexander Paier, Laura Bernado, Thomas Zemen, Oliver Klemp, and Nicolai Czink. "Vehicular channel characterization and its implications for wireless system design and performance". In: *Proc. IEEE* 99.7 (2011-07), pp. 1189–1212 (cit. on p. 77).

[169] Lin Cheng, Benjamin E Henty, Daniel D Stancil, Fan Bai, and Priyantha Mudalige. "Mobile vehicle-to-vehicle narrow-band channel measurement and characterization of the 5.9 GHz dedicated short range communication (DSRC) frequency band". In: *IEEE J. Sel. Areas Commun.* 25.8 (2007-10), pp. 1501–1516 (cit. on p. 77).

[170] J. Kunisch and J. Pamp. "Wideband car-to-car radio channel measurements and model at 5.9 GHz". In: *IEEE VTC-Fall.* 2008-09, pp. 1–5 (cit. on p. 77).

[171] J. Karedal, N. Czink, A. Paier, F. Tufvesson, and A. F. Molisch. "Path Loss Modeling for Vehicle-to-Vehicle Communications". In: *IEEE Trans. Veh. Technol.* 60.1 (2011-01), pp. 323–328 (cit. on pp. 77, 87, 111, 122).

[172] Ian Goodfellow, Yoshua Bengio, Aaron Courville, and Yoshua Bengio. *Deep Learning.* MIT Press Cambridge, 2016 (cit. on p. 80).

[173] Y. Xu, A. Anpalagan, Q. Wu, L. Shen, Z. Gao, and J. Wang. "Decision-Theoretic Distributed Channel Selection for Opportunistic Spectrum Access: Strategies, Challenges and Solutions". In: *IEEE Commun. Surveys Tuts.* 15.4 (2013-Fourth Quarter), pp. 1689–1713 (cit. on pp. 81, 102).

[174] Peter Auer, Nicolo Cesa-Bianchi, and Paul Fischer. "Finite-time analysis of the multiarmed bandit problem". In: *Machine learning* 47.2-3 (2002-05), pp. 235–256 (cit. on pp. 81, 83, 113).

[175] Jean-Yves Audibert, Remi Munos, and Csaba Szepesvari. "Exploration-exploitation Tradeoff Using Variance Estimates in Multi-armed Bandits". In: *Theor. Comput. Sci.* 410.19 (2009-04), pp. 1876–1902 (cit. on pp. 82, 114).

[176] A. Bazzi, C. Campolo, B. M. Masini, A. Molinaro, A. Zanella, and A. O. Berthet. "Enhancing Cooperative Driving in IEEE 802.11 Vehicular Networks Through Full-Duplex Radios". In: *IEEE Trans. Wireless Commun.* 17.4 (2018-04), pp. 2402–2416 (cit. on pp. 87, 122).

[177] F. J. Martín-Vega, B. Soret, M. C. Aguayo-Torres, I. Z. Kovács, and G. Gómez. "Geolocation-Based Access for Vehicular Communications: Analysis and Optimization via Stochastic Geometry". In: *IEEE Trans. Veh. Technol.* 67.4 (2018-04), pp. 3069–3084 (cit. on p. 87).

[178] R. W. L. Coutinho, A. Boukerche, and A. A. F. Loureiro. "Design Guidelines for Information-Centric Connected and Autonomous Vehicles". In: *IEEE Commun. Mag.* 56.10 (2018-10), pp. 85–91 (cit. on p. 99).

[179] J. Liu and J. Liu. "Intelligent and Connected Vehicles: Current Situation, Future Directions, and Challenges". In: *IEEE Commun. Standards Mag.* 2.3 (2018-09), pp. 59–65 (cit. on p. 99).

[180] A. Bhat, S. Aoki, and R. Rajkumar. "Tools and Methodologies for Autonomous Driving Systems". In: *Proc. IEEE* 106.9 (2018-09), pp. 1700–1716 (cit. on p. 99).

[181] R. Molina-Masegosa and J. Gozalvez. "LTE-V for Sidelink 5G V2X Vehicular Communications: A New 5G Technology for Short-Range Vehicle-to-Everything Communications". In: *IEEE Veh. Technol. Mag.* 12.4 (2017-12), pp. 30–39 (cit. on p. 99).

[182] K. P. Divakarla, A. Emadi, and S. Razavi. "A Cognitive Advanced Driver Assistance Systems Architecture for Autonomous-Capable Electrified Vehicles". In: *IEEE Trans. Transport. Electrific.* 5.1 (2019-03), pp. 48–58 (cit. on p. 99).

[183] M. Park, S. Lee, C. Kwon, and S. Kim. "Design of Pedestrian Target Selection With Funnel Map for Pedestrian AEB System". In: *IEEE Trans. Veh. Technol.* 66.5 (2017-05), pp. 3597–3609 (cit. on p. 99).

[184] G. Zhong, S. Niar, A. Prakash, and T. Mitra. "Design of Multiple-Target Tracking System on Heterogeneous System-on-Chip Devices". In: *IEEE Trans. Veh. Technol.* 65.6 (2016-06), pp. 4802–4812 (cit. on p. 99).

[185] X. Wang, L. Xu, H. Sun, J. Xin, and N. Zheng. "On-Road Vehicle Detection and Tracking Using MMW Radar and Monovision Fusion". In: *IEEE Trans. Intell. Transp. Syst.* 17.7 (2016-07), pp. 2075–2084 (cit. on p. 99).

[186] S. Schwarz, T. Philosof, and M. Rupp. "Signal Processing Challenges in Cellular-Assisted Vehicular Communications: Efforts and developments within 3GPP LTE and beyond". In: *IEEE Signal Process. Mag.* 34.2 (2017-03), pp. 47–59 (cit. on p. 99).

[187] S. Darbha, S. Konduri, and P. R. Pagilla. "Benefits of V2V Communication for Autonomous and Connected Vehicles". In: *IEEE Trans. Intell. Transp. Syst.* 20.5 (2019-05), pp. 1954–1963 (cit. on p. 99).

[188] P. Kumari, J. Choi, N. González-Prelcic, and R. W. Heath. "IEEE 802.11ad-Based Radar: An Approach to Joint Vehicular Communication-Radar System". In: *IEEE Trans. Veh. Technol.* 67.4 (2018-04), pp. 3012–3027 (cit. on p. 99).

[189] J. Mei, K. Zheng, L. Zhao, L. Lei, and X. Wang. "Joint Radio Resource Allocation and Control for Vehicle Platooning in LTE-V2V Network". In: *IEEE Trans. Veh. Technol.* 67.12 (2018-12), pp. 12218–12230 (cit. on p. 99).

[190] P. Kapoor, A. Vora, and K. Kang. "Detecting and Mitigating Spoofing Attack Against an Automotive Radar". In: *IEEE VTC-Fall.* 2018-08, pp. 1–6 (cit. on p. 100).

[191] C. Yang, L. Feng, H. Zhang, S. He, and Z. Shi. "A Novel Data Fusion Algorithm to Combat False Data Injection Attacks in Networked Radar Systems". In: *IEEE Trans. Signal Inf. Process. Netw.* 4.1 (2018-03), pp. 125–136 (cit. on p. 100).

[192] M. Amoozadeh, A. Raghuramu, C. Chuah, D. Ghosal, H. M. Zhang, J. Rowe, and K. Levitt. "Security vulnerabilities of connected vehicle streams and their impact on cooperative driving". In: *IEEE Commun. Mag.* 53.6 (2015-06), pp. 126–132 (cit. on p. 100).

[193] S. Feng and S. Haykin. "Cognitive Risk Control for Anti-Jamming V2V Communication in Autonomous Vehicle Networks". In: *IEEE Trans. Veh. Technol.* (accepted, 2019), pp. 1–15 (cit. on pp. 100, 110, 121).

[194] I. Arasaratnam and S. Haykin. "Cubature Kalman Filters". In: *IEEE Trans. Autom. Control* 54.6 (2009-06), pp. 1254–1269 (cit. on pp. 101, 103, 106).

[195] S. Feng and S. Haykin. "V2V Communication-Assisted Transmit-Waveform Selection for Cognitive Vehicular Radars". In: *IEEE CCECE*. 2019-05, pp. 1–6 (cit. on pp. 101, 103).

[196] S. Feng and S. Haykin. "Anti-Jamming V2V Communication in an Integrated UAV-CAV Network with Hybrid Attackers". In: *IEEE ICC*. 2019-05, pp. 1–6 (cit. on pp. 101, 110).

[197] J. Georgy, A. Noureldin, M. J. Korenberg, and M. M. Bayoumi. "Modeling the Stochastic Drift of a MEMS-Based Gyroscope in Gyro/Odometer/GPS Integrated Navigation". In: *IEEE Trans. Intell. Transp. Syst.* 11.4 (2010-12), pp. 856–872 (cit. on p. 106).

[198] J Leo Van Hemmen and Terrence J Sejnowski. *23 Problems in Systems Neuroscience*. Oxford University Press, 2005 (cit. on p. 112).

[199] E. Salahat, A. Kulaib, N. Ali, and R. Shubair. "Exploring symmetry in wireless propagation channels". In: *IEEE EuCNC*. 2017-06, pp. 1–6 (cit. on p. 115).

[200] Xuyu Qian, Ha Nam Nguyen, Mingxi M Song, Christopher Hadiono, Sarah C Ogden, Christy Hammack, Bing Yao, Gregory R Hamersky, Fadi Jacob, Chun Zhong, et al. "Brain-region-specific organoids using mini-bioreactors for modeling ZIKV exposure". In: *Cell* 165.5 (2016-05), pp. 1238–1254 (cit. on p. 133).

[201] Daniel J Felleman and DC Essen Van. "Distributed hierarchical processing in the primate cerebral cortex". In: *Cerebral Cortex (New York, NY: 1991)* 1.1 (1991-01), pp. 1–47 (cit. on p. 133).